ENGEBØ OPEN PIT FEASBILITY STUDY - MINING GEOTECHNICS

Prepared For

Nordic Mining ASA

Report Prepared by

SRK Consulting (UK) Limited
UK7480

SRK Legal Entity:		SRK Consulting (UK) Limited
SRK Address:		5th Floor Churchill House 17 Churchill Way Cardiff, CF10 2HH Wales, United Kingdom.
Date:		June 2018
Project Number:		UK7480
SRK Project Director:	Neil Marshall	Corporate Consultant (Rock Mechanics)
SRK Project Manager:	Max Brown	Principal Consultant (Rock Mechanics)
Client Legal Entity:		Nordic Mining ASA
Client Address:		Nordic Mining ASA, Vika Atrium, Munkedamveien 45, 0250 Oslo, Norway.

Table of Contents: Executive Summary

List of Tables: Executive Summary

List of Figures: Executive Summary

SRK Consulting (UK) Limited
5th Floor Churchill House
17 Churchill Way
City and County of Cardiff
CF10 2HH, Wales
United Kingdom
E-mail: enquiries@srk.co.uk
URL: www.srk.co.uk
Tel: + 44 (0) 2920 348 150
Fax: + 44 (0) 2920 348 199

EXECUTIVE SUMMARY
ENGEBØ OPEN PIT FEASBILITY STUDY - MINING GEOTECHNICS

1 EXECUTIVE SUMMARY

1.1 Introduction

SRK Consulting (UK) Limited ("SRK") is an associate company of the international group holding company, SRK Consulting (Global) Limited (the "SRK Group"). SRK has been requested by Nordic Mining ASA ("NM", hereinafter also referred to as the "Company" or the "Client") to undertake an open pit geotechnical study in support of the Feasibility Study (the "FS") for the Engebøfjellet Rutile Project ("Engebø" or the "Project") located in Norway.

The Engebø rutile project is located in the municipality of Naustdal, Sogn og Fjordane in Norway and lies roughly 125 km North of Bergen and 2.5 km east of the town of Vevring. (UTM: 309 762mE, 6 822 838 mN) (Figure ES 1). The Project is wholly owned by Nordic Mining AS. The deposit was first identified in the 1970s during the construction of a road tunnel, which is currently active. DuPont/Conoco acquired the rights to the deposit in the mid-1990s, and subsequently completed 15,000 m of core drilling over 49 drillholes. The Project was subject to a Pre-Feasibility ("PFS") geotechnical study that was completed in 2016 by Wardell Armstrong International ("WAI").

Figure ES 1: Project location (WAI, 2016)

1.2 Geotechnical Investigations

The Client undertook a geotechnical drilling and logging programme (RMR[89]) which consisted of drilling four specific boreholes located to intersect the proposed pit shell approximately one third to half way up the proposed slope and to fill in data gaps not covered as part of the PFS. The four geotechnical boreholes were subject to geophysical televiewer surveys, and an additional three existing boreholes were also surveyed by televiewer (Figure ES 2). In addition, spinner tests were completed in a number of boreholes and a suite of laboratory strength tests undertaken (UK based laboratory) to define the intact rock strength and discontinuity shear strength to substantiate the point load testing undertaken by SRK. The borehole azimuth was varied with the aim of reducing any bias in the structural information. All rock mass logging, structure picking and structure logging was undertaken by SRK engineers.

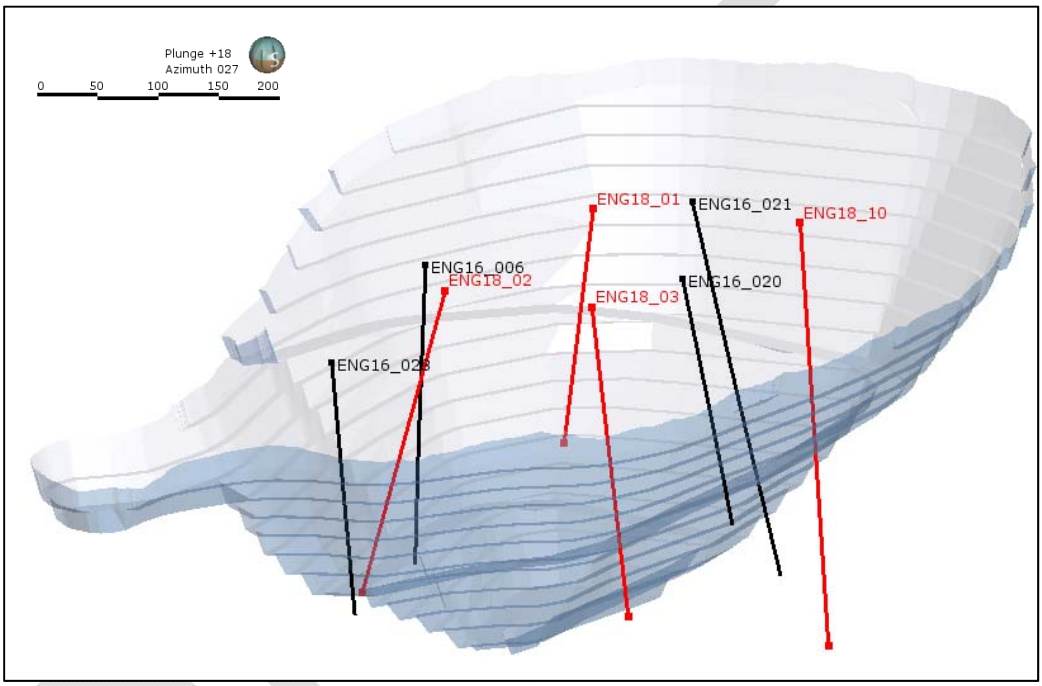

Figure ES 2: Oblique view of geotechnical borehole locations. Note boreholes are placed on an interim pit shell

1.3 Geological and Structural Setting

This report draws upon the Korneliussen et al. (1998) in-depth descriptions of the geological setting and deformation history of Engebøfjellet, who conducted structural, geochemical, and mineralogical studies under the auspices of the Norge Geologiska Undersøkelse, the geological survey of Norway.

Geologically, the Engebø project is comprised of rocks belonging to the Hegreneset complex of the Western Gneiss Region: a highly deformed assemblage of Paleoproterozoic basement amphibolites, eclogites and metagabbroic rocks, together with tonalite-diorite composition gneisses. The rocks comprising the Engebø deposit belong to a lens of highly-deformed Fe- and Ti-rich eclogite which is believed to result from the metamorphism of a Ti-enriched gabbroic intrusion.

A structural geologist spent one week on site with the aim of defining a three-dimensional geological model and also a project-scale major structure model and characterisation of the

geometry of the dominant joint sets present within the pit slopes feed into the development of the geotechnical slope design criteria. The modelled geology of Engebøfjellet is relatively simple, consisting of generally continuous domains of Leuco, Trans and Ferro eclogite, striking East-West and dipping moderately-steeply (50-80º) to the north. Tight foliation is present, especially within the Leuco eclogite, although in general the eclogites are generally massive in nature. Quartz Mica-Garnet ("QMG") veins appear to contain more fractures than other lithologies and the location of such units has been assessed. Whilst there is some scatter, orientations tend to fall into two main groups that dip steeply SSE and NNE, which most likely signify that the majority of the veins are sheared parallel to the predominant foliation.

Nearly all (94%) of the fractured and broken zones logged in the drill core are interpreted to be minor structures based on their negligible fault rock characteristics. Very few faulted and broken intervals were classified as moderate or major structures (<6% of all logged intervals). These intervals include strongly broken and fractured zones of eclogite as well as several intervals where there has been significant core loss or poor recovery. When displayed in 3D, all but one of the faulted intervals classified as moderate and major fall in a planar distribution and are easily correlatable into a planar structure. The interpreted fault has an overall orientation of 53/022, as shown in Figure ES 3.

Several distinct populations of discontinuities have been defined from the televiewer surveys. These generally fall into three sets. Set J1, sub-horizontal joints present in all boreholes. Set J2, steep to sub-vertically dipping, E-W to WNW-ESE striking joints present in most boreholes, but under-represented in the north dipping boreholes due to orientation bias. These joints are controlled by the principal foliation and are present in all of the major lithologies. Set J3, N-S striking sets which are generally characterised by a moderately to steeply west dipping set, while in the Vevring tunnel, an east dipping set was identified. In general, analysis indicates there are no specific structural domains and that the data set collected to date indicates the proposed pit slopes can be structurally characterised by the structural setting described above.

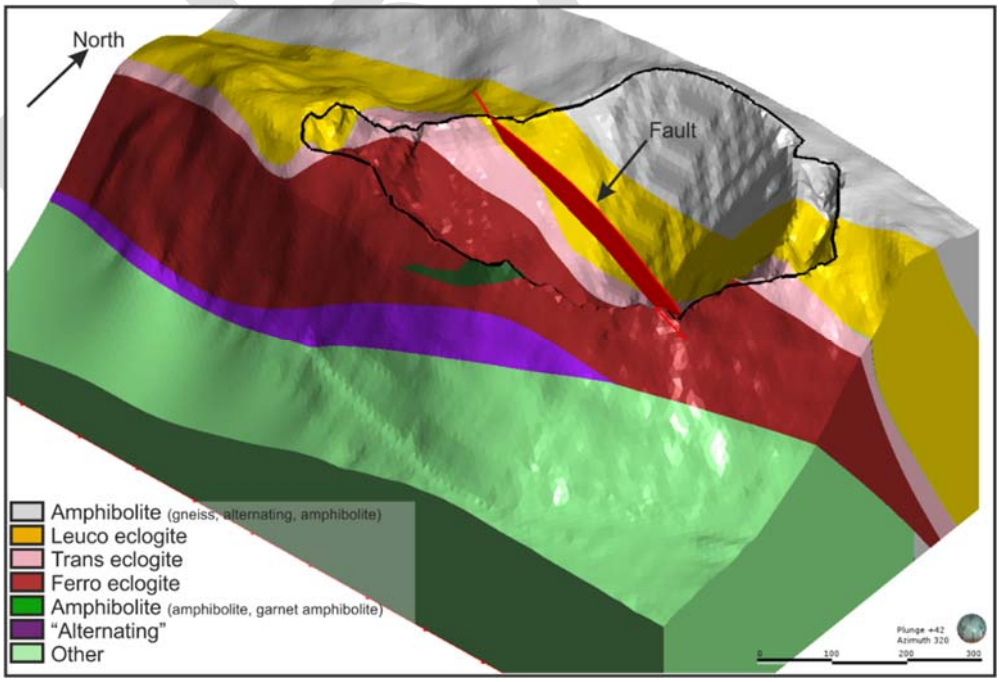

Figure ES 3: Leapfrog geological and structural model of the Engebø deposit

1.4 Rock Mass Strength

Intact strength testing characterised the rock as very strong to extremely strong and rock mass classification returned RMR[89] values in excess of 70 for every major lithology intersected indicating a good rock mass. There was little variability in intact rock strength or rock mass rating between the major lithologies. RMR[89] reduces when potential fault zones are intersected, although, at this stage, it is considered that such zones are discrete and discontinuous. Assessment of the rock mass strength characteristics of the rock forming the final pit slope clearly indicates that slope design and slope performance will be controlled by the structural conditions rather than rock mass strength.

1.5 Structural Analysis

Using the structural architecture as presented in Figure ES 4 and Table ES 1, SRK has used limit equilibrium and probabilistic methods to undertake a kinematic analysis of the proposed pit slopes. Joint shear strength parameters as defined by laboratory (phi 22°, cohesion 0 kPa) testing have been used in the analysis, and stereographic software (Dips) used to define sections of the proposed pit that may be subject to planar, toppling or wedge instability modes. Planar assessment indicates potential for bench scale instability on joint set J3 (70°/245°) within the west dipping slopes (eastern section of the pit), while toppling instability is more likely to occur in the north dipping slopes (southern section of the pit). Given the wide joint spacing and very high intact rock strength, and hence high strength rock bridges, flexural toppling is not considered to be significant.

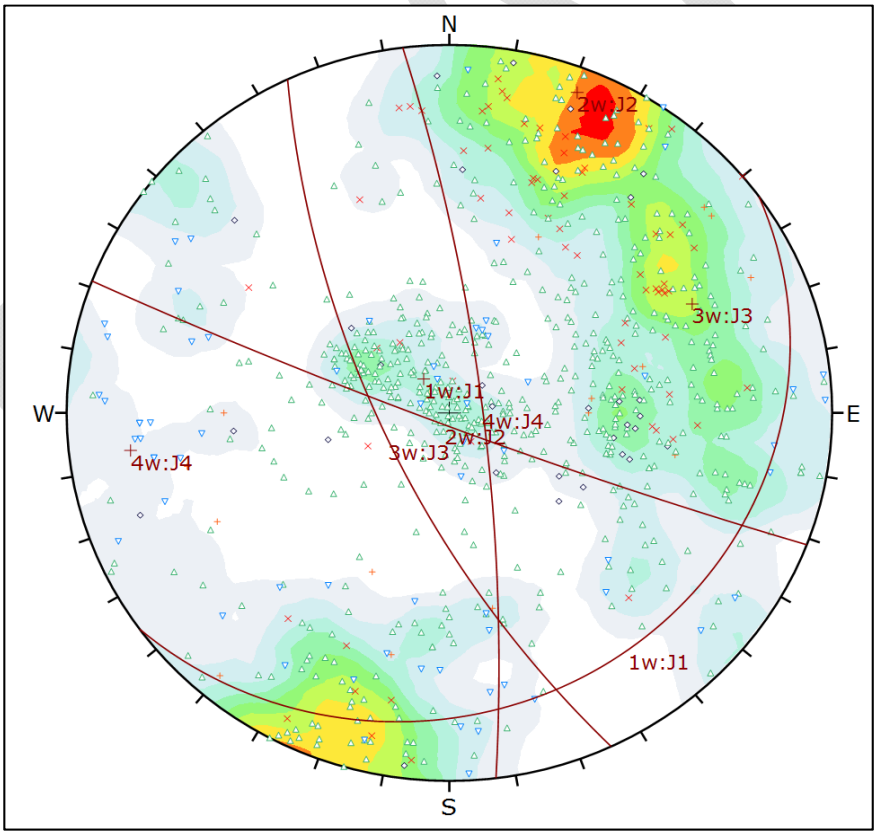

Figure ES 4: Defined joints sets used within structural analyses

Table ES 1: Summary of joint set details

ID	Dip	Dip Direction	Range (= 1*StdDEV) (weighted)	Mean Spacing (m)	Spacing StdDEV (m)	Persistence Max (m)	Persistence StdDEV (m)	Primary Infill
J1	13	142	21	5.6	11.3	30	15	Calcite
J2	86	201	16	2.9	5.7	30	15	Chlorite
J3	70	245	15	3.7	6.9	30	15	Chlorite
J4	80	083	12	-	-	30	15	-

Wedge analysis indicates the kinematically feasible wedges in the west dipping slope and further probabilistic analysis was undertaken using the MWedge software. MWedge uses statistical joint orientation distribution to simulate 10,000 blocks. Each block is formed by the intersection of two joints from any of the joint sets of the domain. A multiple number of joint sets can be loaded in the software and read from an external file. The geometry and volume of each of the 10,000 wedges simulated is calculated. The mode of failure of each wedge is identified and the factor of safety ("FoS") is then calculated. The probability of failure is calculated as the percentage of wedges with a FoS <1. A catchment design threshold of 80% has been chosen as acceptance criteria and designing the slope using the berm width required to hold 80% of the failed wedges means that the bigger wedges, accounting for 20% of the simulated wedges would not be fully retained on the 80% berm width and will spill over the berm. A probability of failure ("PoF") of 50% maximum is generally accepted for the bench design. In general, it was observed that such zones (>50% PoF) fall within the eastern section of the pit. A 5 m berm width is suitable to catch 80% of the likely failure volume for the majority of the pit; however, in the eastern section of the pit, where the probability of wedge instability exceeds 50%, a 6 m berm will be required to contain 80% of the likely failure volume.

1.6 Rockfall Analysis

Given the berm widths required to contain 80% of the likely block failures, a rockfall analysis was also undertaken to verify the suitability of such berm widths. The software Trajec3D (BasRock) was used for these analyses, although it should be remembered that conceptual rockfall analysis is a simplification of reality with the aim to investigate different possibilities. The fall of around 10 cubical blocks of 50 t, 100 t, and 500 t was analysed and the shape and weight used in the analyses were considered to be the most suitable given the known block conditions. The results indicate the rockfall risk can be considered low with the majority of cubic blocks being retained on the first or second bench below the seed point. When rough sphere blocks were assessed, the risk from rockfall increases significantly, although SRK considers a more cubic block shape more likely.

1.7 Finite Element Analysis

Finite element analysis (RS^2) was undertaken to define safety factors for the whole slope along three geotechnical cross-sections developed to intersect the highest sections of the north, south, and east slopes. Inter-ramp and overall slope angles were based on the results of the kinematic assessment. A number of different models were assessed ranging from isotropic homogenous material forming the pit slopes to a joint network model to assess for large scale flexural toppling. Piezometric surfaces were added to the model to simulate groundwater conditions and in all models analysed, acceptable FoS in excess of 3 were returned. Given the very high safety factors, it was not considered necessary to run probabilistic analysis.

1.8 Proposed Slope Geometry

Given the very limited presence of overburden and the fact that fresh rock conditions are observed at surface, SRK has only developed geotechnical design criteria for what can be considered fresh rock slopes.

Based on the structural conditions, kinematic analysis and slope stability modelling SRK has identified two separate design domains (Domain 1 and Domain 2) which are differentiated as function of required berm width (Figure ES 5). Analyses show that the maximum overall slope angles for the fresh rock is constrained by the bench and berm geometry, designed to minimise kinematic instability and trap potential rock fall. It should be noted that the maximum inter-ramp stack height should be 90 m, although a flexible approach to stack height may be required to ensure practical design. If no ramp is planned within the engineered pit slope design, a 17 m geotechnical berm should be constructed at the base of the stack. If a haul ramp is located at the toe of the 90 m stack, SRK recommends that a wider 10 m berm is designed within the stack to protect the ramp from rockfall. The other alternative would be to design wider ramps that can accommodate a rock fall containment trap and catch bund.

Analyses show that steep slope angles can technically be achieved; it may, however, be practically challenging to achieve the recommended inter-ramp angle and will require a strong design implementation strategy. Rock fall analysis results were based on clean berms. Scaling to remove loose rock from the bench faces, followed by clean-up of loose material along the bench toe should be implemented in order to significantly reducing the rock fall hazard. To achieve the recommended berm width, it will be essential to give special attention to blasting in order to minimise crest loss and formation of hard toe. Pre-splitting or good quality limit blasting on the slope face is therefore recommended. In order to maximise berm retention, all berms must be kept clean and free of loose blocks.

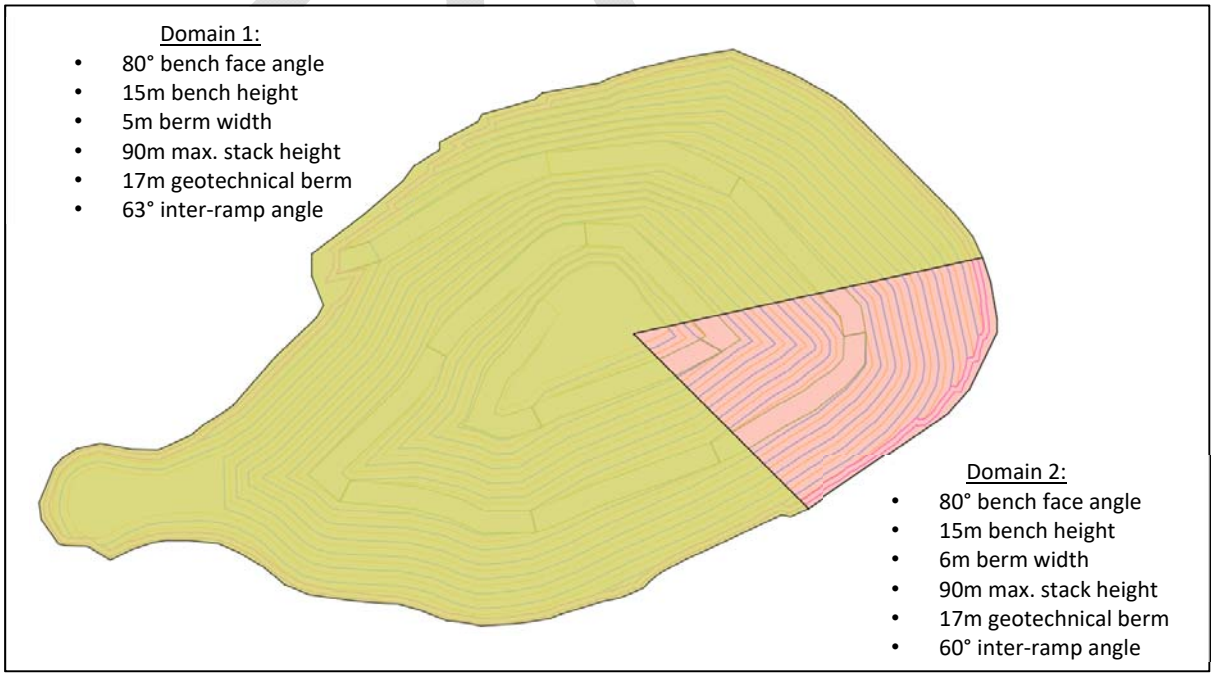

Figure ES 5: Geotechnical design domains

1.9 Underground Infrastructure

A high-level assessment of the geotechnical conditions in the region of the planned underground infrastructure, namely the crusher station and silos has been undertaken. Borehole ENG18_10 intersected the infrastructure area in close proximity and rock mass and structural conditions assessed.

No clear signs of poor ground were noted within Borehole ENG18_10 in the region of the infrastructure although the area is characterised by a number of strong joint sets which will have the potential to form unstable blocks given the likely dimensions of the infrastructure. The modelled fault that dips moderately to the north may intersect the proposed silo region, although core photographs and geotechnical logging indicates a narrow zone of poor ground. The fault may act as a conduit for groundwater flow.

Finite element modelling of the interaction between the proposed infrastructure and the pit slope returns a Strength Reduction Factor ("SRF") in excess of 3.5. Build-up of strain can be observed between the excavations although tangible displacement is not evident. The two-dimensional modelling assumed infinite out of plane geometry, which in this case assumes infinite excavation geometry. In reality, the underground infrastructure will be limited in span and should be modelled in three dimensions when the proposed location is defined.

1.10 Conclusions and Recommendations

SRK has completed a feasibility level geotechnical investigation, analysis, and development of slope design criteria that substantiates the previous pre-feasibility geotechnical work completed on the Engebø project. Analysis of drill core and development of rock mass characteristics indicates a very competent rock mass for all lithologies that will be present within the final pit wall. Furthermore, finite element analysis of the whole slope stability returns high safety factor values in relation to failure through the rock mass and, as such, any significant instability within the proposed pit walls is likely to be controlled by in situ structure.

Due to the likely controlling role of in situ structure within slope design and subsequent performance, SRK has developed a 3D geological and structural model to define the location and geometry major contacts/structures. In addition, downhole televiewer surveys of geotechnical and a number of pre-existing boreholes have provided a high-quality dataset defining pervasive discontinuities. Interpretation of data indicates few major fault intersections while structural data from boreholes indicates similar discontinuity patterns throughout the pit. As a result of the geotechnical investigations, interpretation and subsequent stability and kinematic analysis, SRK has recommended inter-ramp angles of between 60° and 63°. Whilst SRK considers such inter-ramp angles achievable given the existing dataset, high quality final slope blasting practices, state of the art slope monitoring and a rigorous Ground Control Management Plan will need to be implemented to provide the best opportunity to safely achieve such angles. In addition, a constant geotechnical mapping programme, interpretation, updated analysis and if required modifications to interim and final slope design will be required when mining commences.

Table of Contents

List of Tables

List of Figures

List of Technical Appendices

SRK Consulting (UK) Limited
5th Floor Churchill House
17 Churchill Way
City and County of Cardiff
CF10 2HH, Wales
United Kingdom
E-mail: enquiries@srk.co.uk
URL: www.srk.co.uk
Tel: + 44 (0) 2920 348 150
Fax: + 44 (0) 2920 348 199

ENGEBØ OPEN PIT FEASBILITY STUDY - MINING GEOTECHNICS

1 INTRODUCTION AND SCOPE OF WORK

SRK Consulting (UK) Limited ("SRK") is an associate company of the international group holding company, SRK Consulting (Global) Limited (the "SRK Group"). SRK has been requested by Nordic Mining ASA ("NM", hereinafter also referred to as the "Company" or the "Client") to undertake an open pit geotechnical study in support of the Feasibility Study (the "FS") for the Engebøfjellet Rutile Project ("Engebø" or the "Project") located in Norway.

1.1 Background

The Engebø rutile project is located in the municipality of Naustdal, Sogn og Fjordane in Norway (Figure 1-1) and lies roughly 125 km North of Bergen and 2.5 km east of the town of Vevring. (UTM: 309 762 mE, 6 822 838 mN). The project is wholly owned by Nordic Mining AS. The deposit was first identified in the 1970s during the construction of a road tunnel, which is currently active. DuPont/Conoco acquired the rights to the deposit in the mid-1990s, and subsequently completed 15,000 m of core drilling over 49 drillholes.

In 2016, Wardell Armstrong International ("WAI") undertook a mining geotechnical Pre-Feasibility study ("PFS"); this report advances the geotechnical understanding and slope design to Feasibility level.

Figure 1-1: Project location (WAI, 2016)

1.2 Data Sources and Work Programme

1.2.1 Scope of Work

SRK's scope was to carry out field investigations designed to characterize the rock mass and structural conditions of the deposit, and to provide appropriate analysis of such data, for use in mine design studies to feasibility level. The following work program was conducted:

- geotechnical data collection;
- geotechnical model definition;
- determination of final geotechnical domains;
- definition of geotechnical input parameters per domain;
- stability and kinematic analyses;
- pit slope design and configurations; and
- input into the mining design strategy.

1.2.2 Data Sources

Pre-existing data sources included the following:

- Nordic Mining ASA. Engebøfjellet Rutile Project, Naustdal Norway, Slope Design Report. September 2016. Wardell Armstrong. (associated data was also provided).
- A number of reports and presentations related to underground development of the Engebø project prepared by SINTEF.
- Hydrogeological report, Engebøfjellet, Pre-feasibility study. February 2017. SINTEF.
- Numerous Datamine files containing topographic surveys, lithology wireframes and the drill hole database.
- Numerous reports detailing the geology of the project area in addition to student analysis to define open pit slopes.

In addition to the pre-existing data sources, the following geotechnical data collection programmes were implemented as part of the FS:

- drilling of four specific geotechnical boreholes with the aim of enhancing the dataset developed during the PFS;
- rock mass logging to define RMR[89] values;
- rownhole televiewer logging of seven boreholes to define high quality structural information;
- laboratory strength testing of core collected from the 2018 geotechnical drilling programme; and
- downhole hydrogeological testing to define likely inflows in to the proposed pit.

2 GEOTECHNICAL DATA COLLECTION

2.1 Geotechnical Drilling

SRK developed a geotechnical drilling programme with the aim of verifying and enhancing the geotechnical data collected as part of the PFS. Within the PFS, the importance of structure on pit slope design has been identified and, as such, SRK proposed that all new geotechnical boreholes were subject to downhole televiewer logging, in addition to selecting five boreholes from the 2016 drilling programme to be televiewer logged (note that due to communication issues, only three of the five 2016 boreholes were subject to televiewer logging). Where possible, in order to remove any potential bias due to the borehole orientation when defining structural domains and influential small scale joint sets, the geotechnical drilling programme was designed to intersect the preliminary pit walls at different azimuths.

Drilling was supervised by NM staff and was close to completion when SRK attended site to commence the rock mass and structural logging. Table 2-1 presents a summary of the 2016 and 2018 boreholes used within the FS. Figure 2-1 and Figure 2-2 show the location of the geotechnical boreholes.

Table 2-1: Geotechnical drilling programme summary

Hole ID	X Collar	Y collar	Z Collar	Length (m)	Azimuth (°)	Dip (°)	Ori Type
ENG18_01	310305	6822928	308	175	010	70	ATV
ENG18_02	310166	6822840	296	200	315	75	ATV
ENG18_03	310233	6822786	299	185	180	75	ATV
ENG18_10	310401	6822846	309	270	072	85	ATV
ENG16_06	310189	6822917	293	196	009	83	ATV
ENG16_20	310299	6822798	302	150	180	62	ATV
ENG16_21	310358	6822903	312	230	178	62	ATV
ENG16_23	310066	6822797	285	150	190	69	Manual

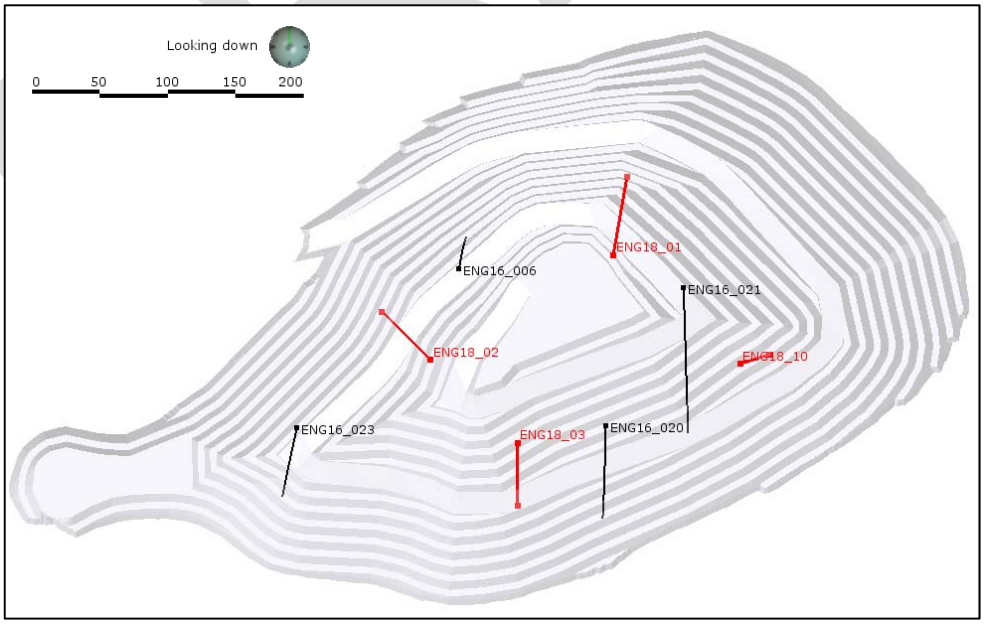

Figure 2-1: 2018 Geotechnical boreholes (red: new boreholes, black: 2016 boreholes subject to televiewer logging)

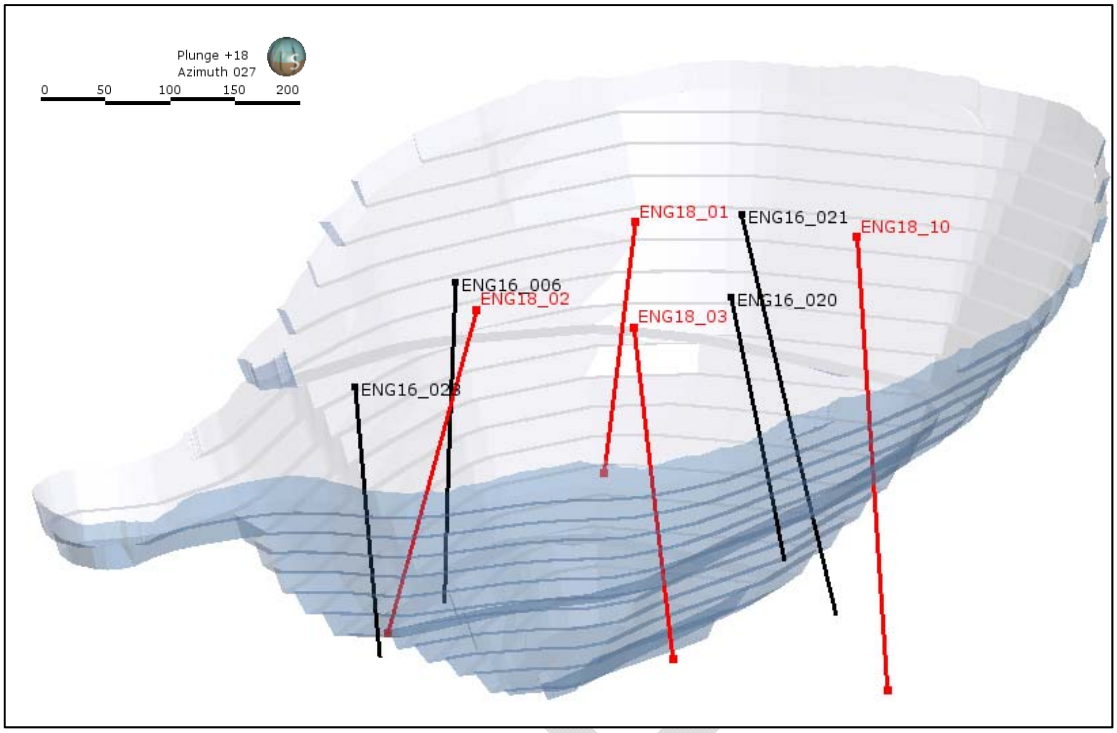

Figure 2-2: Oblique view of borehole locations. Note boreholes are placed on an interim pit shell

2.2 Geotechnical Rock Mass Logging

A Senior SRK Geotechnical Engineer undertook all geotechnical logging.

SRK used Bieniawski's Rock Mass Rating (RMR^{89}) system for rock mass characterisation. During logging, borehole core is divided into contiguous intervals of rock which exhibits similar rock mass characteristics. The rock within each zone or interval will be expected to behave similarly when exposed within the walls of the open pit excavation. The parameters that will influence the stability of each geotechnical zone are:

- thickness of geotechnical zone;
- Rock Quality Designation (RQD);
- quantity of matrix/rock mass defects; such as, faults, shear zones, intense fracturing and zones of deformable material;
- quantity of solid core recovered or observed;
- intact rock strength/hardness (IRS);
- degree and nature of rock weathering;
- spacing between the apparent sets of structures and true spacing (Js);
- total number/density/frequency of structures (FF);
- condition of structures, such as roughness profile, wall alteration and infilling (Jc); and
- ground water conditions.

These parameters are then assessed in accordance with the Bieniawski RMR system (RMR^{89}) and are allocated ratings within the following ranges:

- IRS (Intact Rock Strength) 0 – 15
- RQD 0 – 20

- Js (Joint Spacing) 0 – 20
- Jc (Joint Condition) 0 – 30
- Groundwater conditions 0 – 15

For the slope stability modelling (see Section 9) only, the unadjusted RMR values were used as input parameters. These inputs were then adjusted within the modelling software package for disturbance from production blasting and stress relief due to waste rock removal.

The geotechnical rock mass logging results are presented in Appendix A

2.3 Detailed Structural Logging

Televiewer wireline logging in all geotechnical boreholes was carried out by specialist contractor GeoVista. Using the processed televiewer logs, the interpretation and identification of any natural, open or weakly cemented structures, such as joints or faults, was carried out by comparing the image logs against the drill core. Fractures in the core were logged as open, natural joints if these were also found in the televiewer log. This method ensured that only natural discontinuities are logged and any artificial mechanical breaks caused by the drilling and handling of core are omitted. This approach allows for accurate structural logging with televiewer data substantiated with observations within the drill core. Interpreted televiewer logs are presented in Appendix B.

In addition to the development of dip and dip direction from each structure, roughness, infill, aperture and joint wall strength were defined for each natural structure.

2.4 Geotechnical Laboratory Testing

To accurately determine the strength characteristics of the material forming the proposed pit slopes at Engebø, SRK developed a detailed geotechnical laboratory testing program with tests aimed at defining the following information:

- Uniaxial Compressive Strength Testing (UCS), 30 tests;
- Young's Modulus, 15 tests;
- Poisson's Ratio, 15 tests;
- Natural Joint Shear Strength (NJS), 23 tests; and
- Triaxial Test, 10 tests.

All testing was undertaken at Geolabs, Watford, United Kingdom. Given the consistent nature of the rock mass and lithologies present within the proposed pit slopes, SRK considers the testing programme outlined above to be suitable to define the intact rock strength and shear strength of the major discontinuities.

The results of the testing are presented in Section 6 and the full results transcript from the laboratory presented in Appendix C. Testing was undertaken from samples collected from all geotechnical boreholes.

In addition to the laboratory testing programme, over 500 point load tests were undertaken during the geotechnical logging to ensure a suitable calibration between the laboratory generated UCS values and point load testing.

The results of the laboratory testing are presented in Appendix C.

3 GEOLOGICAL SETTING

In-depth descriptions of the geological setting and deformation history of Engebøfjellet have been written by Korneliussen et al. (1998), who conducted structural, geochemical, and mineralogical studies under the auspices of the Norge Geologiska Undersøkelse ("NGU"), the geological survey of Norway. This report has been relied upon for the background geological framework discussed below. The reader is referred to this report and the numerous references provided therein for a more detailed account.

Engebøfjellet is a small mountain (312 m above sea level) on the northern edge of the Førdefjord, near the village of Vevring, western Norway (Figure 3-1). Geologically, it comprises of rocks belonging to the Hegreneset complex of the Western Gneiss Region: a highly deformed assemblage of Paleoproterozoic basement amphibolites, eclogites and metagabbroic rocks, together with tonalite-diorite composition gneisses.

In western Norway, approximately 425-400 Ma, the rocks of the Hegreneset complex were subject to intense deformation and metamorphism associated with the Caledonian orogeny, a orogenic event spanning northwestern Europe (Sweden, Norway, Greenland, Scotland and Ireland) and the eastern part North America (the Appalachian mountains). Collision of the Laurentia and Baltica continents caused the rocks to be subjected to very high pressure metamorphism, reaching eclogite facies, prior to later amphibolite facies conditions.

The rocks comprising the Engebø deposit belong to a lens of highly-deformed Fe- and Ti-rich eclogite which is believed to result from the metamorphism of a Ti-enriched gabbroic intrusion. The eclogite lens is one of a series of pods of eclogite within the Western Gneiss Region, surrounded by both felsic and mafic rocks of the Hegreneset complex. Metamorphic reactions under eclogite facies metamorphism resulted in the growth of omphacite (augite-jadeite solid solution series) and pyrope (Mg-bearing) garnet; the characteristic minerals of eclogite metamorphism. Additionally, the resultant metamorphism of ilmenite in the gabbroic protolith to rutile is responsible for principal ore mineral.

The full geological and structural geology report is presented in Appendix D.

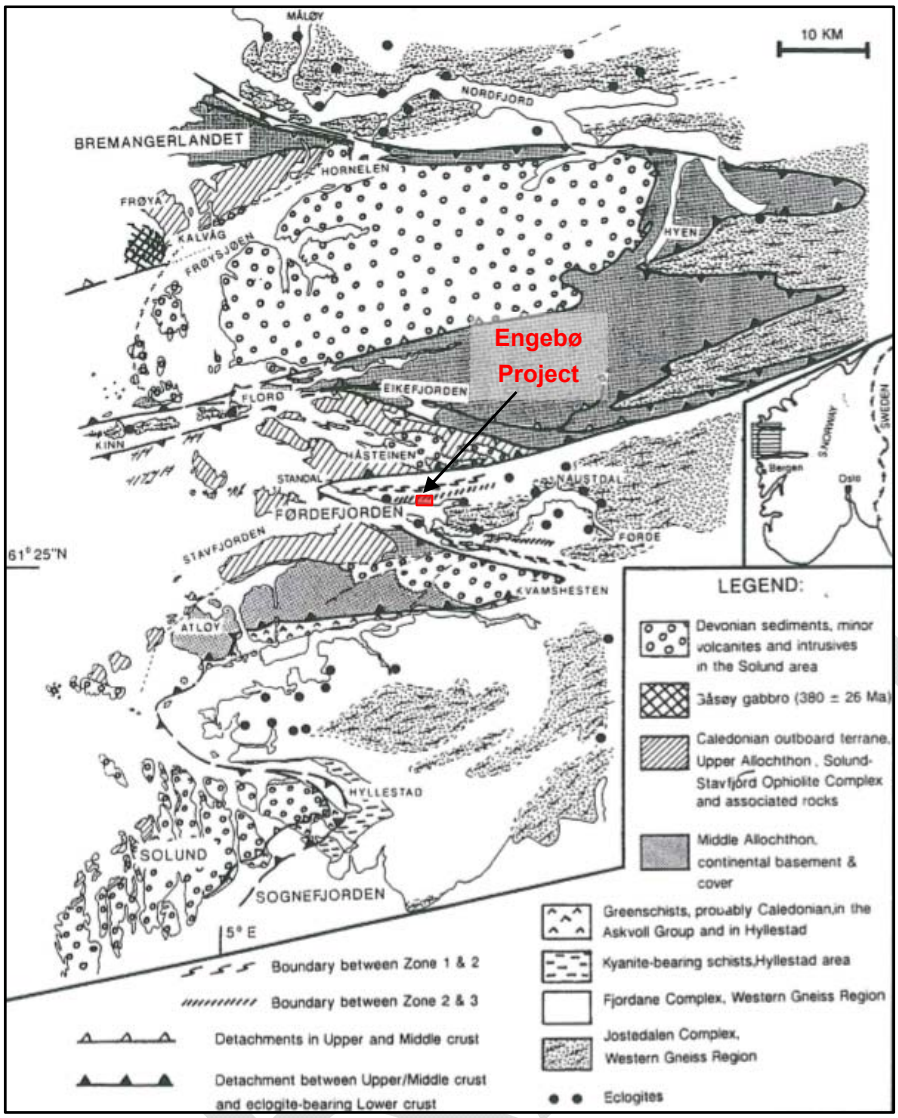

Figure 3-1: Geological map of Sognefjorden to Nordfjord showing the location of the Engebø Project (Andersen & Jamtveit 1990; referenced in Korneliussen et al. 1998)

3.1 Lithologies of the Engebø Project

Lithologies of the Engebøfjellet have been sub-divided by Korneliussen et al. (1998) into eclogitic and non-eclogitic rocks. These classifications have been retained by Nordic Rutile during the exploration of the Engebø deposit.

3.1.1 Eclogites

Three principal types of eclogite have been distinguished based on their iron oxide, titanium oxide, and garnet contents:

- ferro eclogite: >14% Fe_2O_3; >3% TiO_2 and >25% garnet
- transitional eclogite: <14% Fe_2O_3; <3% TiO_2
- leuco eclogite: 6-14% Fe_2O_3; <1.5% TiO_2 (data in Korneliussen et al. 1998)

Images of the three lithologies are shown in Figure 3-2. The transition between these lithologies are geochemically gradational, but are generally distinguished in the field by the content of pink garnets and leucocratic or melanocratic minerals.

Generally speaking, trans and ferro eclogite may be compositionally banded on the decimetre-scale, but do not tend to possess a strong grain shape foliation (schistosity or lineation). This observation is consistent with Korneliussen et al. (1998), who interpreted the omphacite in the eclogite to result from a post-deformation growth during a static metamorphic event (Figure 3-2). Omphacite is interpreted to have overgrown the banding, therefore the trans and ferro eclogites are not fissile; in fact, they are relatively massive in nature.

Leuco eclogite is generally more highly foliated than the ferro and trans varieties, with a moderate-intense schistosity, accompanied by a well-developed mineral stretching lineation in coarser domains. Significantly, from a geotechnical perspective, this lithology has a moderate fissility and, furthermore, tends to be associated with narrow intercalations of highly sheared, very fissile, quartz-mica-garnet schists, which are less competent than the eclogite.

3.1.2 Amphibolite

Amphibolite occurs in the footwall of the eclogites on the southern side of the planned open pit. The lithology is dark green to green grey, comprising medium to coarse grained amphibole. At Engebøfjellet, the lithology occurs in relatively short intervals that are interdigitated (folded and sheared) with the eclogite lithologies and gneiss. The rock is deformed and usually contains a moderately to strongly developed schistosity, together with significant compositional banding defined by subordinate mm-scale leucocratic bands (white mica and quartz) within the more mafic matrix. The rocks are coherent and, although strongly foliated, they do not possess a strong fissility.

The contact relationships between the amphibolite and other units appear to relate to an increase in the deformation fabric, suggesting that the amphibolite (like the leuco eclogite) may form shear zone boundaries around the ferro/trans eclogite.

From a geotechnical perspective, the presence of a stronger shear fabric as well as significant intercalations of quartz-mica-garnet schist in the amphibolite suggests it may have an anisotropic weakness parallel to the shear fabric.

Figure 3-2: **Examples of major lithology type: (a) ferro eclogite (ENG16_012 at 115.9 m); (b) Transitional eclogite (ENG16_012 at 79.7 m); (c) Folded Leuco eclogite (ENG16_012 at 118.4 m); (d) QMGS contact with ferro eclogite (ENG16_023 at 49.3 m)**

3.1.3 Quartz-Mica-Garnet Schist (QMGS)

Within the eclogite units, particularly the leuco eclogite, numerous narrow intervals of white-cream-coloured rock with a mineralogy dominated by quartz and mica (phengite), with variable amounts of garnet occurs. It is referred to as quartz-mica-garnet schist ("QMGS"), but may have been logged as gneiss intervals by NM. The rock possesses a moderate to intense planar schistose fabric, which is not evident, or at least is strongly subdued in the ferro and trans eclogite host rocks, but which may be present in the leuco eclogite.

Zones of QMGS are typically 2-40 cm in thickness and appear as veins or breccia veins. These zones have been strongly attenuated, consistent with the presence of an intense fabric, and indicative of a low relative competency under metamorphic conditions. That is, the QMGS appears to have accommodated localised shearing preferentially over the host rocks.

3.1.4 Granite gneiss

Outside of the planned open pit area, granitic gneiss has been mapped by Korneliussen et al. (1998). The gneiss is believed to represent Proterozoic granite and tonalite intrusives of the Helle Complex that were extensively deformed during the Caledonian orogeny.

4 LARGE-SCALE GEOMETRY OF THE ENGEBØ DEPOSIT

4.1 Constraints

SRK has undertaken a review of structural information within the project area with the aim of developing a structural model to inform the mining geotechnical aspect of the proposed pit slopes.

The principal constraints on the large-scale geometry of the Engebø deposit area are:

- Vevring tunnel: a road tunnel located at a distance of between150 m and 500 m west of the planned open pit, which runs for 630 m in a WNW orientation through the western part of Engebøfjellet. The solid geology of the tunnel was mapped by SRK over a period of 2½ days.
- NGU surface maps (Korneliussen et al. 1998): these have not been ground-truthed by SRK due to snow cover. The maps may be somewhat limited on the southern side of Engebøfjellet due to difficulty of access along the sub-vertically sloping topography.
- Drillholes: historical drillholes, as well as NM's diamond drillholes from 2016 and 2018. Several geotechnical diamond holes are oriented or have televiewer data available, which permit some geometrical constraints to be placed on the subsurface.

4.2 NGU Geological Map

The surface map of Engebøfjellet by the NGU (Korneliussen et al. 1998) is shown in Figure 4-1. The map shows the Engebø eclogitic rocks form a partially-sigmoidal, elongate lens-shaped body, extending E-W for approximately 2.5 km and 0.5 km in width.

Mafic-composition ferro and trans eclogite units form the central part of the lens. These are flanked to the north by leuco eclogite, which is interpreted by Korneliussen et al. (1998) as a lecugabbroic protolith. The eclogites are bound to the north and south by amphibolites and other undifferentiated rocks, referred to here as "amphibolite group".

One of the principal geometrical features indicated in the outcrop pattern are a series of interfingering lobes of eclogite and amphibolite group rocks which are interpreted to result from folding of the contacts. The most likely generation of folding to have caused this geometry, by comparison with field data of Korneliussen et al. (1998), is F_2; however, this needs to be confirmed by field mapping. Many of these lobes have wavelengths at or below the drill spacing and are therefore are not well-defined by the current drillhole data; however, a significant fold defined by a west-facing fold closure in the ferro eclogite (Figure 4-1) occupies the area to the west of the planned open pit area.

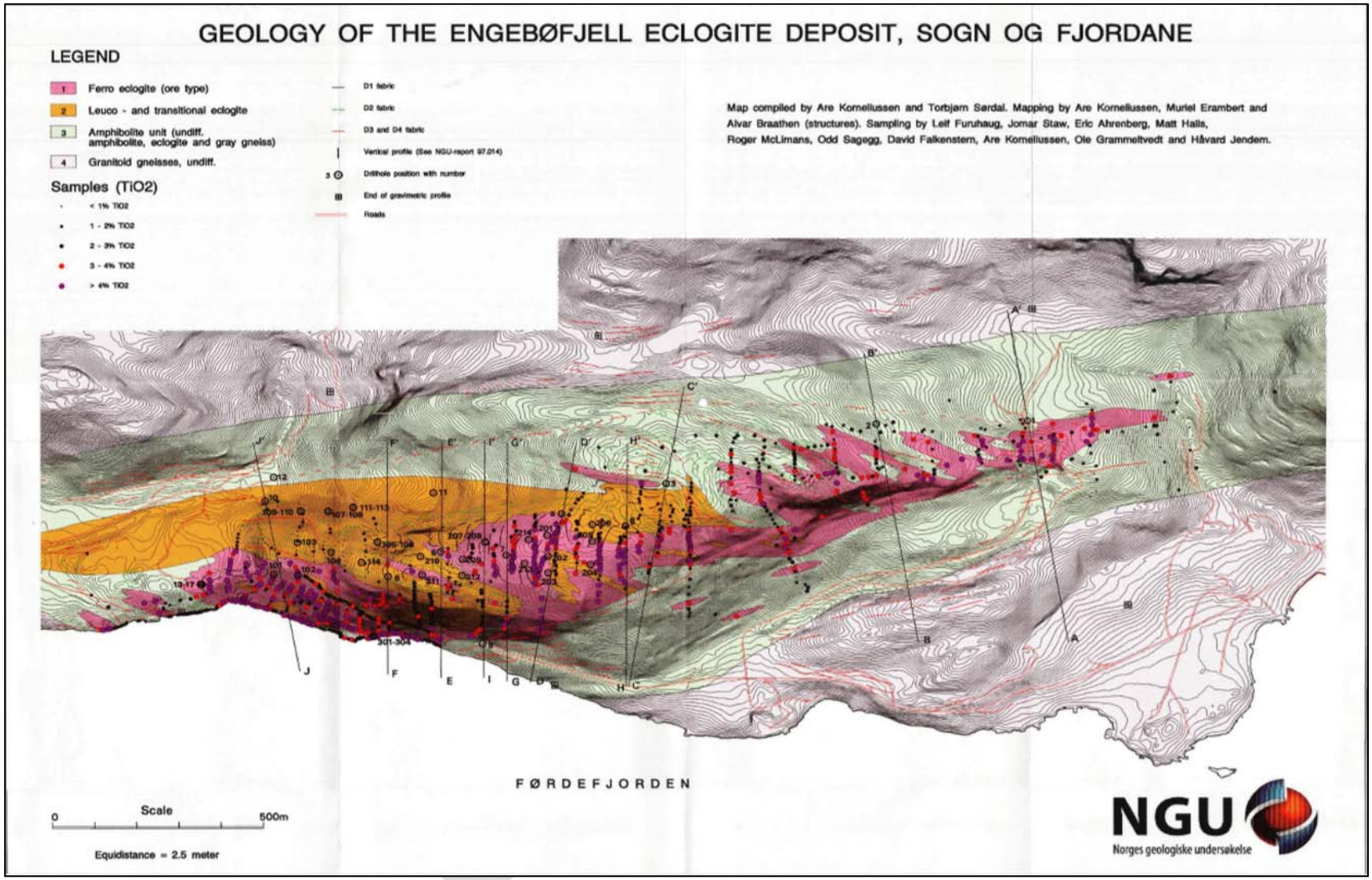

Figure 4-1: Geological map of Engebøfjell (NGU) showing the position of the Vevring Tunnel

4.3 Vevring Tunnel Geology

The Vevring tunnel provides uninterrupted geological outcrop for 630 m, broadly along strike from the Engebø planned open pit area. Fieldwork enabled the structural features recognised in the drill core from Engebø to be placed in greater geological context.

4.3.1 Tunnel domains.

The geology in the tunnel is shown in Figure 4-2 and can be divided into the following domains, from WNW-ESE:

1. Highly foliated leuco eclogite containing sheared QMG veins.
2. Gradational contact into weakly deformed leuco eclogite cut by QMG veins.
3. High strain shear zone in leuco eclogite with increasing content of QMG, which forms a major contact.
4. Minor zone of trans eclogite, banded, but not strongly deformed.
5. Banded ferro eclogite with complex isoclinal folds plunging steeply in roof and banding sub-parallel to the tunnel walls. QMG is restricted to veinlets and fold hinge areas.
6. QMG vein network (stockwork-like) within moderately sheared ferro eclogite.
7. Steeply banded ferro eclogite.
8. Ferro and trans eclogite deformed by complex folding (evidence of three phases).
9. Foliated leuco eclogite containing a minor interval of amphibolite which may relate to the “alternating” lithocode of NM.

4.4 Tentative Interpretation

Tentatively it is interpreted that the Engebø eclogites, primarily ferro and trans, occur in a sliver bound by highly sheared leuco eclogite, amphibolite and gneiss to the north and south. Following the eclogite metamorphic event, the eclogites were affected by at least two folding events giving rise to the complex folding (D_2 and D_3). Evidence of similar folding in Leuco domains at the north and south of the tunnel has not been observed, suggesting the broadly E-W foliation overprinted these structures, perhaps related to stronger sinistral transgressional deformation (D_3) along the flanks of the eclogite lens.

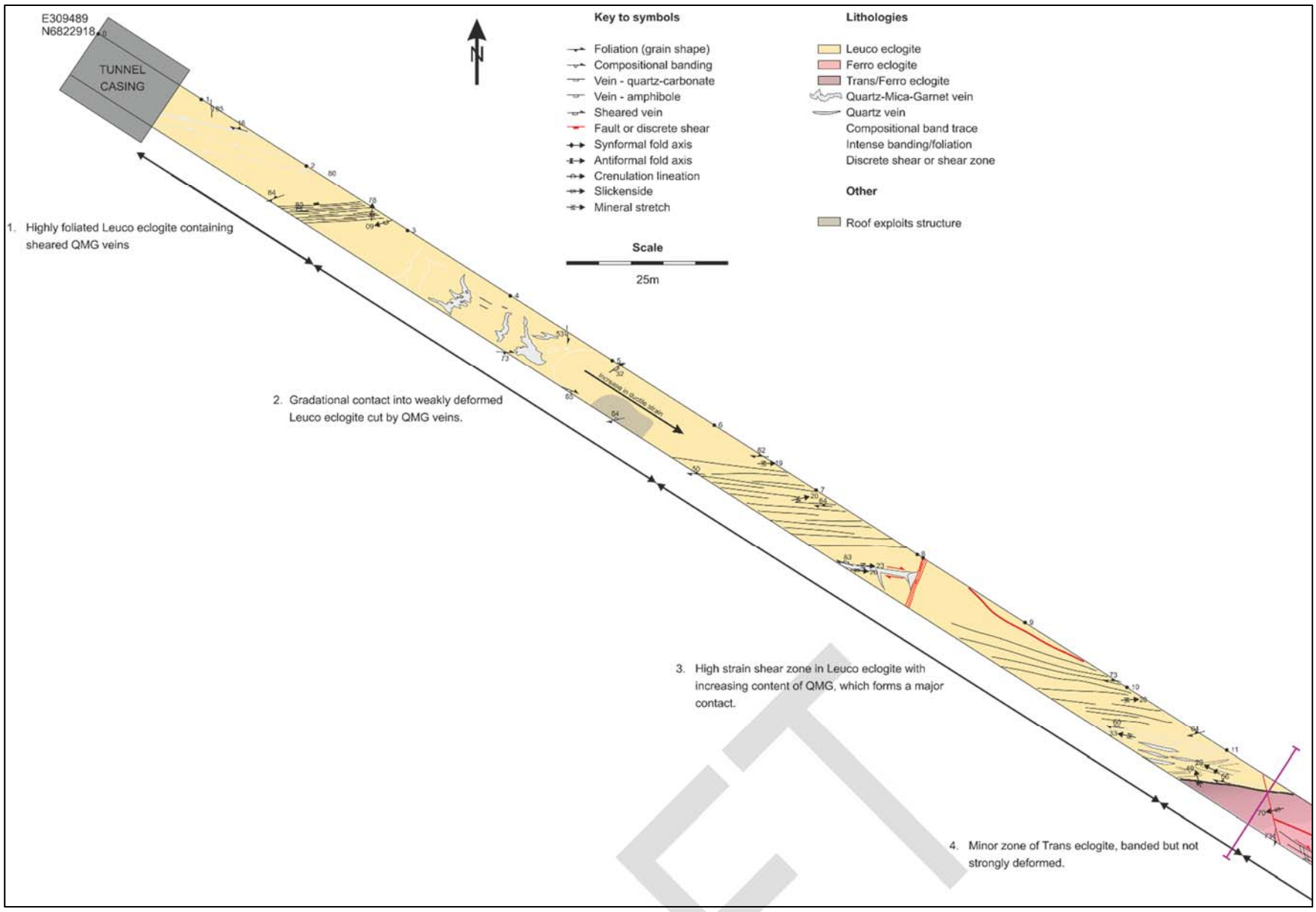
E309489
N6822918
TUNNEL
CASING
N
Key to symbols
Foliation (grain shape)
Compositional banding
Vein - quartz-carbonate
Vein - amphibole
Sheared vein
Fault or discrete shear
Synformal fold axis
Antiformal fold axis
Crenulation lineation
Slickenside
Mineral stretch
Scale
25m
Lithologies
Leuco eclogite
Ferro eclogite
Trans/Ferro eclogite
Quartz-Mica-Garnet vein
Quartz vein
Compositional band trace
Intense banding/foliation
Discrete shear or shear zone
Other
Roof exploits structure
1. Highly foliated Leuco eclogite containing sheared QMG veins
2. Gradational contact into weakly deformed Leuco eclogite cut by QMG veins.
Increase in ductile strain
3. High strain shear zone in Leuco eclogite with increasing content of QMG, which forms a major contact.
4. Minor zone of Trans eclogite, banded but not strongly deformed.

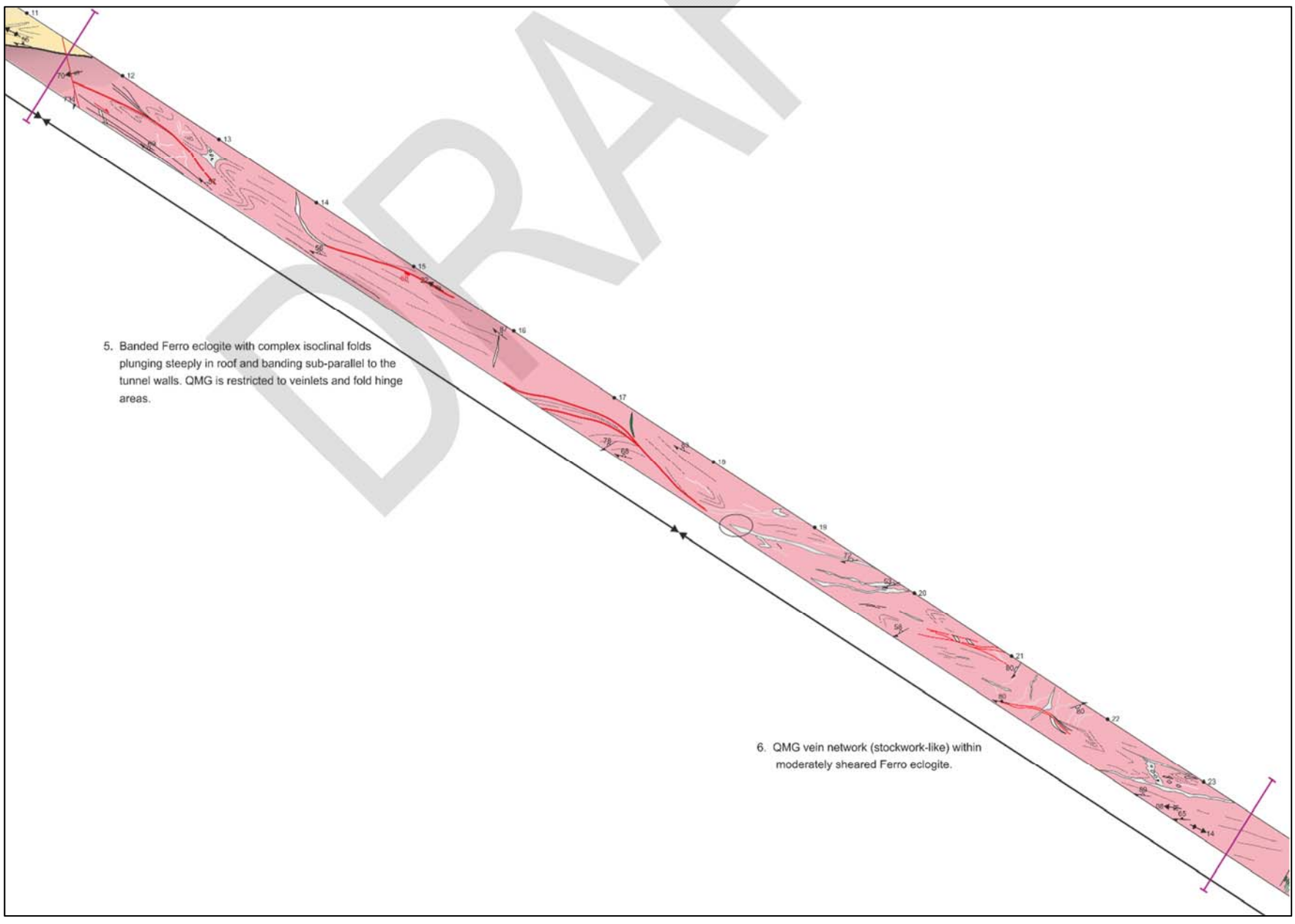
5. Banded Ferro eclogite with complex isoclinal folds plunging steeply in roof and banding sub-parallel to the tunnel walls. QMG is restricted to veinlets and fold hinge areas.
6. QMG vein network (stockwork-like) within moderately sheared Ferro eclogite.

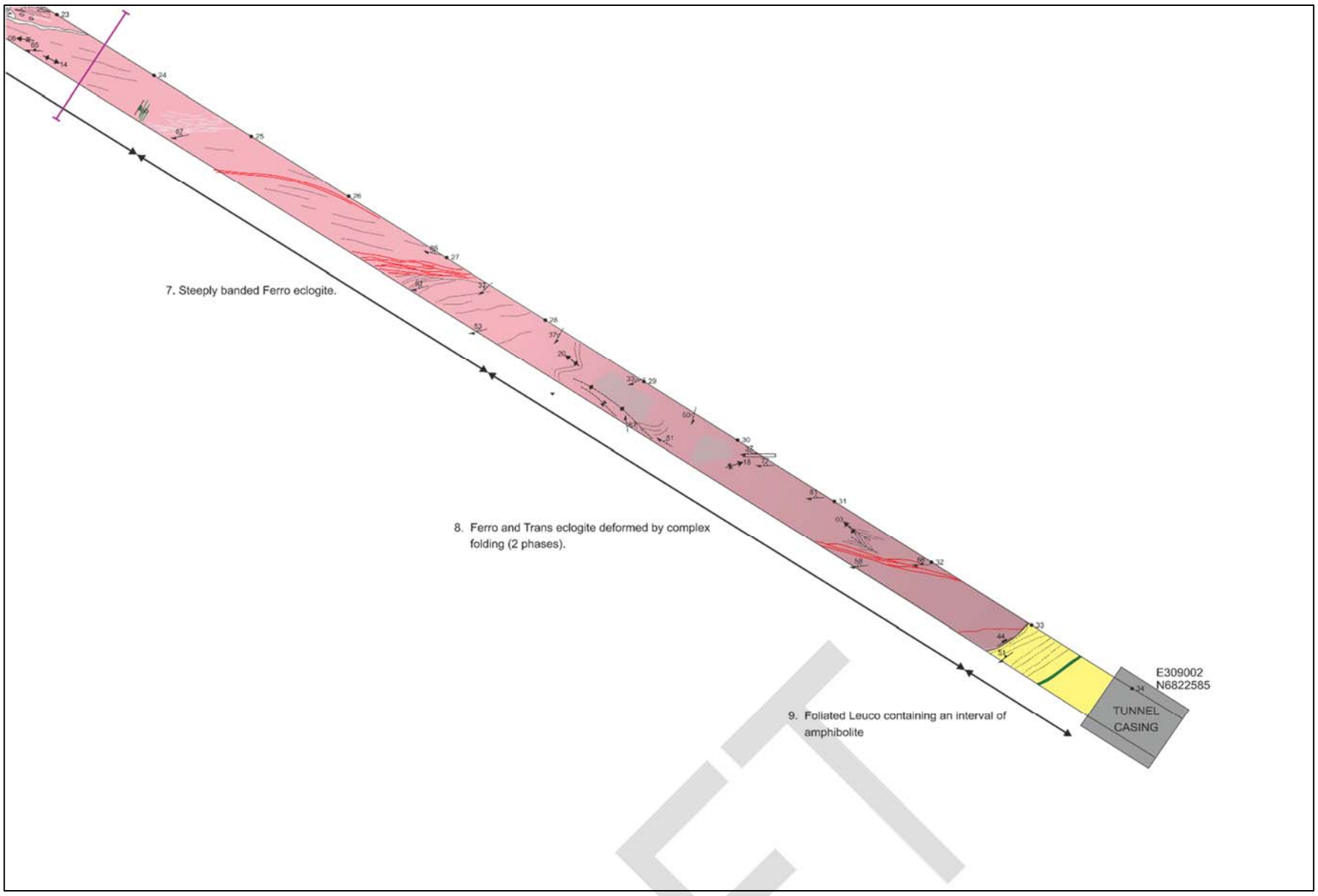

Figure 4-2: Geological map of the Vevring tunnel

4.5 Three-Dimensional Geological Model

A working 3D geological model of the major lithological units is presented in Figure 4-3. The model was developed integrating the drillhole lithological information from NM's exploration campaign and historical exploration, together the NGU surface geological map and SRK's mapping of the Vevring tunnel.

Five major units have been modelled which, from N to S, are:

- **Amphibolite and gneiss:** this unit is not well constrained by drilling. It is defined on the basis of a tentative correlation between the trace of a mapped "amphibolite" (amphibolite, grey gneiss and eclogite) contact on the surface with a zone of mixed lithologies (gneiss, amphibolite and "alternating") according to the NGU map.
- **Leuco eclogite:** a well-constrained unit that is interpreted to step to the south around a steeply plunging antiform and synform pair.
- **Trans eclogite:** the trans eclogite domain captures drillhole intervals that are mostly Trans. However, as this lithology has a gradational relationship with the ferro eclogite the contacts are not definitive.
- **Ferro eclogite:** this domain is well constrained, but contains minor intervals of trans and leuco eclogite. The occurrences of leuco eclogite are particularly associated with a unit of amphibolite in the southern part of the planned open pit area, but have not been modelled explicitly.
- **Amphibolite:** a lense of amphibolite occurs in the southern part of the pit. This is interpreted to be weakly folded parallel to the main antiform defined by the leuco eclogite, but this is not well-resolved in the current drilling data.
- **"Alternating" eclogite:** south of the pit area, a sliver of rock logged by NM as "Alternating" has been modelled. The sliver is effectively a lens-shape <70 m in thickness and modelled for 970 m along strike.
- **Other:** outside the area of the planned open pit, a volume was modelled, but is not reflective of any major lithology. Rather, it limits the area of well-constrained subsurface geology.

The lithological model is a simplification of the logged and mapped lithologies for two main reasons:

- Logged and mapped lithologies are not entirely consistent with surface traces from the NGU map.
- Minor intercalations of subordinate lithologies cannot be modelled (such as minor gneissic intervals in leuco, or minor trans intervals in ferro are not represented).

It is also noteworthy that some lithologies terminate abruptly between drillholes (for example, the eastern continuation of the amphibolite lens). It is not clear whether this is a true feature of the geology or is a result of some inconsistency in the logging.

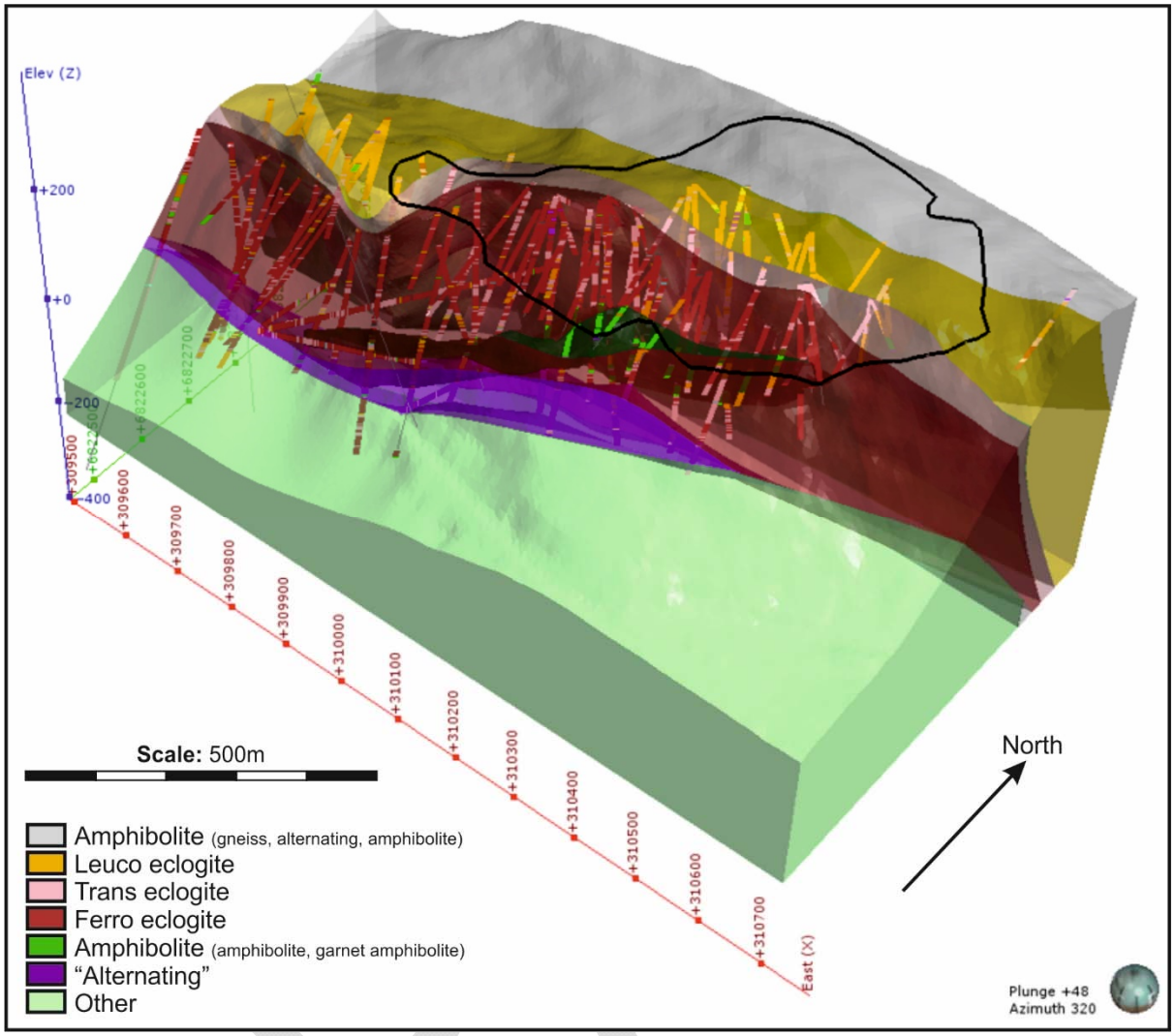

Figure 4-3: 3D lithological model of the Engebø project area relative to the trace of the optimised open pit

4.5.1 Geometry

The modelled geology of Engebøfjellet is relatively simple, consisting of generally continuous lithologies of leuco, trans and ferro eclogite, striking E-W and dipping moderately-steeply (50-80º) to the N. Contacts mapped in the tunnel correlate closely with those logged from historical and recent diamond drillhole logs, indicating reasonable geological continuity of the major units along strike; however, whereas SRK mapped leuco eclogite lithology in the SE of the tunnel, this correlates with a zone logged as "Alternating" by NM.

At the resolution of the drillhole data, the main modelled structures are an antiform-synform fold pair that has caused the belt to left-step, just west of the current planned open pit (Figure 4-3). The fold is a simple reflection of the mapped geometry from NGU map, and generally there is a broad reasonable agreement between the positions of the major contacts of the main lithologies. In the area of the fold, however, the mapped surface contacts could not always be utilised in the model without significantly complicating the interpretation due to conflicts between mapped and logged geology. Moreover, the plunges of the modelled folds are only constrained by the drillhole data and there is considerable potential for modification of the fold interpretation.

Over the area of the planned open pit, four of the geological lithologies are continuous. Only the amphibolite lithology is discontinuous, occurring as a lens-shaped sliver (Figure 4-3 - purple lens shaped zone).

4.5.2 Limitations: Resolution Effects and Drill Coverage

Geometrical complexities within the deposit range from cm-scale structures (such as Figure 3-2c) to folds with wavelengths of 230 m, according to the NGU map. Drillhole spacing in the main area of the deposit varies, but is generally <70 m; therefore, there are significant geological features that cannot be modelled directly by the data. Although most of the modelled contacts between lithological units are relatively planar in nature, these should be considered as a simplification. Indeed, some of the undulosity of the modelled surfaces may be due to only partial-resolution of folds affecting the contacts.

The northern part of the planned open pit area is not well-covered by drilling and therefore cannot be modelled with any real certainty.

There are some considerable discrepancies between the modelled geology and outcrop pattern of the NGU. In particular, an amphibolite sliver has been modelled with an overall trend of 070-250º based on drillhole data that does not tally with the mapped folded eclogites and amphibolites at surface. Further work is clearly required to test these relationships.

From a geotechnical perspective, the most significant limitation to the geological interpretation is the relatively poorly constrained geology of the hangingwall rocks on the northern side of the pit, due to relatively sparse drilling information. Additionally, the geological model has a limited extent to the east of the pit due to insufficient geological constraints.

Remapping of the surface outcrops of Engebøfjellet is planned by NM and will be important in further refining the 3D geological model. It may also be desirable to undertake some re-logging of drill core in areas where inconsistencies between surface and subsurface geology remain, and also where the lithological units terminate abruptly.

5 STRUCTURAL GEOLOGY

5.1 Shear Zones and Deformation Fabrics

The Ferro and Trans eclogite lithologies are typically massive in nature; however, subtle compositional banding highlighted by garnet-rich and -poor zones is evident within the rocks (Figure 3-2a). The compositional banding is not reflected in a grain shape fabric, suggesting the omphacite and garnet crystallised or re-crystallised following an earlier deformation, consistent with the observations of Korneliussen et al. (1998). Banding of the ferro and trans eclogite of the Vevring tunnel was strongly affected by folding and also rotated by shears.

Deformation fabrics within the eclogite are most obvious where the host rock is brecciated by quartz-mica(phengite)-garnet (QMG) vein networks, described in Section 5.2

In the Vevring tunnel, foliation intensity is more pronounced in the leuco eclogite lithology in the west-northwest and east-southeast, relative to the trans and ferro eclogite. In the Leuco domains, the weak- to moderately-developed schistosity dips moderately-steeply towards the north, striking broadly E-W. A high strain ductile shear zone, approximately 5m wide, comprises the southern contact of the northern Leuco domain (Figure 4-2).

In contrast, in the Trans and Ferro eclogite zones, E-W or WNW-ESE striking shear zones are only localised and limited to zones <5 m in width. It is only in ferro and trans zones containing higher QMG content that this orientation of shear zone is prominent (Figure 4-2; between distance markers 18-23).

Extrapolating observations from the Vevring tunnel to the planned open pit area, it is anticipated that the main body of the ferro and trans eclogite zones are poorly foliated, other than in localised, metre-scale, E-W trending shear zones. The leuco eclogite, in drillholes from the pit area, is very similar to that in the Vevring tunnel: moderately-highly foliated by a schistose fabric, with frequent intercalations of deformed QMG.

The northern part of the planned open pit is located in rocks grouped as amphibolites and gneiss. From a brief review of drill core photos from this pit sector (ENG16-06, 07 and 17) it appears that the amphibolite, gneiss, “alternating” and leuco eclogite rocks within this zone are similarly highly foliated to the main leuco zone, consistent with them belonging to a wider shear zone. Similarly, in the southern pit wall, the modelled amphibolite lens (Figure 4-3) is associated with higher foliation intensity locally and minor intervals of leuco eclogite. Overall, it is interpreted that the rocks without the ferro/trans domain constitute a sheared envelope around the less deformed eclogite sliver.

5.2 Quartz-Mica-Garnet Veins and Vein Breccias

As described earlier, the QMG generally occurs as veins and breccias which have been preferentially deformed (Figure 5-1). In the northwestern part of the Vevring tunnel, these range from 2cm to 40cm in width and are arranged in a stockwork-like pattern, isolating clasts of eclogite up to several meters in diameter. The veins themselves may contain smaller clasts of host rock, apparently in equilibrium.

Many QMG veins show strong deformation fabrics defined largely by coarse (up to 3 mm) elongate white mica (phengite; Figure 5-1c). Fabrics within the veins commonly include both a strong planar schistosity and mineral stretching lineation. Deformation within these brecciated and veined areas is clearly partitioned into the gneissic veins owing to their relative lower

competency under the prevailing metamorphic conditions.

Mechanically, the QMG veins were often associated with mechanical breaks in the drill cores reviewed; the rock parting along the vein margins. In the tunnel, flat lying veins in the western third clearly control the roof geometry and appear to have acted as releasing planes for slabs to break away. Therefore, from a geotechnical perspective, the veins appear to present a mechanical weakness.

Drillhole photo-logging of the intervals in the 2016 and 2018 drilling campaigns has been undertaken to evaluate the distribution of these intervals. The results of the logging are shown in Figure 5-2 and tabulated in Table 5-1. It is evident that the QMG occurs throughout all of the logged lithologies but varies in frequency with lithology. Of the major lithologies the highest normalised downhole spacing (and by corollary the frequency) occurs in the leuco eclogite and amphibolite (including garnet amphibolite category). The frequency of QMG intervals in the leuco eclogite is approximately double that in Trans and almost four times higher than their occurrence in Ferro. Precise QMG interval thicknesses have not been measured; however, the majority of QMG veins in the Vevring tunnel are <10 cm true thickness (Figure 5-1).

Table 5-1: Occurrence of QMG intervals per lithology (2016 holes only)

Lithology	QMG Intervals logged	Total lithological interval (m)	Average downhole spacing (m)*
Leuco	265	4445.3	16.8
Trans	164	5241.8	32
Ferro	169	9733	57.6
Amphibolite (incl. Garnet Amphibolite)	30	713.2	23.8
Gneiss	11	341.9	31.1
Alternating	46	1226.3	26.7

*indicative value only as not corrected for hole orientation or attitude of QMG interval.

A stereoplot of the orientations of QMG zones from drillhole logs, ATV surveys and tunnel mapping are shown in Figure 5-3. Whilst there is some scatter, orientations tend to fall into two main groups that dip steeply SSE and NNE, which most likely signify that the majority of the veins are sheared parallel to the predominant foliation. The scatter of poles towards the centre of the stereoplot indicates that a portion of the QMG intervals are shallow-dipping, in numerous directions. Shallow dipping veins of QMG were observed in the tunnel and, in several cases, clearly acted as release-structures where slabs had detached from the roof; however, given that the majority of drillholes are steep, these should be well-sampled relative to steep structures (which would tend to be under-sampled). Therefore, their relative scarcity indicates that they are significantly less frequent than steeply-dipping foliation parallel zones. It is likely that the SSE dipping features are also over-represented in the current dataset which is derived largely from hole ENG18_01, a hole oriented to the NNE through leuco eclogite.

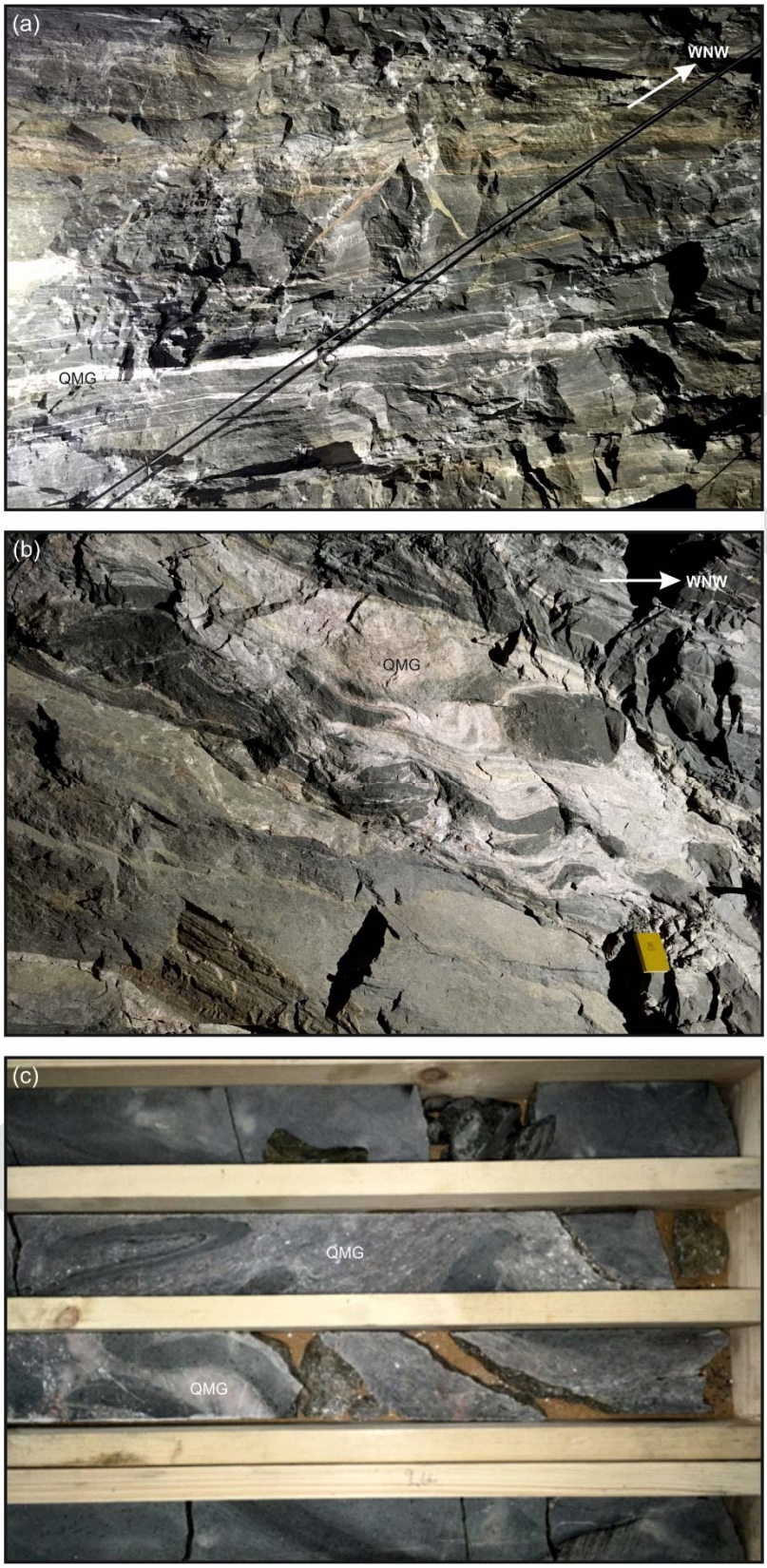

Figure 5-1: Quartz-mica-garnet intervals: (a) highly-sheared veins of QMG in sheared Leuco eclogite, Vevring tunnel; (b) ductilely-deformed QMG breccia, Vevring tunnel; (c) sheared and folded interval, similar to (b) from hole ENG16_002 at 34.4 m.

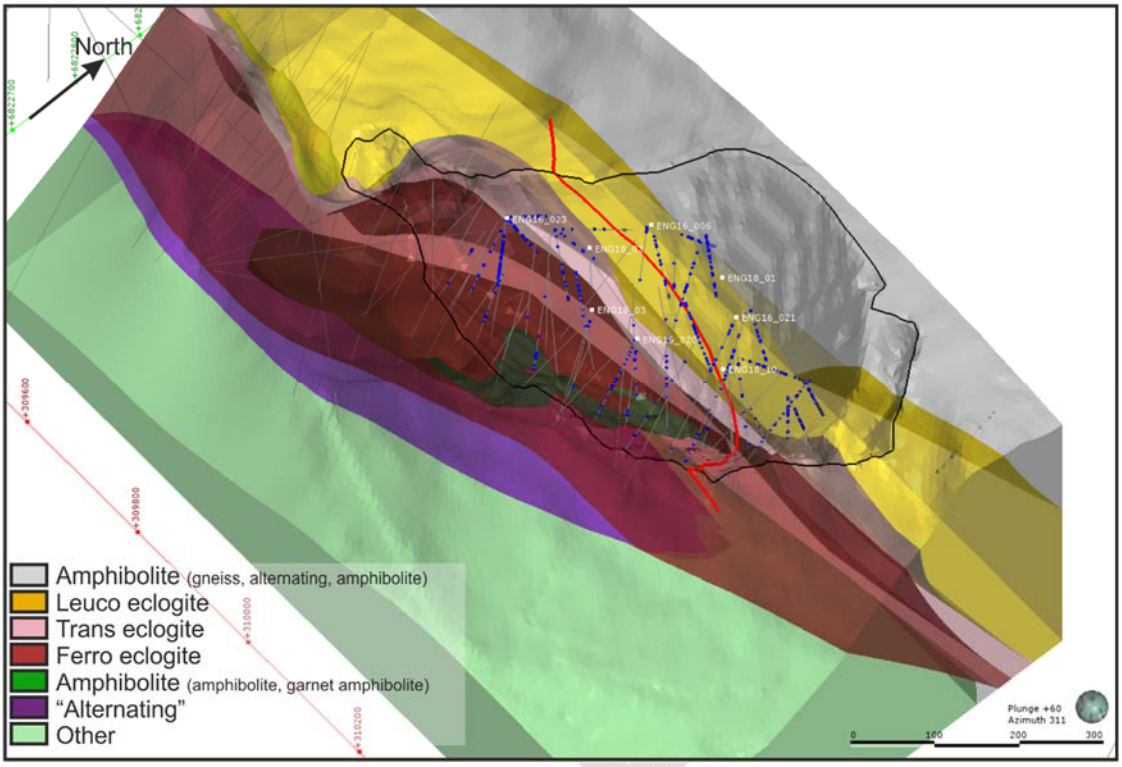

Figure 5-2: Distribution of QMG drillhole intervals relative to the planned open pits and major lithological contacts

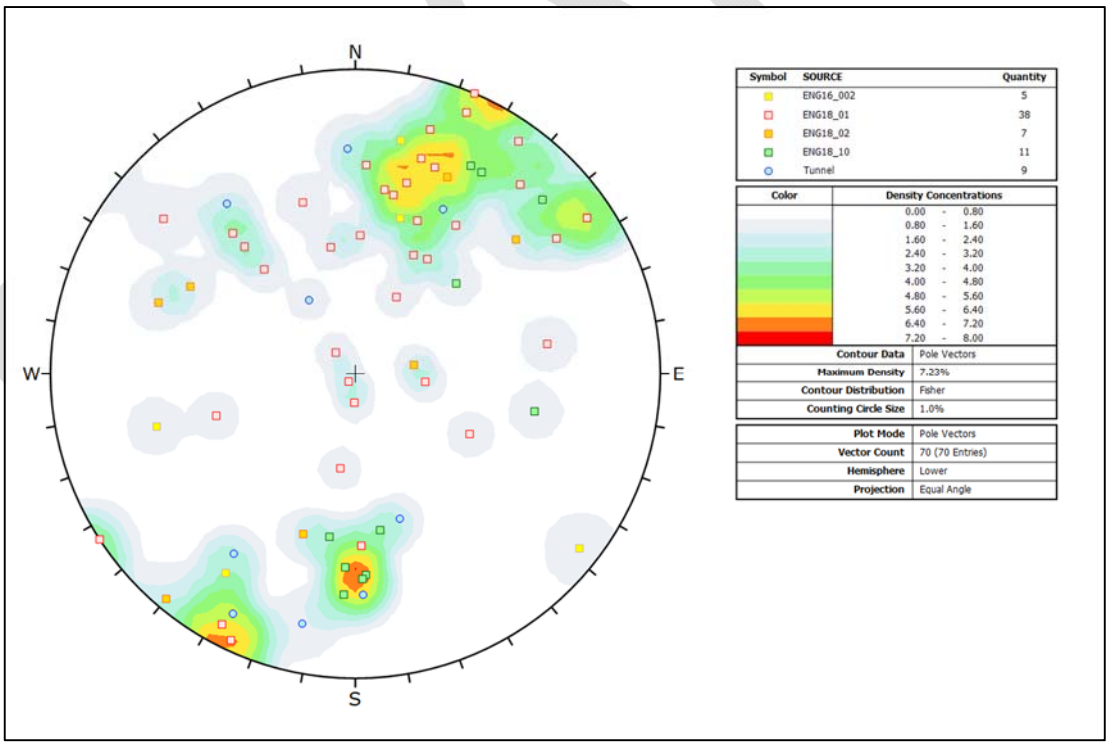

Figure 5-3: Stereoplot of QMG zones measured in drillholes and the Vevring Tunnel

5.3 Faults and Fractures

5.3.1 Shears

Within the central part of the tunnel (between markers 9-18; Figure 4-2), the roof is cut by several marked shear planes trending NW-SE. Some of these were defined by narrow brittle ductile zones comprising narrow shears containing QMG, whilst others varied from a single centimetre-wide shear zone to a sheared quartz vein (Figure 5-4). Unfortunately, most were not accessible to measure, therefore orientation data from them is scarce (Figure 5-5). Where these could be measured, they are steeply dipping and appear to have localised in zones where the fabric (compositional banding or schistosity) had already been rotated into a NW-SE orientation (by earlier folding?). These were associated with shallow-plunging quartz slickensides which, together with drag of foliation and a local quartz vein arrays indicate the shears accommodated sinistral transcurrent movement. Displacements are believed to be minor (tens of metres, or less), but appear to die-out rapidly into zones of veining or ductile deformation and are unlikely to be correlatable in drillholes.

Figure 5-4: Shears in the Vevring tunnel: (a) Narrow zone of shearing along north wall (distance marker 9) consisting of highly sheared narrow zones of QMG in leuco eclogite; (b) Sub-vertical sheared quartz vein which grades into a narrow discrete shear (distance marker 17)

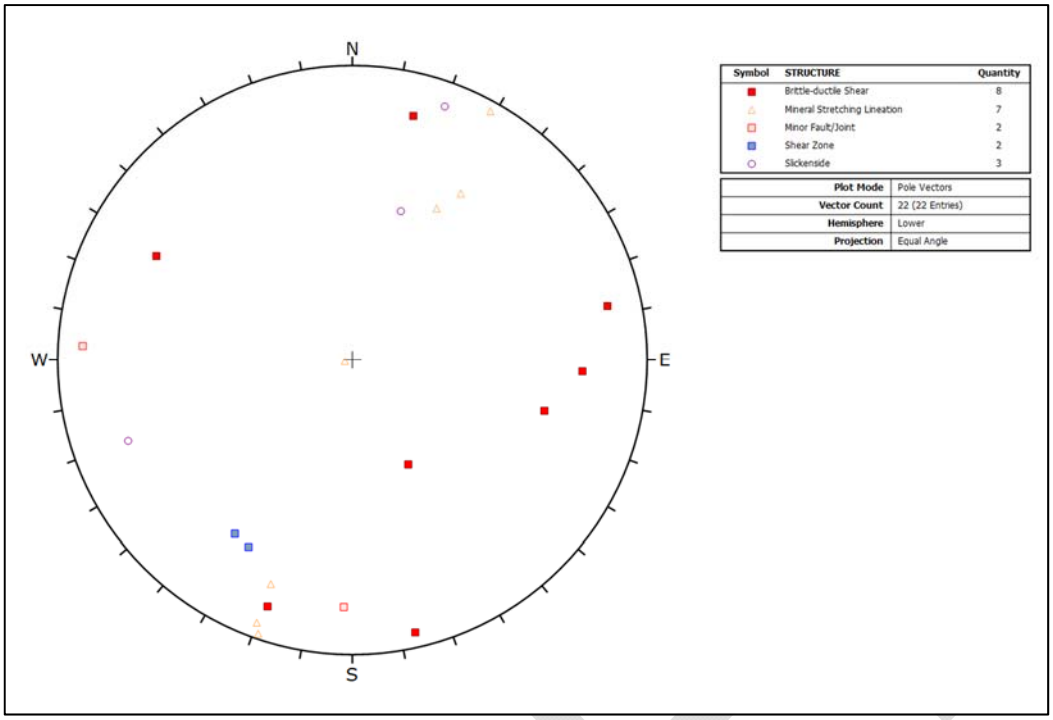

Figure 5-5: Orientations of faults, minor faults, brittle-ductile shears (planar) and slickenside and mineral stretching lineations

5.3.2 Faults

In order to better understand the faults within the Engebø Project area, drill core photographs from the entire 2016 and 2018 campaigns were logged for fractured and faulted zones. A total of 98 fractured zones were logged from the drill core photos and were classified according to their apparent significance (minor, moderate, or major), based on the degree of fracturing, presence or absence of significant quantities of fault gouge or breccia, and width of the overall deformation zone, or extensive core loss.

Minor Faults and Fractures

Nearly all (94%) of the fractured and broken zones logged in the drill core are interpreted to be minor structures based on their negligible fault rock characteristics. An empirical relationship exists between fault displacement and fault rock and fault zone thickness (Childs et al. 2009), and displacement and length (Walsh & Watterson, 1998). On the basis of these relationships, these minor fractures are not likely to be correlatable within the drillhole dataset: their lateral continuity is likely to be tens of metres, and their displacements limited to a few metres or less. Moreover, individual fracture zones have no distinguishing characteristics. A relatively typical minor fault within a core interval is shown in Figure 5-6. Minor faults at Engebø are typically comprised of fracture surfaces with negligible fault rock other than a millimetre-scale fracture cement or coating of quartz, chlorite, and carbonate. Weak striations are evident on many of these fracture surfaces, indicating they accommodated minor shear displacements.

The fractures occur at a low angle to the axes of drill cores, usually indicating that they are moderate to steeply dipping. Several drill cores have semi-continuous zones of fracturing which are interpreted to result from a single fault which trend sub-parallel to the core axis, intersecting the drillhole several times.

Figure 5-6: Minor fault typical of most broken intervals: fracture zone intersecting core at very low-angle; negligible fault rock

Moderate and Major Fault Intervals

Very few faulted and broken intervals were classified as moderate or major structures (<6% of all logged intervals. These intervals include strongly broken and fractured zones of eclogite as well as several intervals where there has been significant core loss or poor recovery (Figure 5-7).

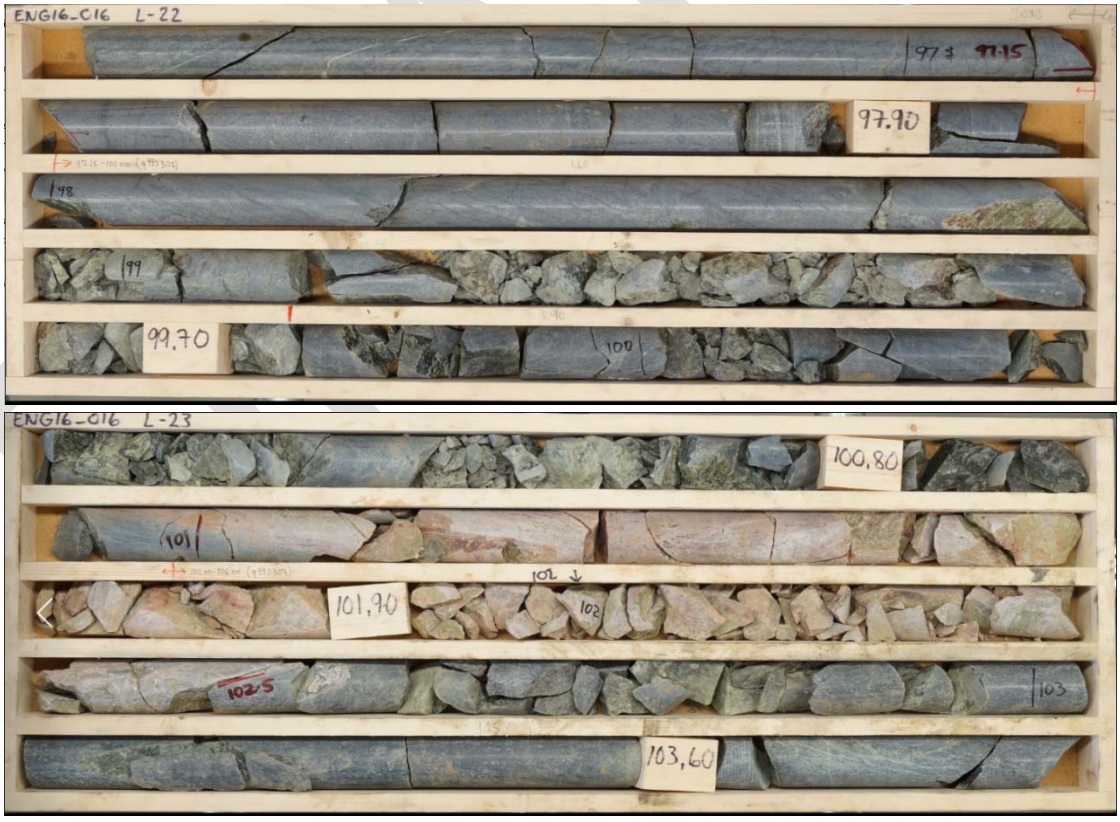

Figure 5-7: Significant fault logged in ENG16-016

When displayed in 3D, all but one of the faulted intervals classified as moderate and major fall in a planar distribution and are easily correlatable into a planar structure. The interpreted fault, shown in Figure 5-8, has an overall orientation of 53/022. The orientation of this structure is similar to some brittle-ductile shears observed within the Vevring tunnel which supports the interpretation.

Although this structure is correlatable over a distance of >350 m, the fault does not appear to accommodate any discernible displacement based on the drillhole lithological data. Overall, the structure is not interpreted to be a large displacement feature and surfaces that it intersects have not been offset in the 3D model.

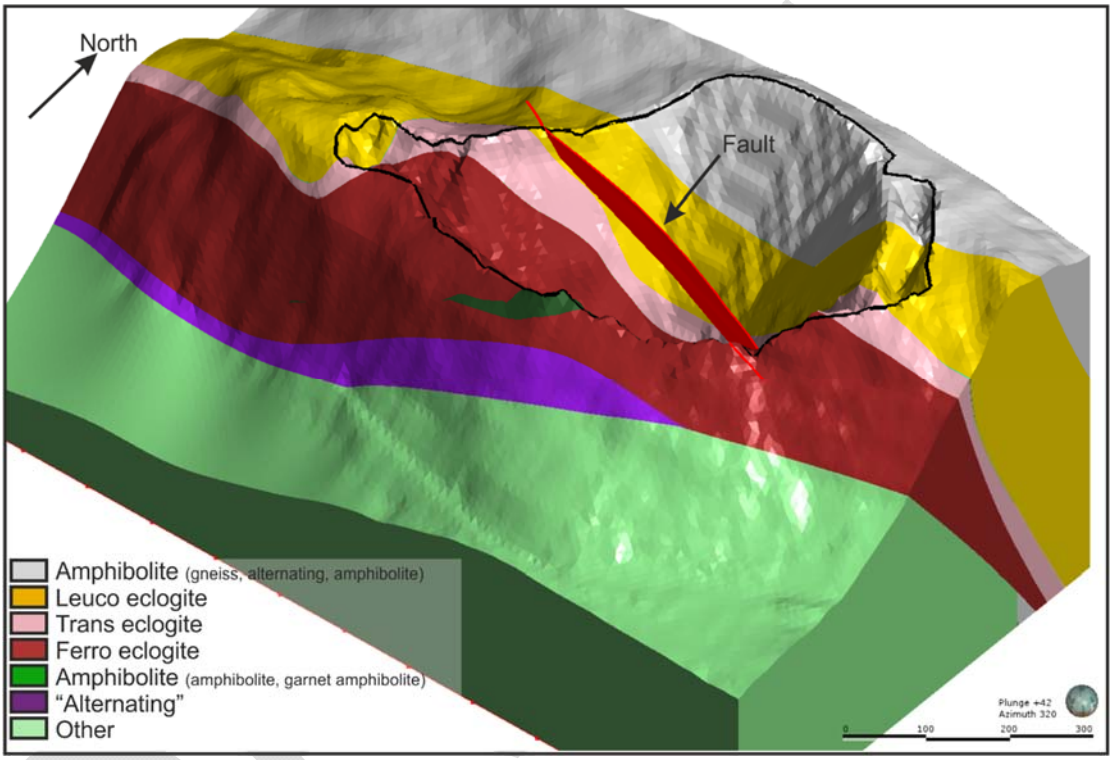

Figure 5-8: Leapfrog model of the single correlated fault from the Engebø deposit

5.3.3 Joints and Discontinuities

Stereoplots of the results of joint and fracture surveys of the drill holes and tunnel from various studies (SRK, this commission and 2016) are shown in Figure 5-9.

The stereoplots of the joint data show some variability in the populations of fractures across the planned open pit area related to drilling orientation bias; however, several distinct populations can be defined from the stereoplot. These are described below and summarised in Table 5-2.

- **Set 1: Sub-horizontal joints:** a well-defined grouping of joints is present in all holes except ENG16_06. These joints are also well-represented in the tunnel data.
- **Set 2: Steep to sub-vertically dipping, E-W to WNW-ESE striking joints:** this group is evident in most stereoplots, but is under-represented in the north-dipping holes because of drilling orientation bias (holes: ENG16_06; ENG18_01; ENG18_02), but are present in the tunnel data (Figure 5-9). These joints are controlled by the principal foliation and shear zone orientations in the tunnel and are present in all of the major lithologies.

- **Set 3/4: N-S striking joints:** these structures have been tentatively broken into two subsets based on their dip:
    - **Set 3:** Moderate west-dip: within all sectors of the pit, a population of discontinuities dips ~45-90 west or northwest; however, these structures have not been recorded in the tunnel datasets and do not appear to be controlled by a pre-existing structural feature or fabric.
    - **Set 4:** Sub-vertically dipping: a very well-established joint set in the Vevring tunnel, but not represented in the planned open pit area. This may largely be due to the N-S orientation bias of the drilling. In the tunnel, these structures are not controlled by pre-existing rocks fabrics.

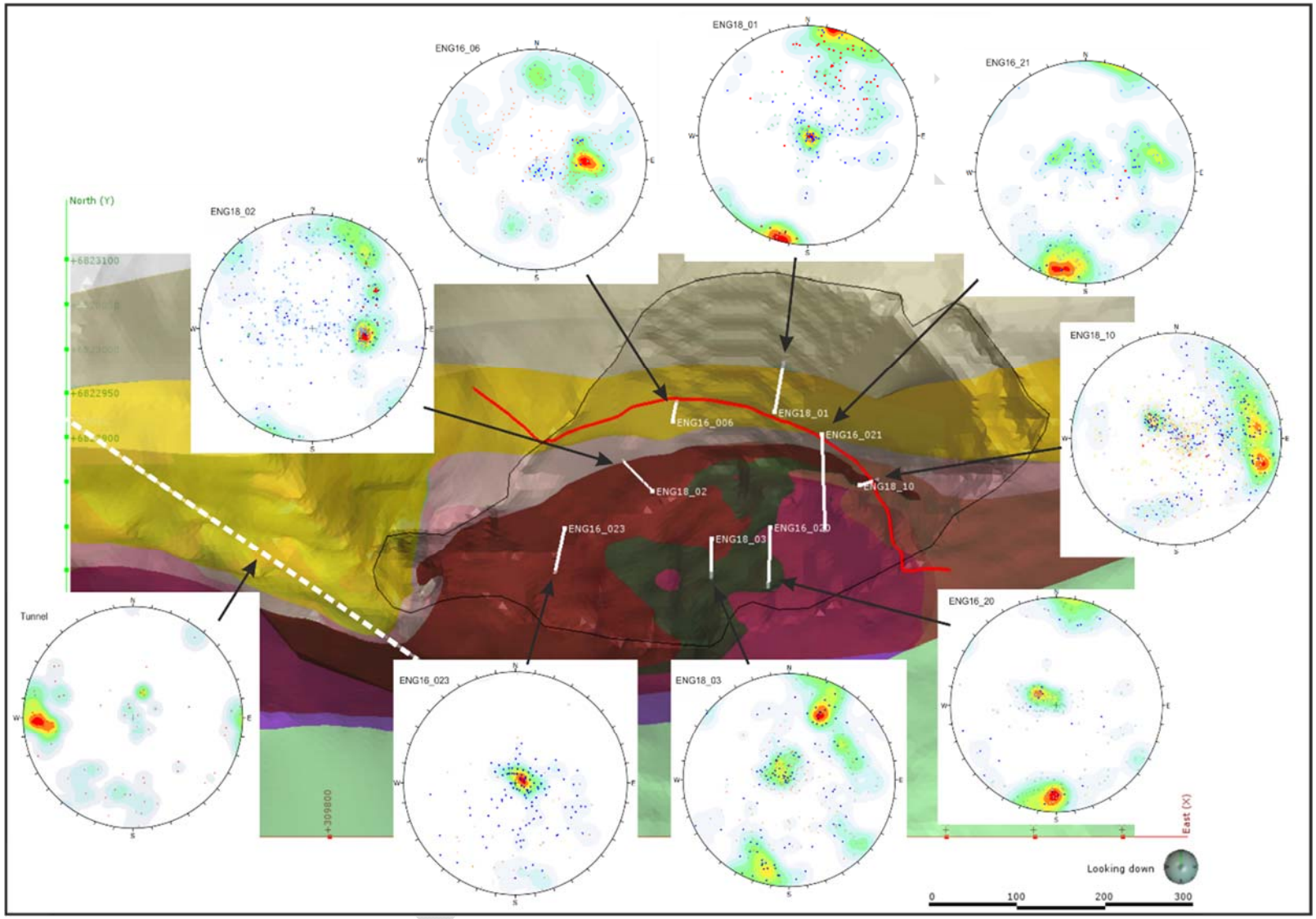

Figure 5-9: Stereoplots of discontinuity orientations from geotechnical drill holes and tunnel survey of SRK (2016)

Table 5-2: Summary of orientation discontinuity orientation characteristics from geotechnical drillholes

Drillhole	Hole Orientation	Set 1	Set 2	Set 3	Set 4
ENG16_06	83/010	11/335	69/181	47/273	-
ENG16_20	62/180	16/126	84/009	86/304	-
ENG16_21	62/178	19/143	79/018	56/261	-
ENG16_23	69/190	10/225	73/356	55/290	-
ENG18_01	70/010	03/256	74/199	64/252	-
ENG18_02	75/315	31/120	79/203	50/276	-
ENG18_03	75/180	12/147	84/019	62/235	-
ENG18_10	85/072	22/133	61/001	68/263	-
Tunnel	01/124	12/214	73/006	-	80/090

5.3.4 Amphibole Veins

Planar veinlets of amphibole, 1-2 mm in thickness, are relatively common features of the eclogite domain. The veins occur in weak clusters and are not deformed ductilely, but cross-cut foliation and compositional banding. They are interpreted to have formed during retrograde metamorphism. As they are minor structures which are strongly cemented they are not considered to be geotechnically significant.

5.4 Potential Controls on Groundwater Circulation

The maximum depth of the tunnel below the surface is about 175 m below topography. Mapping of the Vevring tunnel was carried out during a period of snow melt. Despite this, the tunnel remained dry throughout, with the exception of zones 20-30 m away from either tunnel opening, where the depth of the tunnel shallowed and fractures within the rocks were affected by near surface weathering.

The rock mass is clearly very tight (low porosity and permeability) and therefore fracture flow is of key importance. In SRK's opinion, the structures with potential to contribute significantly to groundwater circulation are the three main joint sets, outlined above (section 5.3.3), the modelled significant fault and smaller scale sinistral shears in ferro eclogite, where they have been reactivated by brittle shears (section 5.3.1).

As these main joint patterns recorded in televiewer data from 2016 and 2018 holes do not show major differences in the different lithologies (data not presented here), it is not clear from this structural review if any of the structures has the potential to dominate the groundwater circulation patterns.

As mentioned previously, vuggy openings have been identified along several minor features in drill core. Overall, their scale and general low abundance means that they are probably not significant in terms of groundwater flow.

6 ROCK MASS STRENGTH

The assessment of the strength of the intact rock at Engebø is based on field estimation, point load testing ("PLT") and uniaxial compressive strength ("UCS") tests. Average strength values were derived for the main lithological domains presented in Section 3.1.

6.1 Logged Intact Rock Strength

Intact rock strength ("IRS") was estimated as part of the geotechnical logging, using the standard International Society of Rock Mechanics ("ISRM") empirical guidelines. These field tests provide a 'first pass' estimation of rock strength variability.

Results, presented in Table 6-1, show similar IRS values across the three main domains for the oxide and transition materials. All rocks were in general classified as Very Strong Rock according to the ISRM (1981) strength classification.

Table 6-1: Average logged IRS per major lithology

Lithology	Average Logged IRS (MPa)	Min Logged IRS (MPa)	Max Logged IRS (MPa)	StDev Logged IRS (MPa)
ALT	142	75	175	52
Amph	175	33	300	80
Ferro	137	33	300	73
GAM	183	75	300	98
Gar_Amph	130	130	130	
Gneiss	147	120	180	31
Leuco	170	33	300	58
Trans	153	1	300	74

6.2 Point Load Testing Results

The point load data results (Is_{50}) were converted to UCS equivalent (UCS_{eq}) values by means of a conversion factor (K). This conversion factor is the ratio between the UCS and the Is_{50} value. In general, the uniaxial compressive strength is about 20 to 25 times the point load strength although tests on many different types of rock show that the ratio can vary between 15 and 50, especially for anisotropic rocks. Consequently, the most reliable results are obtained if uniaxial calibration tests are carried out. K factors were generated from 30 valid UCS results and the corresponding Is_{50} result from the PLT test. Similar failure modes were considered in the calculation of the K values; that is, if the UCS sample was failing through foliation, only the PLT results failing through foliation were considered to calculate the K factor. The mean K values, calculated for each lithology, as presented in Figure 6-1, were then used for the calculation of the UCS_{eq} for the entire PLT database. If no K was derived for a lithology, a default K of 16 (based on engineering judgement) was applied to calculate UCS_{eq}.

Using the conversion factors defined in Figure 6-1, equivalent UCS values by lithology for the point load testing is presented in Table 6-2. As per the field logging, all lithologies can be defined as Very Strong Rock. Both axial and diametral point load testing was undertaken to assess for the influence of anisotropy; however, in general, the results indicate similar strength values with each direction of testing. Figure 6-2 displays UCS variability with depth, it is clear that there is little change in strength with depth and the presence of a reduced intact rock

strength zone near surface as a result of weathering or alteration processes can be discounted.

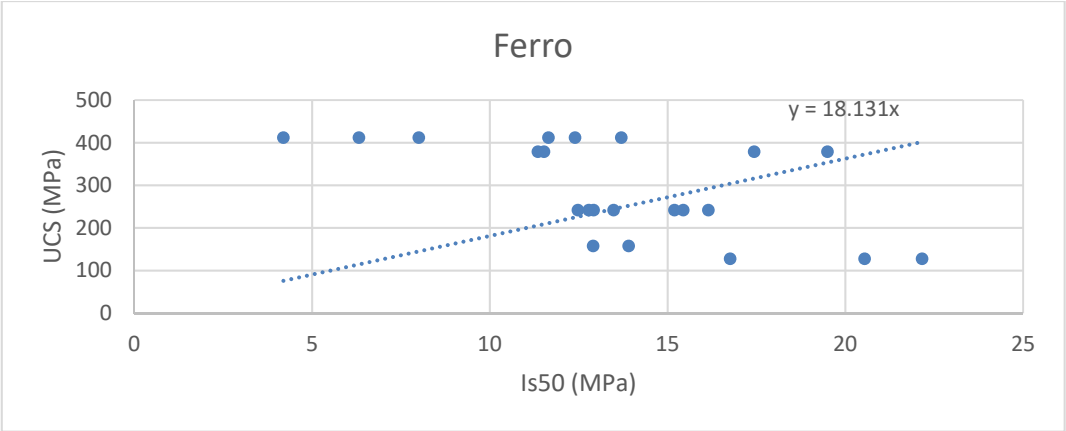

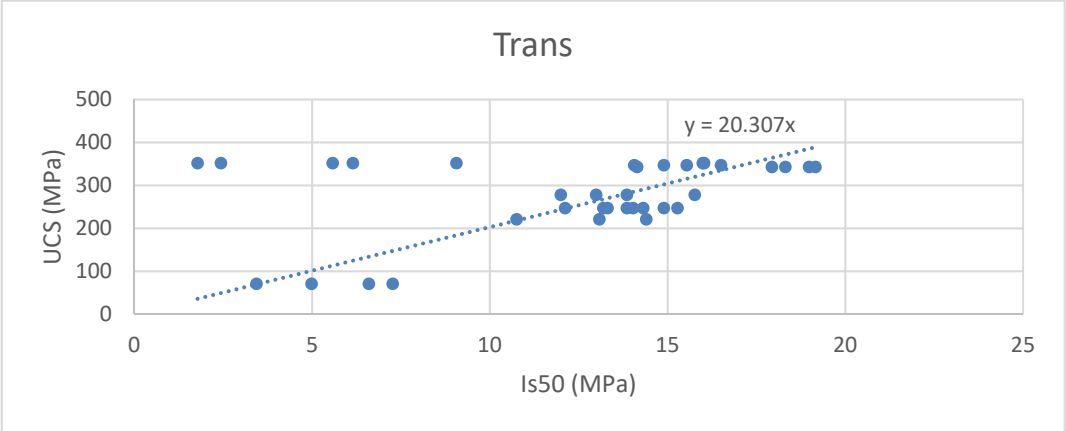

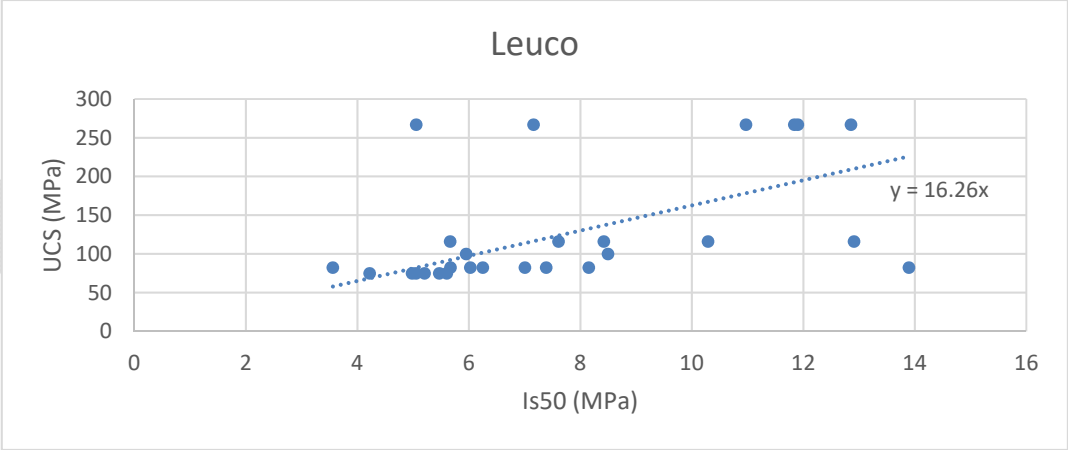

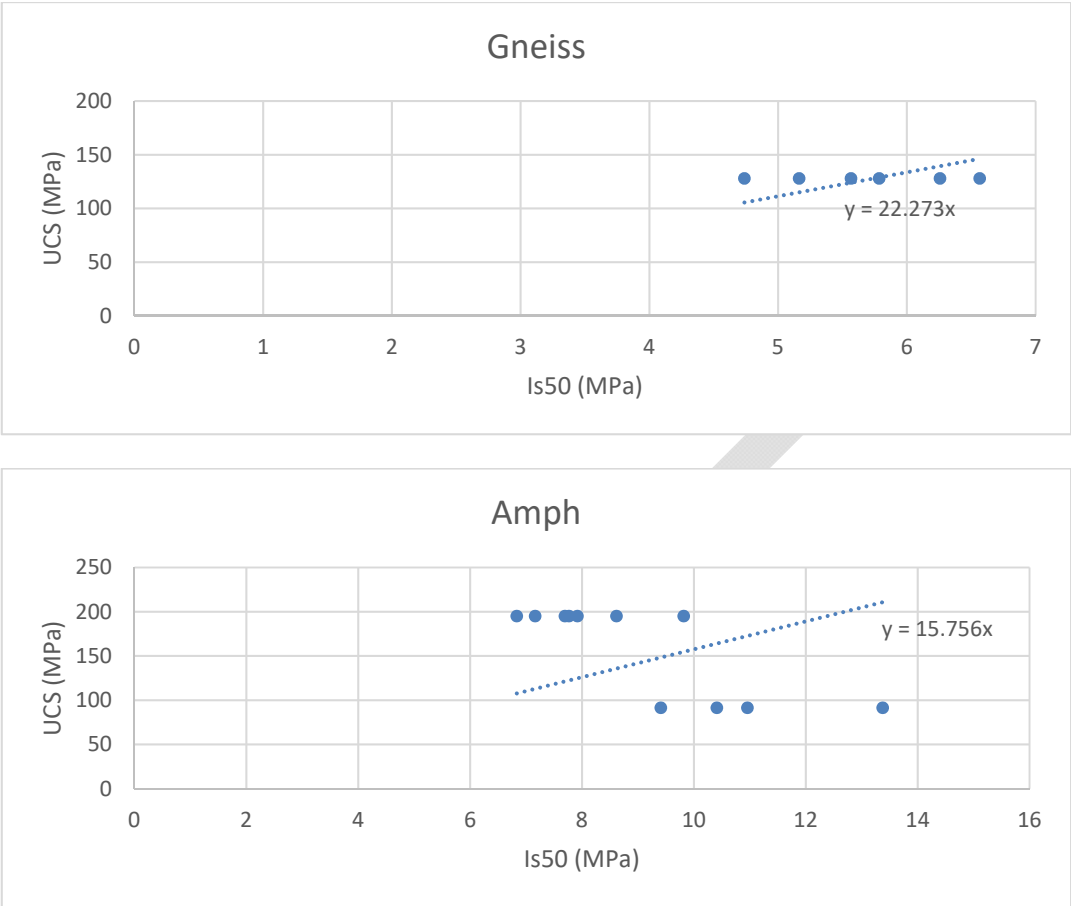

Figure 6-1: K factor generation for each major lithology

Table 6-2: Equivalent PLT UCS by lithology

Lithology	Mean PLT UCS (MPa)	Min PLT UCS (MPa)	Max PLT UCS (MPa)	StDev PLT UCS (MPa)
Amph	144	107	210	31
Ferro	254	24	401	69
Gneiss	126	106	146	15
Leuco	154	38	301	63
Trans	254	36	458	83

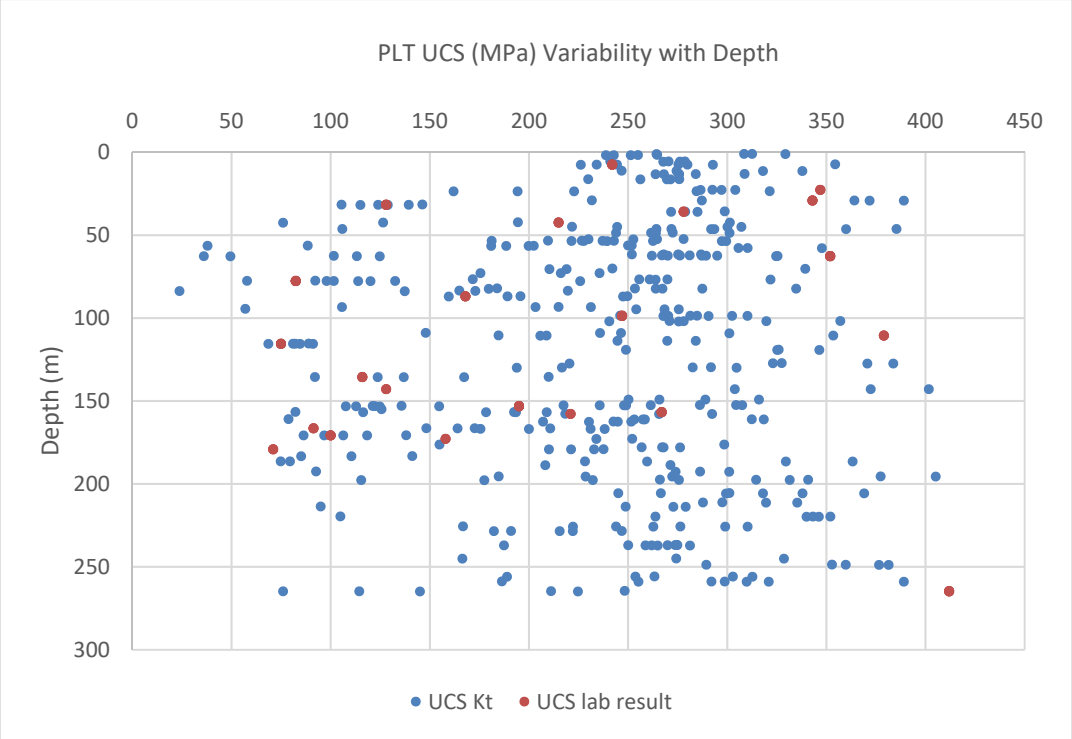

Figure 6-2: Variability of PLT UCS with Depth

6.3 Laboratory Testing Results

As part of the geotechnical programme, samples for UCS, natural joint shear and triaxial laboratory testing were selected. Testing was performed according to the ISRM: 2007: Suggested Methods.

6.3.1 UCS Test Results

Average UCS values obtained in the laboratory for each lithology and mode of failure are presented in Table 6-3. These statistics show that samples failing through the rock are stronger than sample failing through a joint or foliation plane (Table 6-4). Where samples have failed along foliation planes, however, the intact rock strength remains high, indicating minimal impact on intact rock strength due to the presence of anisotropy. Laboratory test results are broadly in line with the logged IRS field estimates and point load testing results. Figure 6-3 shows the distribution of all intact rock strength testing.

Table 6-3: UCS results: Failure through intact rock

Lithology	Average UCS (MPa)	Min UCS (MPa)	Max UCS (MPa)	StdDev UCS (MPa)
Amph	195	195	195	-
Ferro	290	128	412	131
Gneiss	126	123	128	4
Leuco	207	116	267	64
Trans	289	71	387	107

Table 6-4: UCS results: Failure along foliation plane

Lithology	Average UCS on Foliation (MPa)	Min UCS on Foliation (MPa)	Max UCS on Foliation (MPa)	StdDev UCS on Foliation (MPa)
Amph	91	91	91	-
Ferro	219	158	280	86
Leuco	108	75	168	35
Trans	194	167	221	38

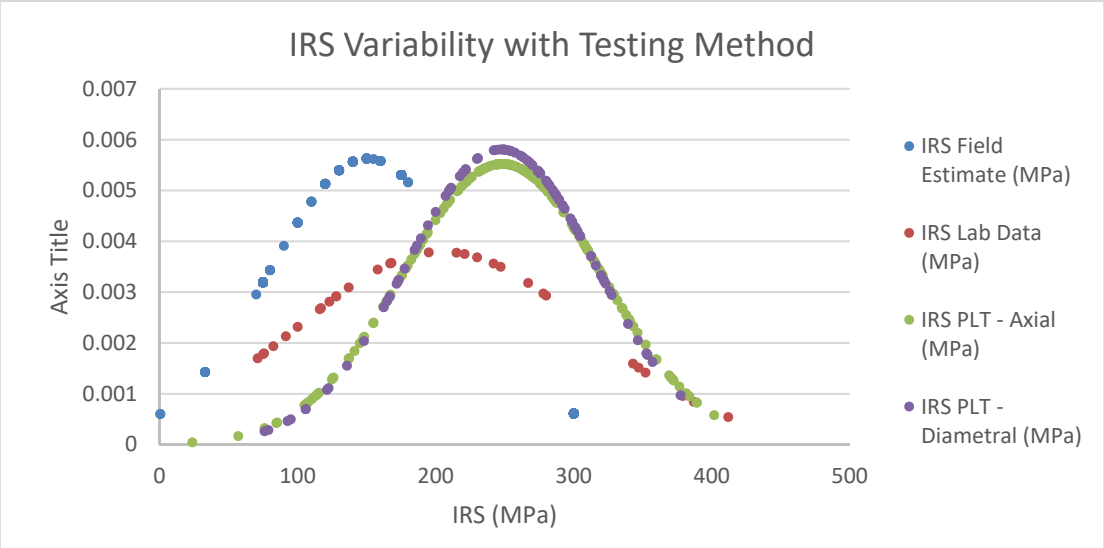

Figure 6-3: IRS variability with testing method

6.3.2 Deformation Modulus Test Results

The results of the deformation modulus testing are presented in Table 6-5.

Table 6-5 Deformation modulus testing results

Lithology	Average Young's Modulus (GPa)	Average Poisson's Ratio
Amph	323	0.36
Ferro	136	0.17
Leuco	102	0.16
Trans	126	0.20

6.3.3 Triaxial Test Results

Triaxial tests were carried out for each main lithology. Each test corresponds to a suite of three samples, with each sample is tested at a different normal stress simulated to simulate the effects of loading at a bench and inter-ramp scale. Triaxial tests enables the extraction of fundamental material parameters, including the angle of shearing resistance, apparent cohesion, dilatancy angle and *mi* value. Triaxial test results are detailed in Table 6-6.

Table 6-6: Summary of triaxial results

Lithology	Confining Pressure 1 (15 MPa)	Confining Pressure 2 (30 MPa)	Confining Pressure 3 (60 MPa)	Friction Angle (°)	Cohesion (MPa)
Amph	312	399	514	39	61
Amph	415	499	641	41.7	77
Ferro	483	-	-	-	-
Ferro	451	554	692	42.8	83
Ferro	523	643	728	38.6	116
Ferro	79.1	110	167	18.7	18
Leuco	259	-	-	-	-
Leuco	265	305	401	30.4	62
Trans	281	-	-	-	-
Trans	265	343	469	39.5	48

6.4 Strength of Structural Defects

Joint infill and surface micro roughness were recorded as part of the systematic geotechnical logging. The main infill minerals observed on joint surfaces are chlorite (40% across the pit areas) and calcite (35% across the pit areas). About 9% of all logged joints show no infill. The main infill mineral distributions for each pit area are presented in Figure 6-4. Cumulatively, these four main types of infill account for 93% of the logged infill. Joint surface roughness distributions are presented in Figure 6-5. Most of the joint logged across all pits are slightly rough and rough (49% and 24% of all joint logged respectively).

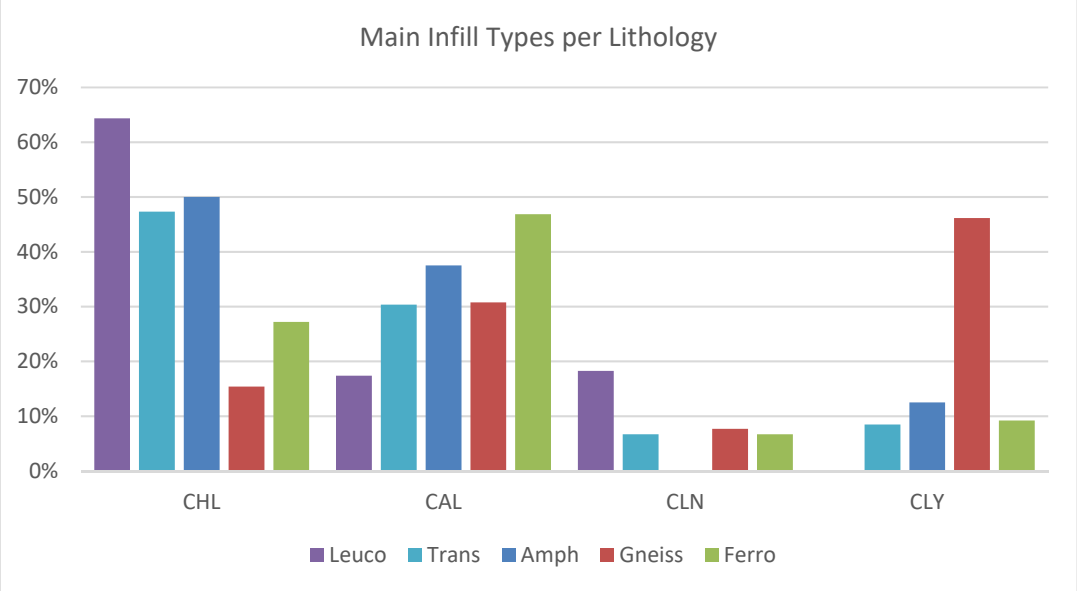

CHL=Chlorite, CAL=Calcite, CLN=Clean, CLY=Clay

Figure 6-4: Main joint infill distribution

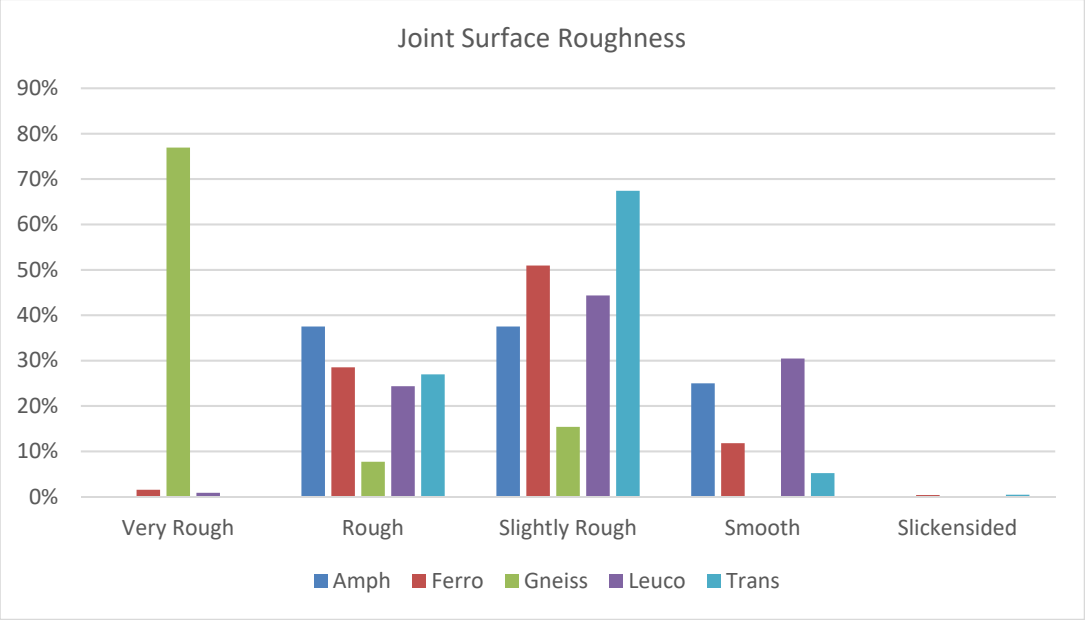

Figure 6-5: Joint micro roughness distribution

Direct shear testing was carried out to estimate the shear strength of the discontinuities. Multistage direct shear tests were conducted under increasing normal loads on natural joints recovered from the core. A total of 23 natural joint shear tests were undertaken on the main lithologies. Table 6-7 presents the peak results by major lithology and Table 6-8 presents the peak results based on infill type. The peak shear strength results appear to be appropriate based on observations made during the core logging, with 'Amph' and 'Trans' material have a higher friction angle than the 'Ferro' and 'Leuco' rock types. Shear strength by infill type has generated consistent results although joints logged as clean (CLN) have the lowest friction angle. When undertaking shear testing on natural joints, it is likely that damage to the surface was sustained during the first stages of loading with natural asperities being sheared off. It is considered that the values obtained from testing can be thought of as lower bound values.

As a result of the presence of infill within many of the joint surfaces tested, the Barton-Bandis criterion was not used to scale the joint shear strength. A friction angle of 22° was used within the kinematic analysis. Figure 6-6 shows the shear/normal plot of each lithology.

Table 6-7: Joint shear strength by lithology

Lithology	Average Peak Cohesion (kPa)	Min Peak Cohesion (kPa)	Max Peak Cohesion (kPa)	StdDev Peak Cohesion (kPa)
Amph	258	258	258	-
Ferro	244	34	517	184
Leuco	616	88	1144	396
Trans	308	88	730	214
Lithology	**Average Peak Friction Angle (°)**	**Min Peak Friction Angle (°)**	**Max Peak Friction Angle (°)**	**StdDev Peak Friction Angle (°)**
Amph	28	28	28	-
Ferro	21	16	26	4
Leuco	20	14	25	5
Trans	24	19	30	4

Table 6-8: Joint shear strength by infill type

Infill	Average Peak Cohesion (kPa)	Min Peak Cohesion (kPa)	Max Peak Cohesion (kPa)	StdDev Peak Cohesion (kPa)
CAL	383	34	1144	306
CHL	317	88	730	261
CLN	151	151	151	-
CLY	325	133	517	272
Infill	**Average Peak Friction Angle (°)**	**Min Peak Friction Angle (°)**	**Max Peak Friction Angle (°)**	**StdDev Peak Friction Angle (°)**
CAL	22	14	30	4
CHL	22	15	28	5
CLN	19	19	19	-
CLY	23	17	29	8

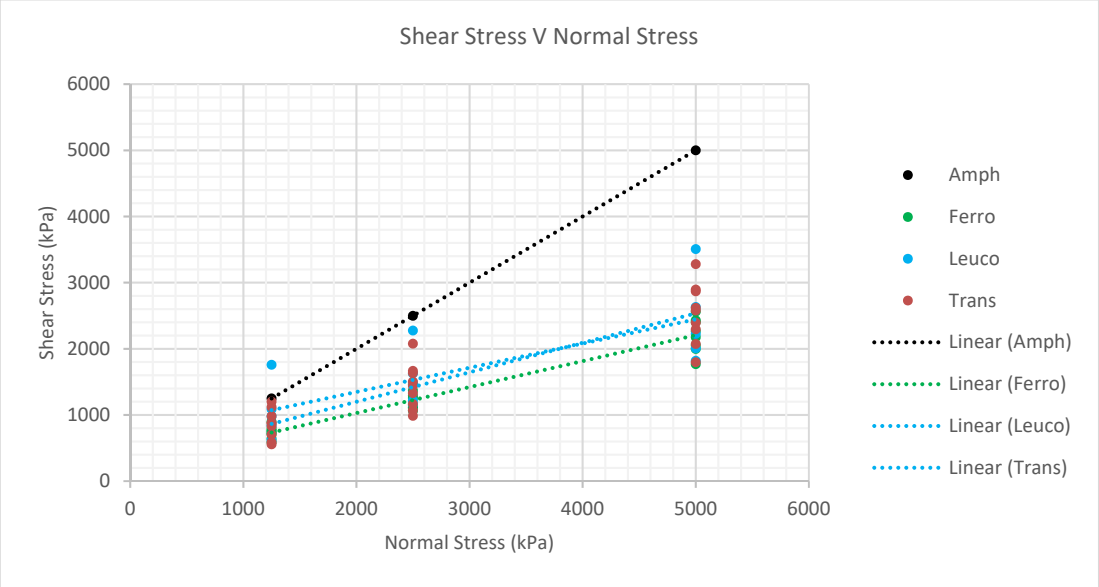

Figure 6-6: Shear/Normal plot: Joint shear strength

7 HYDROGEOLOGICAL SETTING AND CONSIDERATIONS

7.1 Introduction

Mining geotechnical related aspects of the Hydrogeological Study undertaken in support of the overall Feasibility Study are summarised below. The full Hydrogeological Study report is included in Appendix E.

7.2 Data Collection

7.2.1 Groundwater level measurement

Static water levels were measured in a number of holes across the deposit. Due to the inclined nature of the exploration holes (<70°), a dip meter was not able to be used in all holes as the tape stuck to the damp borehole wall; however, this was overcome by using the water level logged from OTV/ATV logging.

7.2.2 Downhole impellor flowmeter (spinner) testing

Groundwater flow in the bedrock at Engebø is expected to be fracture controlled. Downhole impellor flow logging or "spinner" testing was therefore carried out to identify the location of fractures that are open to groundwater flow. Spinner logging was undertaken by Geovista between 7 and 14 March 2018, with SRK being present for QA/QC checking of field methods on 7 and 8 March 2018.

The boreholes were logged under static conditions. Static spinner logging involves the calibrated impellor flowmeter (spinner) being lowered down the borehole at a constant speed controlled by an electrical winch to produce a baseline log identifying flow anomalies. Ambient flow between discrete fractures intersected by the borehole are driven by natural differences in head in each fracture and these are identified as flow anomalies in the spinner logs. Fractures with similar head cannot be identified with static logging and derivation of fracture transmissivity is not possible. Pumped tests were not possible due to problems with the pump.

Full details of the spinner testing undertaken are included in Appendix E1.

7.3 Data Analysis

7.3.1 Groundwater Levels

Groundwater levels (shown in Appendix E2) do not follow topography and are likely controlled by structures, that is, fractures that represent areas of preferential porosity, and, if interconnected with other fractures, groundwater flow. This is common in fractured rock and represents compartmentalisation of groundwater determined by higher and lower permeability structures. Groundwater flow in this environment will be controlled by the occurrence, transmissivity and degree of interconnectivity of fractures, as well as variability in recharge.

7.3.2 Structural Controls on Groundwater Flow

Logged structures do not show a clear trend based on lithology, size or infill and are not focussed in a particular area.

Most logged fractures are between 2 and 7 mm, although some were logged as being greater than 30 mm. It should be noted, however, that aperture data from geotechnical drilling often has a positive bias depending on the angle at which the drill bit intersects the structure.

Mine to regional scale structure is particularly important in terms of controlling groundwater flow, a detailed interpretation of which is included in Section 5. Only one correlatable regional scale fault was able to be mapped to a planar structure with an overall orientation of 53/022 and crossing the approximate centre of the proposed pit from east to west. None of the holes logged with the spinner intersected this fault.

A number of minor faults were observed to have vuggy openings which are not restricted to the fractures localised to certain fractures and are unlikely to constitute a major element of the permeability structure.

7.3.3 Spinner Tests

Flow logs were analysed and geotechnical logging and flow logging data was compared to see whether flows were related to fractures and joints with particular characteristics. Most flowing features identified during spinner testing can be correlated to a nearby geotechnically logged structure. Table 7-1 summarises the interpretation of the spinner testing data and interpolation to the nearest geotechnically logged feature where this flow likely originates.

Table 7-1: Spinner logging analysis

Hole ID	Geotechnical Log Features					Spinner Log Features		
	Dip	Azimuth	Depth (m)	Aperture (mm)	Infill	Depth (m)	Flow (L/s)	Confidence*
ENG16_06	39.7	277.7	105.35	19.4	n/a	104.2	0.041	Average
	88.1	64.5	110.97	0.6	n/a	111.0	0.041	Average
	46.9	247.0	165.26	12.1	n/a	165.0	n/a	Average
	43.8	247.8	175.69	7.7	n/a	175.0	n/a	Average
ENG16_20	No clear flowing fractures							
ENG16_21	35.8	139.6	215.33	5.6	n/a	216.8	0.036	Average
ENG18_01	14.8	257.6	167.01	2.0	CAL	168.8	0.041	High
ENG18_03	74.9	28.9	152.59	3.0	CHL	153.0	0.052	Average
	8.1	93.6	163.16	4.8	CAL	161.2	n/a	Average
ENG18_10	31.2	105.6	208.24	14.8	CLY	209.5	0.083	High
	75.5	21.0	246.43	2.5	CHL	247.5	0.062	High

Note: Confidence is a function of coincidental changes in tool speed, consistency in up versus down versus temperature log, and size of anomaly versus noise.

No clear relationship between fracture aperture and flow was observed and the apertures of flowing structures vary significantly, between 0.6 mm and 19.4 mm. This is not unexpected, as groundwater flow is controlled by the minimum aperture along a given fracture, which is likely to be significantly smaller than the aperture intersected by the drill bit and logged from optical or acoustic televiewer.

7.4 Conceptual Hydrogeological Model

The Engebø deposit comprises medium to high grade metamorphic rocks including eclogites, gneisses, and amphibolites; crystalline rocks with low primary porosity and permeability. Deformation events have led to the formation of several sets of structures that contribute to secondary porosity and permeability.

There is little or no overburden across most of the site area. Thin layers of soil and moraine can be found where topography is flat enough to allow this to accumulate.

Recharge to the Engebø deposit is through infiltration of rainfall or snowmelt either directly into outcropping rock or via the very shallow surface soils present in some areas of the deposit. Recharge is likely to be spatially dependent on the occurrence of fractures.

Three sets of joints have been identified and a significant number of these structures are open and therefore have the potential to act as pathways for groundwater. Groundwater flow is controlled by the interconnectivity and transmissivity of these structures. The spinner testing undertaken identified several transmissive structures at different orientations with no discernible trends. Furthermore, only a small number of flow features were identified during the spinner testing compared to a large number of structures that were logged during the acoustic televiewer logging as open and clean.

Groundwater levels vary significantly across the site and do not conform to topography. This suggests that the interconnectivity of fractures is limited at a site-wide scale.

Groundwater discharge from the system is from springs at the foot of the Engebø deposit, which in turn feed into small surface water courses.

7.5 Geotechnical Modelling Considerations

7.5.1 Limit equilibrium analysis

SRK produced estimated piezometric surfaces as an input into limit equilibrium slope stability modelling. Given the extremely high rock strength and lack of major structural features (faults), the model was found to be insensitive to pore water pressure. For this reason, a conservative piezometric surface was used, notwithstanding the significant limitations of using piezometric surfaces over pore water pressure grids in limit equilibrium analysis.

The following additional affects which are likely to further depressurise the walls in the case of the low permeability rocks present at Engebø:

Overbreak due to blasting. The overbreak zone (also referred to as the blast damage zone) is a zone of weakened rock in the pit walls. Blast damage enlarges structures and therefore potential new flow pathways allowing groundwater to drain.

Lithostatic unloading effects. Unloading as the pit is mined out is likely to result in increase in fracture aperture and a commensurate increase in transmissivity. As a rule of thumb, this response is typically seen in rocks with a hydraulic conductivity of 10^{-8} m/s or lower.

Freeze back. Groundwater daylighting in the pit walls will likely freeze during the winter months which will lead to a temporary build-up of pore water pressures behind the pit slope.

7.5.2 Kinematic analysis

Friction angle for kinematic analysis was set at 22° as a result of the presence of infill (see Section 9.2). Any planar failures due to unfavourable joint set orientations in the pit is therefore driven by this low friction angle and the kinematic analysis was found to be insensitive to water filling of discontinuities.

8 ROCK MASS MODEL

SRK has interrogated the RMR^{89} logging data to define rock mass classification values for each major lithology. With the exception of a very thin layer of overburden (which has not been accounted for in the geotechnical analysis), the rock slope can be considered to contain only 'fresh' rock with no weathering or significant alteration.

8.1 Fresh Rock

Based on the results of the geotechnical logging, the rock mass according to RMR^{89} can be considered 'Good to Very Good'. Zones of poor ground are typically associated with fault zones and are in general discrete, not extensively intersected by the geotechnical drilling and difficult to correlate between boreholes. In general, all lithologies can be described as very strong, massive crystalline rock with wide to very wide joint spacing,

Table 8-1 shows the range of RMR^{89} values generated for each of the major lithologies intersected during the drilling programme with all lithologies classified in the upper end of the 'good rock' category. Figure 8-1 presents the RMR^{89} distribution curves of the major lithologies.

Table 8-1: RMR^{89} for each major lithology

Lithology	Average of Calc RMR^{89}	Weighted RMR^{89}	Min RMR^{89}	Max RMR^{89}	StdDev RMR^{89}
ALT	75	75	63	82	9
Amph	75	76	51	86	10
Ferro	74	75	15	94	8
Gneiss	76	80	67	81	8
Leuco	76	77	15	96	13
Trans	73	75	15	90	10

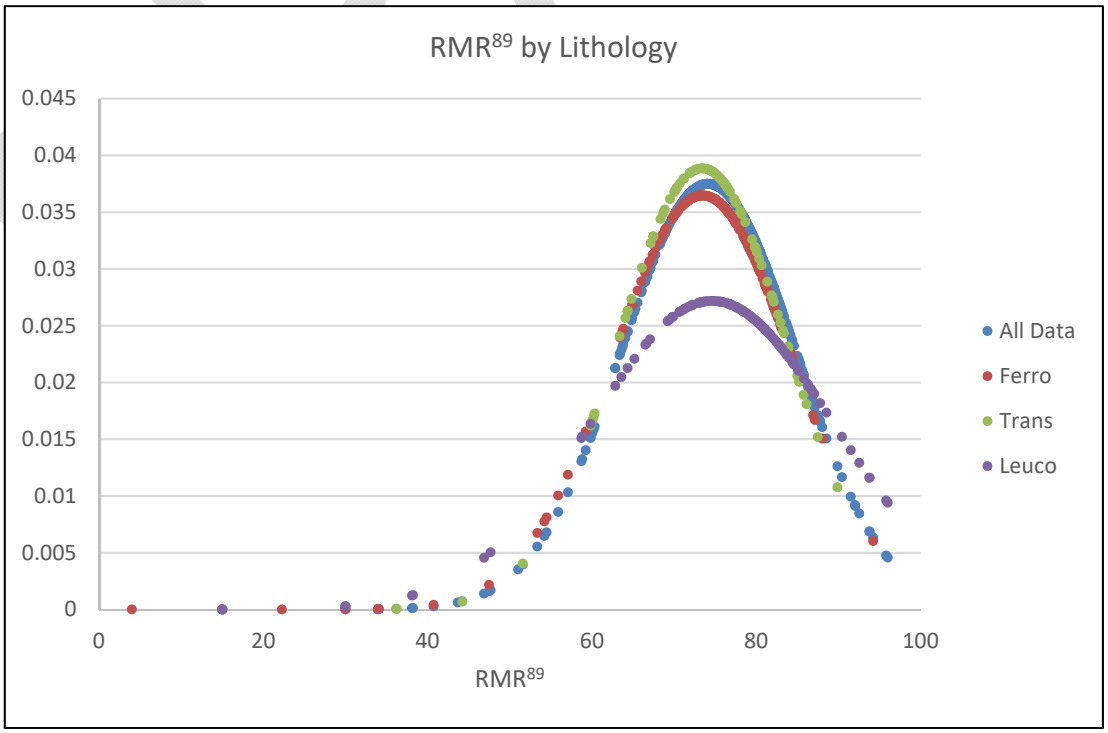

Figure 8-1: RMR^{89} for each major lithology

Figure 8-2 shows the distribution of RMR^{89} values on a borehole by borehole basis. Again, there appears to be consistency between boreholes with no specific areas of decreased ground conditions. Figure 8-3 shows the variation of RMR^{89} with depth for each major lithology. With the exception of a few data points, there is little variability with depth and high RMR89 values are intersected immediately below the topographic surface. Figure 8-4 to Figure 8-7 show representative examples of each major lithology.

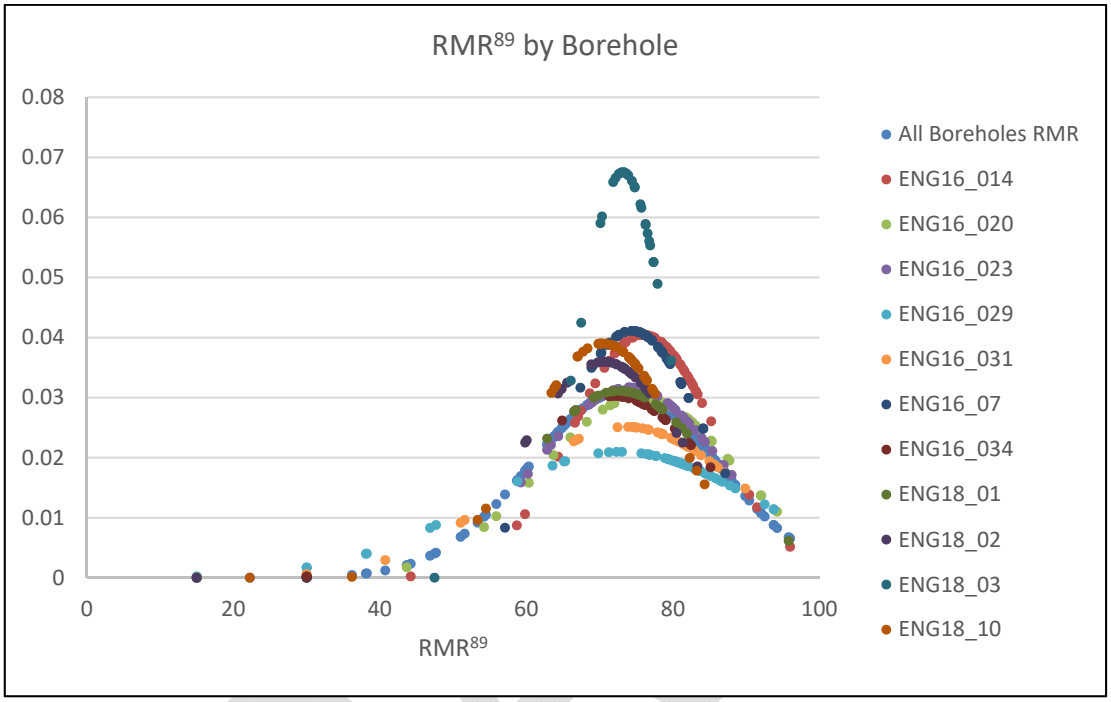

Figure 8-2: RMR^{89} by borehole

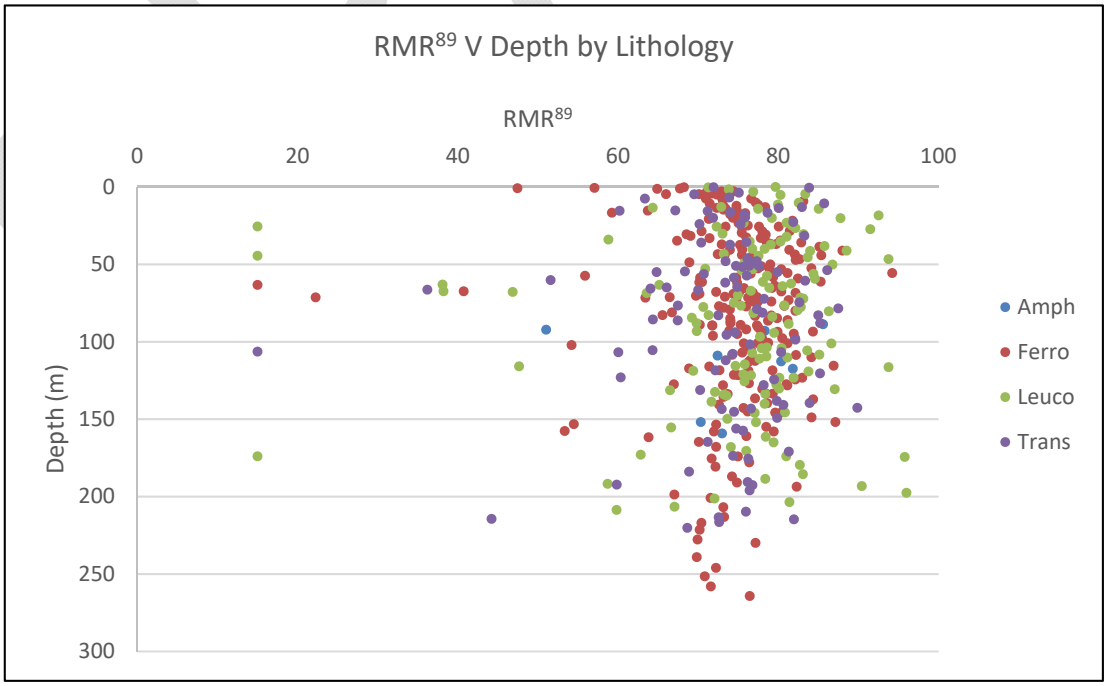

Figure 8-3: RMR^{89} with depth for each major lithology

Figure 8-4: Amphibolite, Borehole ENG16-31

Figure 8-5: Ferro, Borehole ENG18-03

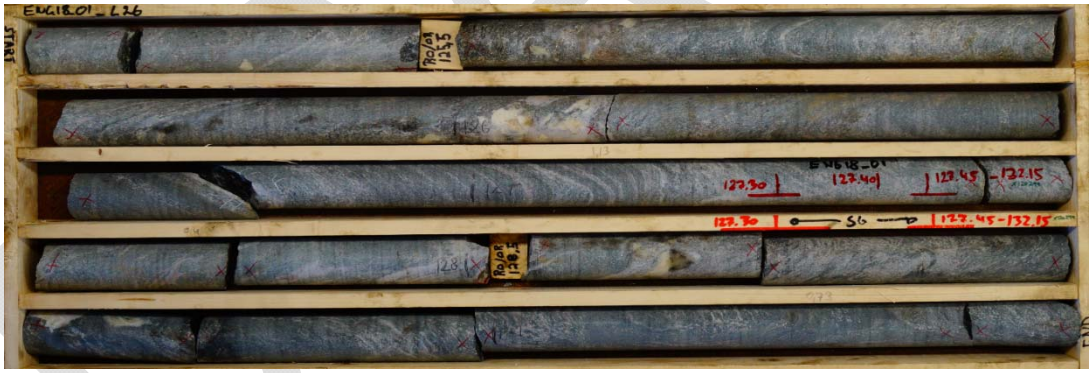

Figure 8-6: Leuco, Borehole ENG18-01

Figure 8-7: Trans, Borehole ENG18-02

9 STRUCTURAL ANALYSIS AND KINEMATIC ASSESSMENT

9.1.1 Summary of Structural Features of Geotechnical Significance

Overall, Engebø is characterised by a strong rock mass with relatively few features that are perceived to pose a significant geotechnical risk. The principal features that should be considered are:

Joint discontinuities

- These do not appear to be strongly controlled by lithology and are the most pervasive discontinuity type and therefore are perceived as the principal consideration when evaluating pit slopes.

Foliation

- Where the rocks are foliated they can locally control the orientation of discontinuities.
- Although the gross orientation of the foliation is known, it is clear that, locally, foliation orientation can change markedly and therefore may be an issue where macroscopic (5-10 m scale) folding occurs.
- The presence of QMG zones will exacerbate the weakness caused by the foliation.

Shears in eclogite

- Steep, narrow shears mapped in the ferro eclogite in the tunnel are generally sub-vertical and are therefore unlikely to be a major geotechnical issue.

Significant faults

- The fault interpreted here is not believed to be a major structural feature. Moreover, its geotechnical significance is limited as the fault dips into the pit wall.

9.1.2 Structural Domains

The planned open pit area has been divided into two structural domains, North Wall Domain and South Wall Domain, as shown in Figure 9-1. The characteristics of each domain are summarised below, highlighting the main structures and potential adverse conditions.

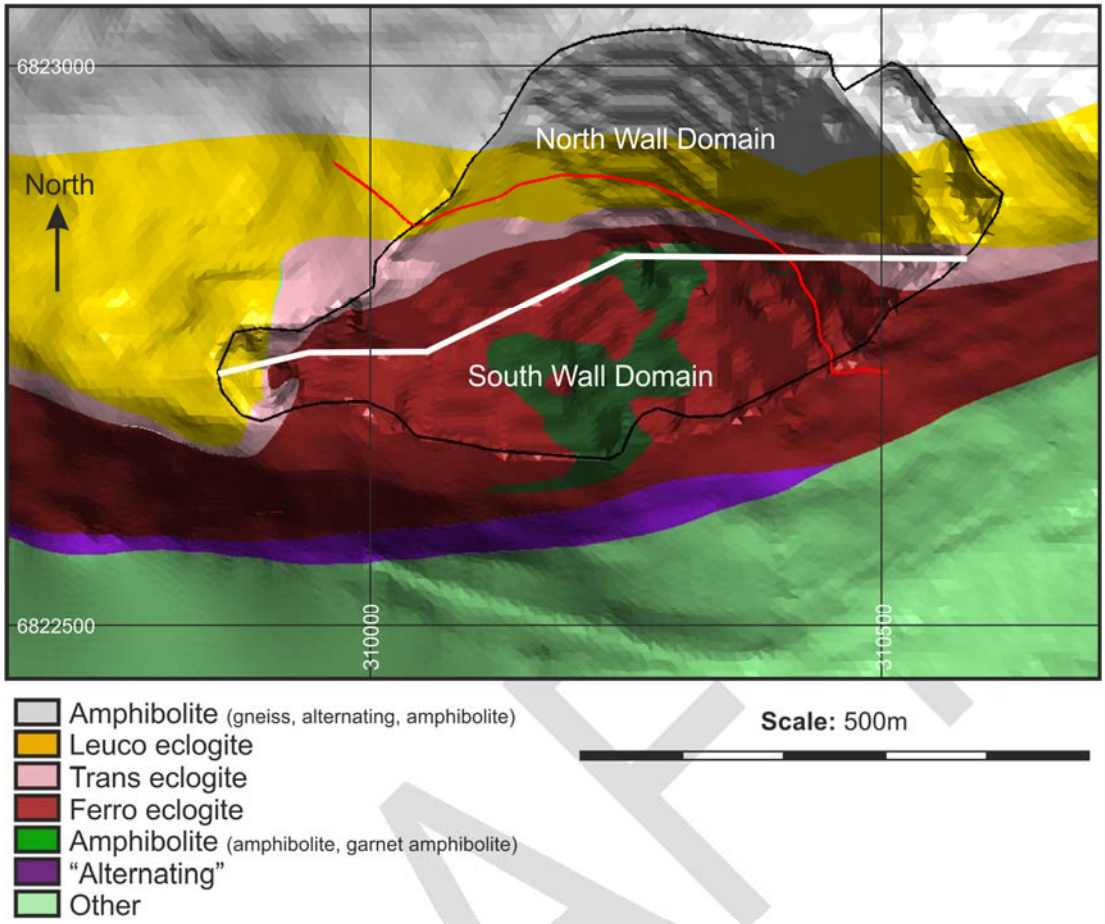

Figure 9-1: Structural domains superimposed on the 3D lithological model of the pit cut to the current optimised pit shell (red line indicates fault trace on pit shell)

North Wall

- Lithologies: dominated by leuco and amphibolites/gneiss with intercalations of QMG.
- Foliation: the foliation predominantly dips steeply to the N or NNE, striking E-W or WNW-ESE. Foliation is well-developed and is likely to intensify in shear zones and at contacts between the litho types.
    - The northern part of this domain is not well constrained by drilling and it is unclear if the foliation over steepens and dips to the south, as is partially indicated in the cross-sections of Korneliussen et al. (1998).
    - An antiformal fold occurs in the western part of this domain which, it is interpreted, the foliation in the leuco will reflect the fold hinge region, dipping towards the west and northwest.
    - Although the predominant foliation dips towards the north, the foliation and compositional banding in the ferro/trans eclogite is likely to vary significantly due to small folds.
- Fault: the single fault interpreted from drillhole data intercepts the north wall of the pit with a trace trending approximately WNW-ESE overall, dipping into the face of the pit.

- Joint sets: as shown in Figure 9-2; joint sets J1, J2 and J3 are well-represented in the domain.
- Potential risks: the main risks posed by the structures in the North Wall domain are believed to be related to toppling failure where joints along the steeply north-dipping foliation (Set J2) act as releasing structures. This risk may be particularly exacerbated by the higher frequency of highly foliated and less competent QMG veins within the foliated rock mass.

South Wall

- Lithologies: the domain is dominated by ferro eclogite in the main, but in the central southern part of the domain a sliver of amphibolite (and lesser leuco, not modelled) occurs.
- Foliation: foliation in the ferro/trans units is weak or preserved as compositional banding, in the generally massive rocks. In the vicinity of amphibolite lens, however, foliation increases pockets of intense foliation occur. The present planned position of the south wall of the pit transects the amphibolite lens.
- Fault: the major fault interpreted in the pit does not affect the South Wall domain except within the very eastern part of the pit.
- Joint sets: as shown in Figure 9-2; joint sets J1, J2 are well-represented in the domain. Joint set J3 appears slightly more variable but, potentially significantly, is the predominant joint set
- in the east of the pit.
- Potential risks: the main risks identified are:
    - Failure along foliation-parallel joints (set J2) which may daylight on bench faces resulting in bench-scale failure. This is more likely in the area where intense foliation and QMG are present in the vicinity of the amphibolite lens.
    - Set J3 discontinuities daylighting on benches in the eastern-most part of the pit, and/or, in conjunction with set J2 joints causing wedge failures in the southeast part of the pit.

In general, there appears to be little structural variability between boreholes, although when such variability is evident, it is most likely a function of drill hole bias and the 'blind spot' associated with orientated core drilling. As such, SRK has combined the mid and high confidence orientation data to define a structural data set that can be considered to cover the proposed open pit slope area (Figure 9-3 and Table 9-1). No joint persistence data is available from the project area outcrops due to snow cover at the time of the site visits, although observations from the tunnel and site photographs taken when no snow was on the ground gives an idea of likely persistence. Accurate data on persistence can only be defined when fresh rock intersections are exposed during mining.

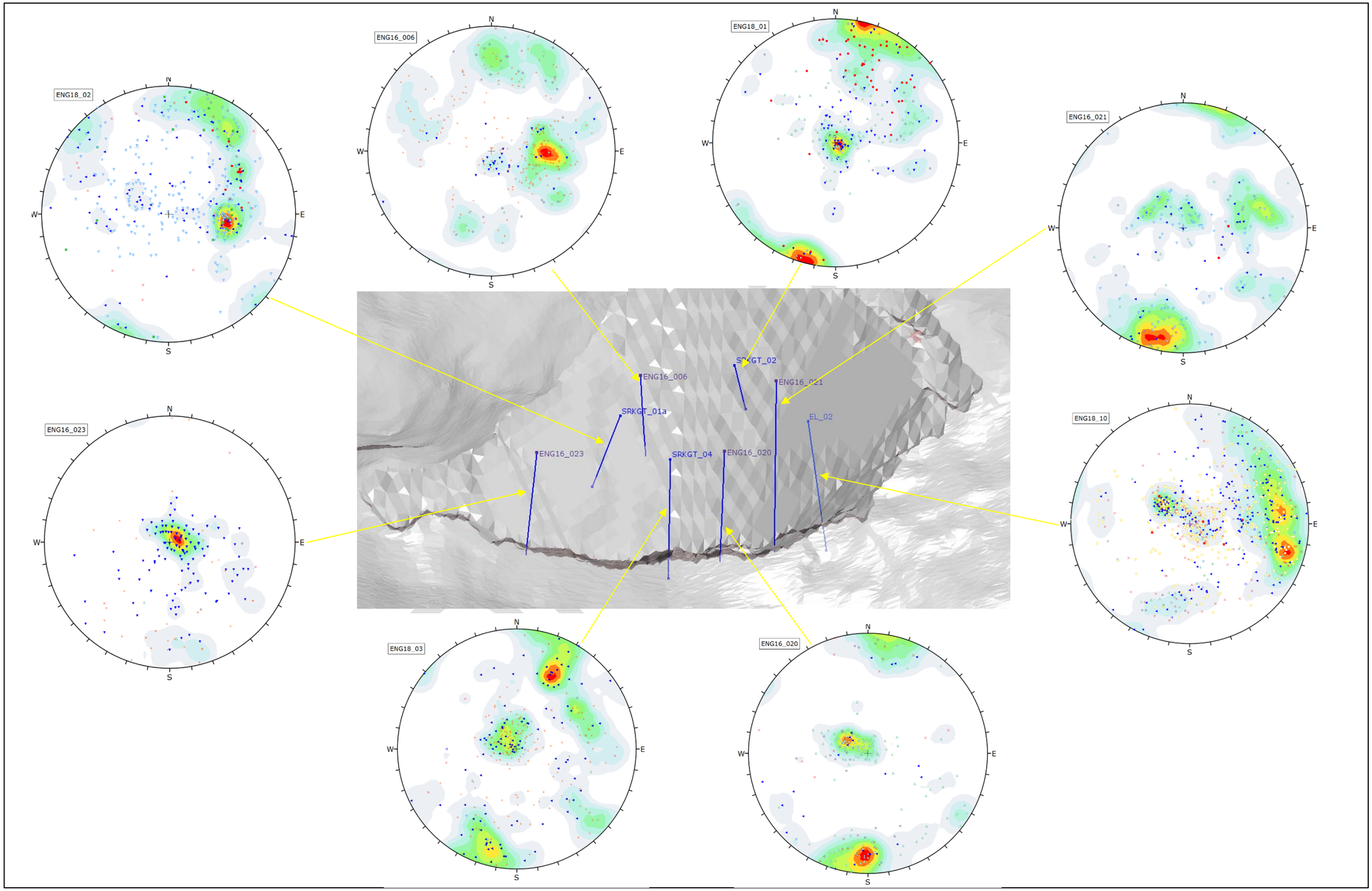

Figure 9-2: Borehole stereoplots

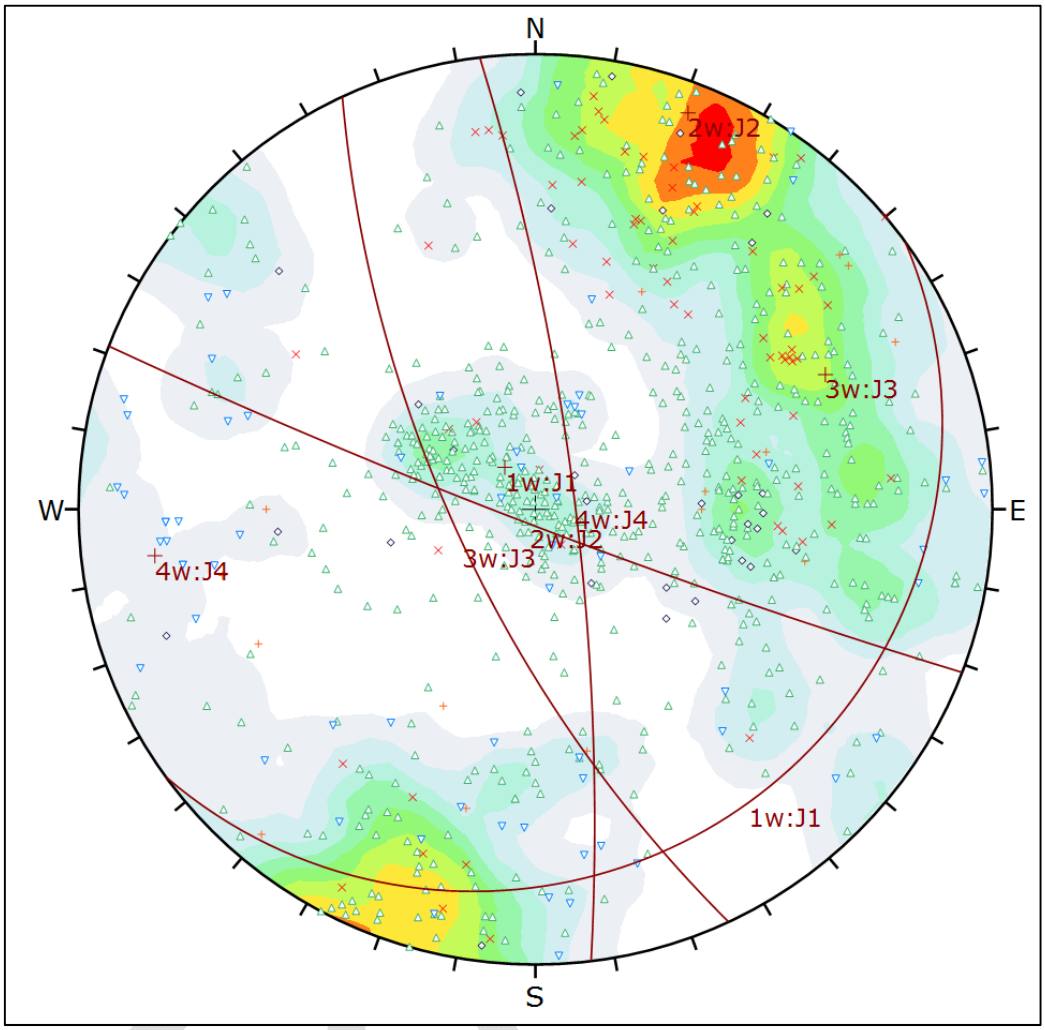

Figure 9-3: Defined joints sets used within structural analyses

Table 9-1: Summary of joint set details

ID	Dip	Dip Direction	Range (= 1*StdDev) (weighted)	Mean Spacing (m)	Spacing StdDev (m)	Persistence Max (m)	Persistence StdDev (m)	Primary Infill
J1	13	142	21	5.6	11.3	30	15	Calcite
J2	86	201	16	2.9	5.7	30	15	Chlorite
J3	70	245	15	3.7	6.9	30	15	Chlorite
J4	80	083	12	-	-	30	15	-

9.2 Kinematic Analysis

9.2.1 Evaluation Modes

From a strictly kinematic standpoint, rock failures in an open pit are often classified into three basic failure types (Hoek and Bray 1981). The basic concepts behind these failure mechanisms are discussed below. A key parameter in any kinematic analysis is joint persistence. Whilst it is not possible to accurately determine joint persistence from drill core, it was possible to define joint persistence from the pit mapping data. Where faults or major structures have been recorded in the pit slopes but have not been assigned part of a joint set, they have been included

in the kinematic analysis and the recorded persistent assigned to each structure utilised.

Toppling analysis involves plotting a plane, representing the bench face slope angle and a slip limit; the latter is defined as a plane with a dip direction parallel to the pit slope, and a dip equal to the bench face angle, minus the joint friction angle (for example, 75° (BFA) – 22° (friction angle) = 45° (slip limit)). The confined toppling region indicates where toppling failure is likely located. By comparing the number of joint and major structure poles within the confined zone with the total number of poles in the parent cluster, it is possible to determine the qualitative probability for toppling failure for a given rock type and pit slope orientation.

Planar Sliding failure is characterised by slip on a pre-existing near-planar surface that dips out of the rock face. Depending on the excavation geometry, there may be releasing planes on either side of the failure and a tension joint behind the failure. The pre-existing structure upon which sliding occurs could be a fault plane, a fracture, or a joint set, but is very often layering-parallel (sedimentary or metamorphic) jointing/partings that dip into the excavation at angles greater than the friction angle of the said surface. It is quite common in open pits for layering on one side of the pit to be unfavourably orientated and to create a sliding type slope stability problem on a single side of the pit.

Planar failure analysis is undertaken by employing a friction cone and a daylight envelope to test for combined frictional and kinematic scenarios where planar sliding is possible. Any poles falling within the envelope are kinematically free to Slide, if frictionally unstable. Any pole falling outside of the frictional cone represents a plane that could Slide if kinematically possible. The crescent shaped zone formed by the daylight envelope and the pole friction circle therefore encloses the region of planar sliding, where planes are free to Slide both frictionally and kinematically. Again, by comparing the number of poles in the parent cluster, it is possible to determine the qualitative probability of planar failure for a given rock type and pit slope orientation.

Wedge failure is characterised by slip of a wedge shaped block of rock along the intersection line of two discontinuity planes; in which case, the intersection line plunges into the pit at an angle that is steeper than the friction angle of the said surfaces (Hoek and Bray 1981). This is a very common failure type that can utilise combinations of pre-existing planar structures, including large fracture or fault planes to potentially cause failure on the scale of an entire slope.

The wedge analyses were undertaken by using the variable pit slope faces and a friction cone representing the plane friction angle. Wedge sliding may occur if the intersection points of two major planes fall within the zone identified by the friction cone and the pit slope. Wedge analyses were carried out on both the inter-ramp and bench scales.

The potential and level of risk related to wedge instability, both on an inter-ramp and bench scale, was evaluated with MWedge software. For impacted pit slope dip direction ranges, wedge risk is limited to ±45º from the midpoint of the selected pole feature.

Persistence length up to 30 m for all joint sets was assumed, along with a standard deviation of 15 m. A designed joint cohesion of 0 kPa and friction angle of 22º was used in the analyses. Bench height of 10 m was analysed.

Kinematic analysis was performed at 30º slope direction intervals to cover all critical slope dip directions and for 70º, 75°, 80°, 85° and 90º bench face angles.

9.2.2 Planar Assessment

A quantitative assessment of planar instability was undertaken, considering the proportion of critical planar sliding poles for a range of bench face angles and dip direction, as presented in Table 9-2 and Figure 9-4. These percentages give an estimate of 'probability of failure' with respect to all planes logged for the critical joint sets at Engebø. Results show that the risk of planar failure is highest for the eastern/north eastern slopes of the pit (that dip to the west/southwest) as a result of the intersection of the pit slope and joint sets J2 (86/201) and J3 (70/245) with the likelihood of instability increasing as the bench face angle increases. Given the sub-vertical nature of J2 and J3 it is considered that in general, planar instability would be confined to bench scale instability with minor crest loss.

Table 9-2: Planar instability showing likelihood of kinematic instability on critical joint set

Slope Dip Direction	70° BFA	75° BFA	80° BFA	85° BFA	90° BFA
0	Low	Low	J2 7%	J2 14%	J2 20%
20	Low	Low	J2 14%	J2 22%	J2 37%
40	Low	Low	J2 6%	J2 8%	J2 18%
60	Low	Low	Low	Low	Low
80	Low	Low	Low	Low	Low
100	J1 19%	J1 19%	J1 19%	J1 19%	J1 19%
120	J1 28%	J1 28%	J1 28%	J1 28%	J1 28%
140	J1 21%	J1 21%	J1 21%	J1 21%	J1 21%
160	J1 13%	J1 13%	J1 13%	J1 13%	J1 13%
180	J1 10%	J1 10%	J2 16%	J2 22%	J2 28%
200	J1 5%	J2 17%	J2 34%	J2 47%	J2 61%
220	J3 19%	J3 29%	J3 41%	J3 47%	J3 47%
240	J3 31%	J3 60%	J3 72%	J3 78%	J3 78%
260	J3 23%	J3 54%	J3 60%	J3 60%	J3 60%
280	J3 6%	J3 16%	J3 22%	J3 22%	J3 22%
300	Low	Low	Low	Low	Low
320	Low	Low	Low	Low	Low
340	Low	Low	Low	Low	Low

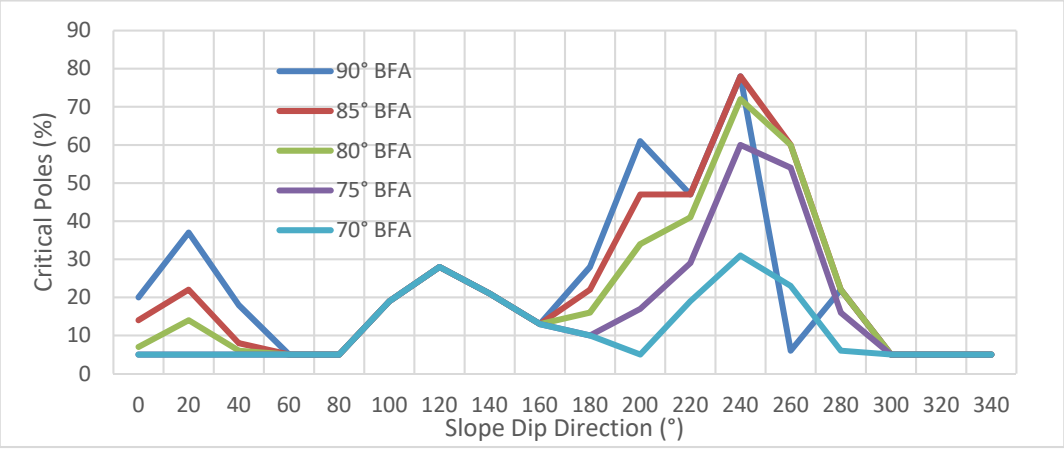

Figure 9-4: Planar failure assessment results

9.2.3 Toppling Assessment

A quantitative assessment of flexural toppling instability was undertaken, considering the proportion of critical toppling poles for a range of bench face angles and dip direction, as presented in Table 9-3 and Figure 9-5. These percentages give an estimate of 'probability of failure' with respect to all planes logged for the critical joint sets at Engebø. Results show that the risk of toppling failure is highest for the southern slopes of the pit (that dip to the north) as a result of the intersection of the pit slope and joint set J2 (86/201). In addition, within the northern slope, joint set J1 (13/144) dips to the south and may potentially form a basal release surface for sliding. Given the wide spacing of the prevalent joint sets and high intact rock strength, toppling instability is not considered to be a ubiquitous failure mode within the pit and will likely be confined to localised failures.

Table 9-3: Toppling instability showing likelihood of kinematic instability on critical joint set

Slope Dip Direction	70° BFA	75° BFA	80° BFA	85° BFA	90° BFA
0	J2 28%	J2 28%	J2 28%	J2 28%	J2 28%
20	J2 61%	J2 61%	J2 61%	J2 61%	J2 61%
40	J3 47%	J3 47%	J3 47%	J3 47%	J3 47%
60	J3 78%	J3 78%	J3 78%	J3 78%	J3 78%
80	J3 60%	J3 60%	J3 60%	J3 60%	J3 60%
100	J3 22%	J3 22%	J3 22%	J3 22%	J3 22%
120	Low	Low	Low	Low	Low
140	Low	Low	Low	Low	Low
160	Low	Low	Low	Low	Low
180	J2 20%	J2 20%	J2 20%	J2 20%	J2 20%
200	J2 37%	J2 37%	J2 37%	J2 37%	J2 37%
220	J2 18%	J2 18%	J2 18%	J2 18%	J2 18%
240	Low	Low	Low	Low	Low
260	Low	Low	Low	Low	Low
280	Low	Low	Low	J1 14%	J1 18%
300	Low	Low	Low	J1 22%	J1 27%
320	Low	Low	Low	J1 13%	J1 20%
340	Low	Low	Low	Low	J1 13%

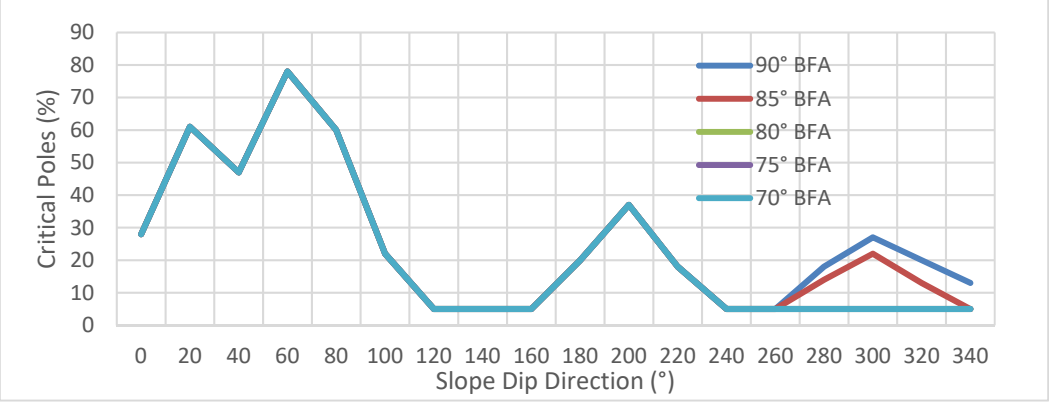

Figure 9-5: Toppling failure assessment results

9.2.4 Wedge Assessment

A quantitative assessment of wedge instability was undertaken, considering the proportion of critical plane intersections for a range of bench face angles and dip directions, as presented in Table 9-4 and Figure 9-6. These percentages give an estimate of 'probability of failure' with respect to all planes logged for the critical joint sets at Engebø. Results show that the risk of planar failure is highest for the eastern slopes of the pit (that dip to the west/southwest) as a result of the intersection of the pit slope and joint sets J2 (86/201) and J3 (70/245). Given the sub-vertical nature of these joint sets, it is likely that wedge geometry would be restricted although larger wedges may have the potential to develop as a result of the variable orientation of the J2 and J3 joint sets.

To further understand the likelihood of wedge instability, probabilistic wedge simulation analyses were undertaken in MWedge. MWedge uses statistical joint orientation distribution to simulate 10,000 blocks. Each block is formed by the intersection of two joints from any of the joint sets of the domain. A multiple number of joint sets can be loaded in the software and read from an external file. The geometry and volume of each of the 10,000 wedges simulated is calculated. The mode of failure of each wedge is identified and the factor of safety ("FoS") is then calculated. The probability of failure is calculated as the percentage of wedges with a FoS <1.

Table 9-4 presents the results of the wedge analysis and Figure 9-6 providing the berm widths required to contain 80% of failed material for a 15 m bench height. The tables show the berm widths required to hold all the failed wedges generated in the analysis (100%), in addition to 90% or 80% of the failed wedges. A design threshold of 80% have been chosen as acceptance criteria. Designing the slope using the berm width required to hold 80% of the failed wedges means that the bigger wedges, accounting for 20% of the simulated wedges would not be fully retained on the 80% berm width and will spill over the berm. A probability of failure of 50% maximum is generally accepted for the bench design.

Within Table 9-5, the cells highlighted red indicate zones of the pit where the probability of wedge instability is greater than 50%. In general, it can be observed that such zones fall within the eastern section of the pit. It can be seen that a 5 m berm width is suitable to catch 80% of the likely failure volume for the majority of the pit. In the eastern section of the pit, where the probability of wedge instability exceeds 50%, a 6 m berm will be required to contain 80% of the likely failure volume (Figure 9-7).

Table 9-4: Wedge instability showing likelihood of kinematic instability on critical joint set

Slope Dip Direction	70° BFA	75° BFA	80° BFA	85° BFA	90° BFA
0	22%	22%	27%	31%	36%
20	15%	15%	20%	25%	31%
40	13%	13%	16%	19%	24%
60	14%	14%	16%	19%	22%
80	16%	16%	17%	20%	22%
100	18%	18%	20%	22%	24%
120	20%	20%	23%	25%	28%
140	22%	22%	24%	27%	31%
160	24%	24%	27%	31%	35%
180	25%	25%	30%	35%	40%
200	28%	28%	35%	41%	47%
220	34%	34%	42%	48%	53%
240	41%	41%	47%	52%	55%
260	42%	42%	47%	51%	54%
280	40%	40%	45%	48%	52%
300	36%	36%	40%	44%	47%
320	33%	33%	36%	39%	43%
340	28%	28%	32%	36%	40%

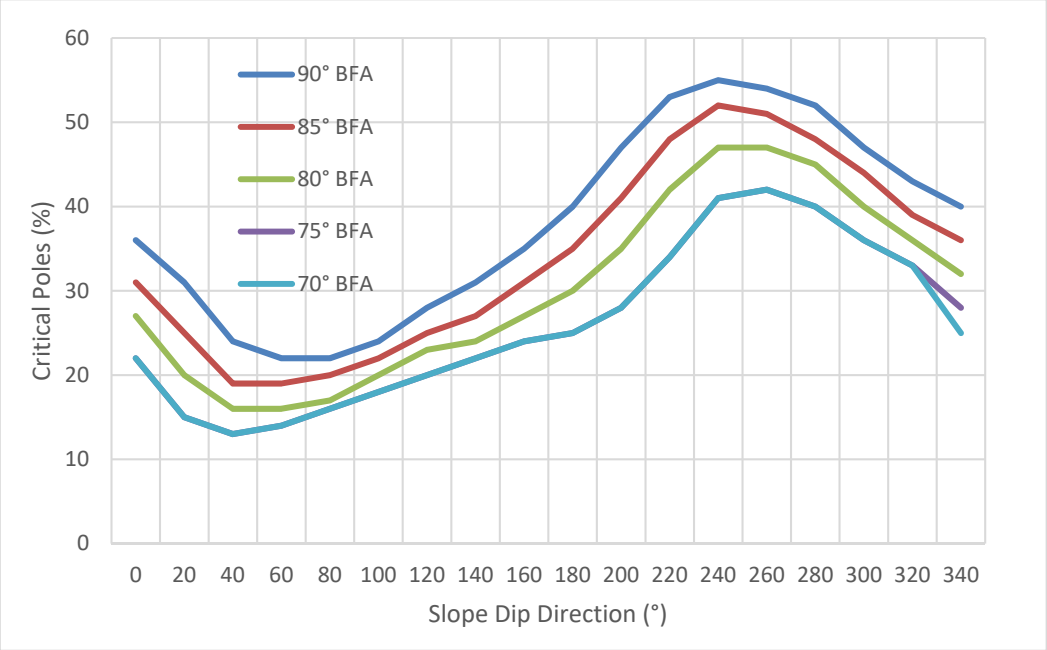

Figure 9-6: Wedge failure assessment results

Table 9-5: Summary of probabilistic wedge analysis

Slope Dip Direction (°)	Slope Dip (°)	PoF (%)	Max Berm Required to retain 80% Wedges	Max Berm Required to retain 90% Wedges	Max Berm Required to retain 100% Wedges	Max unstable Wedge Volume (m^3)
0	70	18.8	3.5	4	9	288
30	70	8.6	3.5	4	8	207
60	70	15.6	4.5	5.5	9	321
90	70	18.4	4.5	5.5	9	289
120	70	18.6	5	5.5	9	297
150	70	19.4	5	6.5	9.5	328
180	70	24.4	5	6	9	300
210	70	26.7	5	6	11	506
240	70	40.7	3.5	4.5	9	265
270	70	53.7	4	5	9.5	363
300	70	50.3	4	5	8.5	230
330	70	40.3	4	4.5	8	204
0	75	26.8	3.5	4.5	10	368
30	75	11.1	3.5	4	9.5	329
60	75	16.4	5	6	10.5	430
90	75	19.3	5	6	9	277
120	75	19.7	5	6	9.5	292
150	75	19.9	5.5	6	9.5	296
180	75	26.7	5	6	10	364
210	75	33.4	5	6	10.5	423
240	75	51.1	3.5	4.5	9.5	333
270	75	59.2	4.5	5.5	10	336
300	75	54.9	4.5	5.5	9.5	300
330	75	48.5	4	4.5	8.5	227
0	**80**	**32.6**	**4**	**5**	**10.7**	**424**
30	**80**	**21.6**	**4**	**4.5**	**8.3**	**204**
60	**80**	**29.3**	**4.5**	**5.5**	**9.3**	**281**
90	**80**	**36.1**	**4**	**5**	**8.7**	**251**
120	**80**	**34.5**	**5**	**6**	**9.7**	**323**
150	**80**	**32**	**5**	**6**	**10.3**	**386**
180	**80**	**32.3**	**5**	**6**	**9.8**	**334**
210	**80**	**34.8**	**5.5**	**6.5**	**9.8**	**334**
240	**80**	**41.4**	**4**	**5**	**9.4**	**292**
270	**80**	**53**	**5.5**	**6**	**10.2**	**371**
300	**80**	**56**	**5**	**6**	**9**	**259**
330	**80**	**51**	**4.5**	**5.5**	**8.6**	**223**
0	85	46.6	4.5	5.5	9.5	271
30	85	19.4	4	5	9.5	269
60	85	18.5	6	6.5	10	303
90	85	21.8	5	6	10	288
120	85	21.3	5.5	6.5	9.5	246
150	85	23.9	5.5	6.5	10	306
180	85	31.4	5.5	6.5	11	390

Slope Dip Direction (°)	Slope Dip (°)	PoF (%)	Max Berm Required to retain 80% Wedges	Max Berm Required to retain 90% Wedges	Max Berm Required to retain 100% Wedges	Max unstable Wedge Volume (m^3)
210	85	49.8	5.5	6.5	12	546
240	85	58.5	4.5	5.5	12	500
270	85	63.9	6	7	10.5	349
300	85	61.2	5.5	6.5	10	313
330	85	58.6	5	6	9	218
0	90	55.4	5	6	11	400
30	90	26.7	4	5	9.5	231
60	90	20.4	6	7	10.5	343
90	90	23.1	5.5	6.5	10	265
120	90	23.4	5.5	6.5	10.5	318
150	90	25.4	5.5	6.5	10	297
180	90	34.4	5.5	6.5	12	481
210	90	53.5	5.5	6.5	11	391
240	90	59.3	4.5	6	12.5	538
270	90	65.9	6.5	7.5	10.5	346
300	90	62.3	6	7	10.5	310
330	90	60.1	5.5	6.5	9.5	249

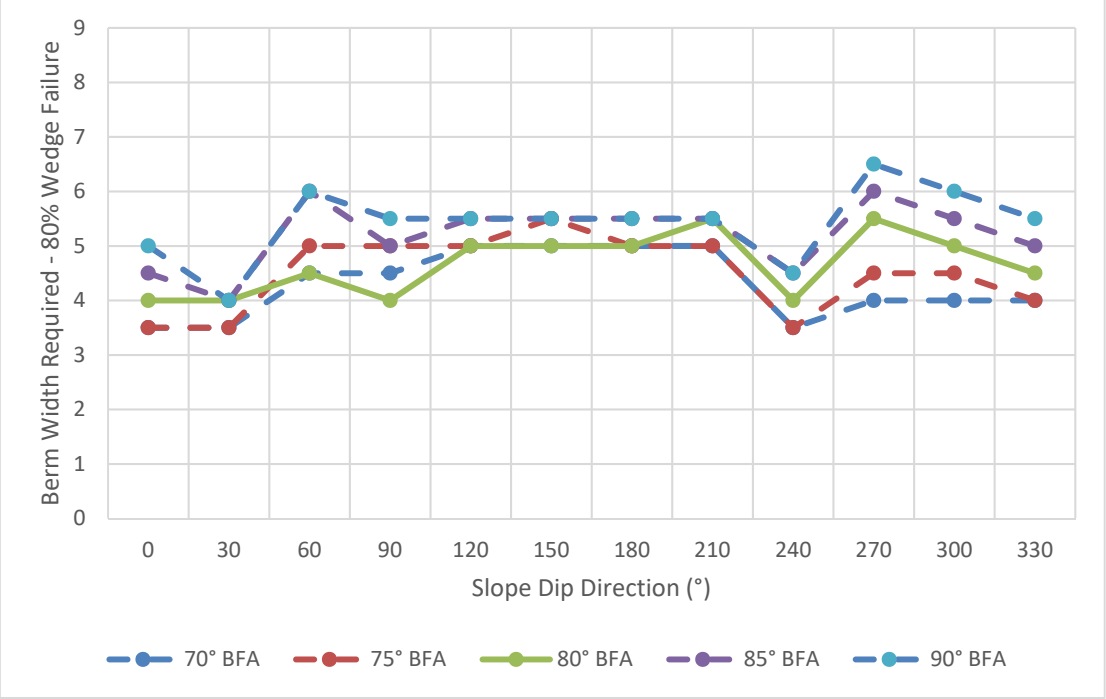

Figure 9-7: Berm width requirement: 15 m bench height (80% retention)

9.3 Rockfall Analysis

In view of the risk that part of the failed material could spill over the berms below, rock fall analyses were carried out to determine how far down the slope the overspill material would fall. The software Trajec3D (BasRock) was used for these analyses. Trajec3D is a three-dimensional rigid body rock fall analysis program that can simulate the trajectory of volumetric bodies during free fall, bouncing, sliding and rolling. Trajec3D enables the quick assessment of many scenarios to better understand potential trajectories that dislodged rocks could follow, the time it should take to reach areas of interest, and an estimate of the energy along the trajectory. Trajec3D is a simplification of reality with the aim to investigate different possibilities. This software does not take into account the breakage of blocks during their fall, thus giving conservative results.

The weight distribution of all unstable wedges generated in MWedge for the most critical slope direction (80°/270°) are presented in Figure 9-8. These distributions show that for both pit, 80% of the simulated unstable wedges have a mass less than 50 t.

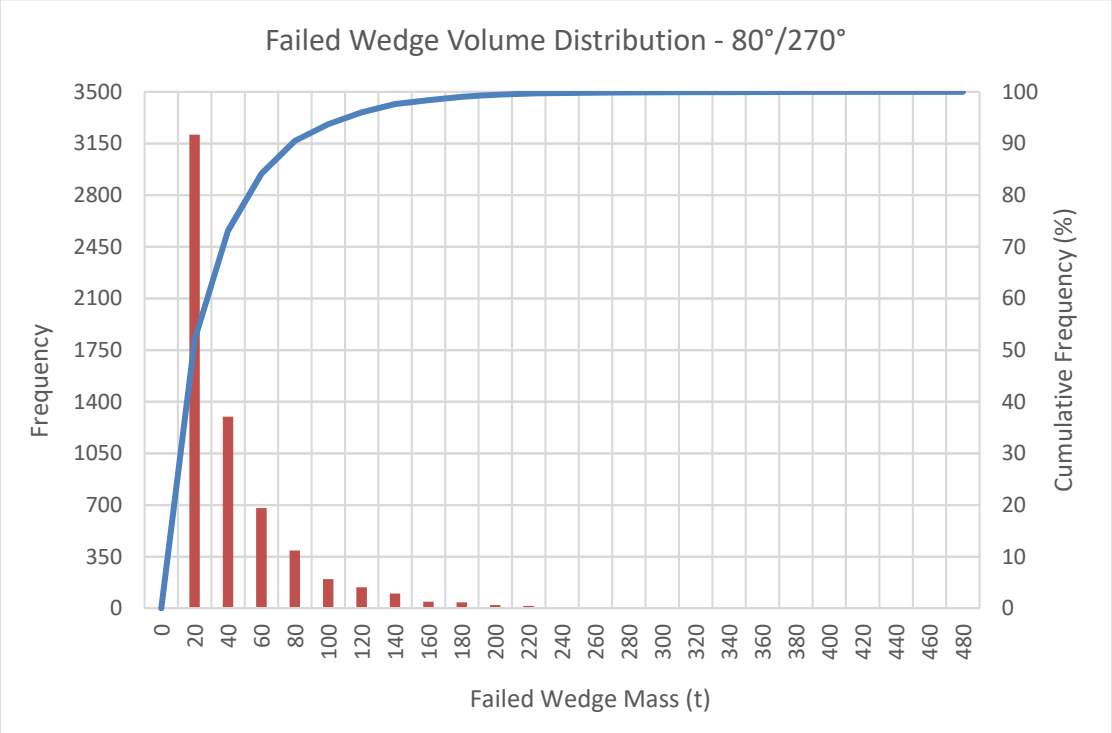

Figure 9-8: Weight Distribution of Failing Wedges

Generic inter-ramp models were generated for each scenario, based on the MWedge results. The fall of around 10 cubical blocks of 50 t, 100 t, and 500 t was analysed. Trajec3D only allows the use of a fixed range of weights. The shape and weight used in the analyses were considered to be the most suitable. Five runs were tested for each scenario. No initial speed was entered; no interaction between the blocks was possible.

For each run, the number of blocks stopping on the first, second, third benches and below was counted. Image capture of Scenario 1, run 5 is presented on Figure 9-9. All simulation results and an assessment of 'rockfall risk' are summarised and in Table 9-6. Rockfall risk is estimated as follows:

- Low risk if over 60% of the failing wedges are stopped on the first or second bench.
- Moderate risk if between 40 and 60% of the wedges are retained on 1st or 2nd bench.
- High risk if less than 40% of the unstable wedges are retained on the 1st or 2nd bench.

When analysing the path of cubic blocks, the rockfall risk can be considered low with the majority of cubic blocks being retained on the first or second bench below the seed point. When rough sphere blocks were assessed, the risk from rockfall increases significantly, although SRK considers a more cubic block shape more likely.

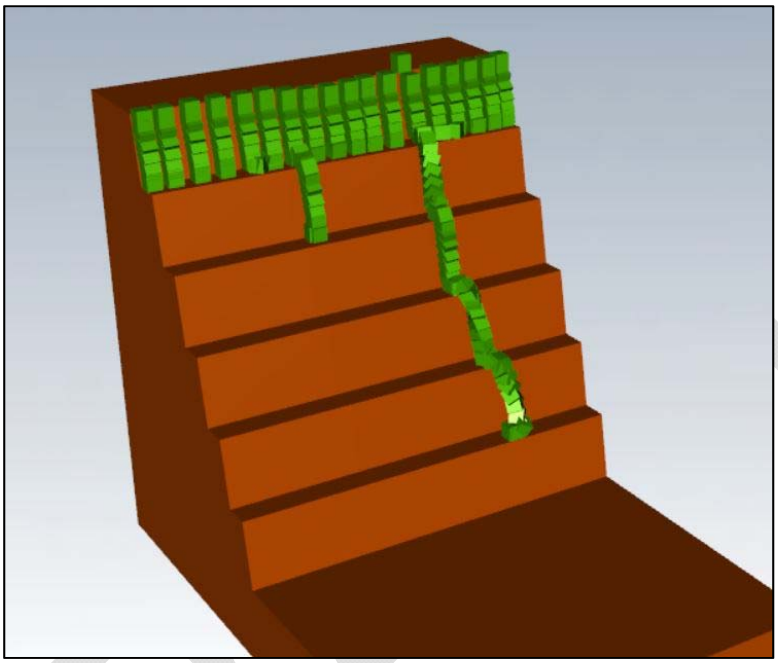

Figure 9-9: Trajec3D Results: Scenario 1, run 5

Table 9-6: Trajec3D results summary

BFA (°)	Berm Width (m)	Block Mass (t)	Block Shape	% Blocks retained on 1st or 2nd bench	Rockfall Risk
80	5	100	Cubic	97	Low
80	5	500	Cubic	100	Low
80	5	50	Cubic	100	Low
80	5	100	Rough Sphere	51	Moderate
80	5	500	Rough Sphere	3	High

10 FINITE ELEMENT MODELLING

10.1 Approach

Finite Element Analysis ("FEA") has been undertaken with the aim of considering the stability of representative overall slope configurations. Results from the FEA stability analysis are used in combination with those of the kinematic analysis to define the final slope configuration recommendations presented within this document. Note that staged pit walls (non- final walls) have not been analysed at this time.

Overall slope stability analysis was undertaken using the FEA program, RS², (Rocscience, 2011). RS² was selected for this assessment due to its ability to model stresses distribution within the slope and provide an indication of the location and shape of any potential failure surface.

The program undertakes stability analysis by the procedure of strength reduction where the factor of safety (the Strength Reduction Factor or "SRF") is obtained by progressively weakening the rock mass until the slope "fails". The SRF is deemed to be the factor by which the rock mass strength needs to be reduced to reach failure. Numerically, the failure occurs when it is no longer possible for the program to obtain a converged solution because the equations of stress-strain formulation are beyond the point of limiting equilibrium.

10.2 Acceptance Criteria

Historically, the most used criterion has been the FoS, a deterministic measure of the ratio between the resisting and driving forces in the system. A state of balance or limiting equilibrium occurs when the FoS has a value of 1.0. As the FoS is a deterministic measure, the uncertainty in its value is usually accounted for by setting a prescribed minimum design acceptance value, derived from experience.

Typically accepted FoS and Probability of Failure ("PoF") values are presented in Table 10-1 (Read & Stacey, 2009). The selection of an acceptable FoS values depends on the permanence of the slope and the consequences of failures. At this stage, neither the location of the access ramp nor number of access ramps is known. For the purpose of this study, it is assumed that access ramps will be permanent, needing to be safe throughout the life of mine. A consequence of slope failure of the pit walls is therefore regarded as high. Based on the data in Table 10-1, SRK considers a FoS of 1.3 and a PoF of 5% as appropriate overall slope acceptance criteria for the Engebø pit. A FoS of 1.2 was chosen for the overburden slope design.

Table 10-1 Acceptance criteria

Slope Scale	Consequences of Failure	Acceptance criteria		
		FoS (min) (static)	FoS (min) (dynamic)	PoF (max) P[FoS≤1]
Bench	Low-high	1.1	n/a	25-50%
Inter-ramp	Low	1.15-1.2	1.0	25%
	Moderate	1.2	1.0	20%
	High	1.2-1.3	1.1	10%
Overall	Low	1.2-1.3	1.0	15-20%
	Moderate	1.3	1.05	10%
	High	**1.3-1.5**	**1.1**	**5%**

10.3 Geotechnical Cross Sections

The FEA 2D models were created by consideration of the available 3D geological model, the established rock mass domains and the kinematic constraints. The applicable wireframe CAD models were investigated and the completed critical sections imported into RS². Each digitised polygon was then converted to a FEA mesh and coded with representative material properties in addition to apply a fracture network to certain cross-sections. For the stability models, inter-ramp slope angles were set to match the likely maximum allowable kinematic design.

Due to the simplicity of the current available geological model, in addition to the consistency of material from rock mass characterisation of the major lithologies, SRK has developed a geotechnical model that incorporates a single fresh rock domain primarily containing:

- Trans
- Amph
- Leuco
- Ferro
- Gneiss

SRK has developed three geotechnical cross-sections that intersects north, south, and east walls of the proposed pit. Inter-ramp stack heights have been limited to a maximum of 90m with inter-ramp angles at 63°. A single groundwater surface has been modelled on each section and takes into account the understanding of the likely drawdown resulting from mining.

Figure 10-1 shows the location of the geotechnical cross sections and Figure 10-2 an example of a geotechnical cross section.

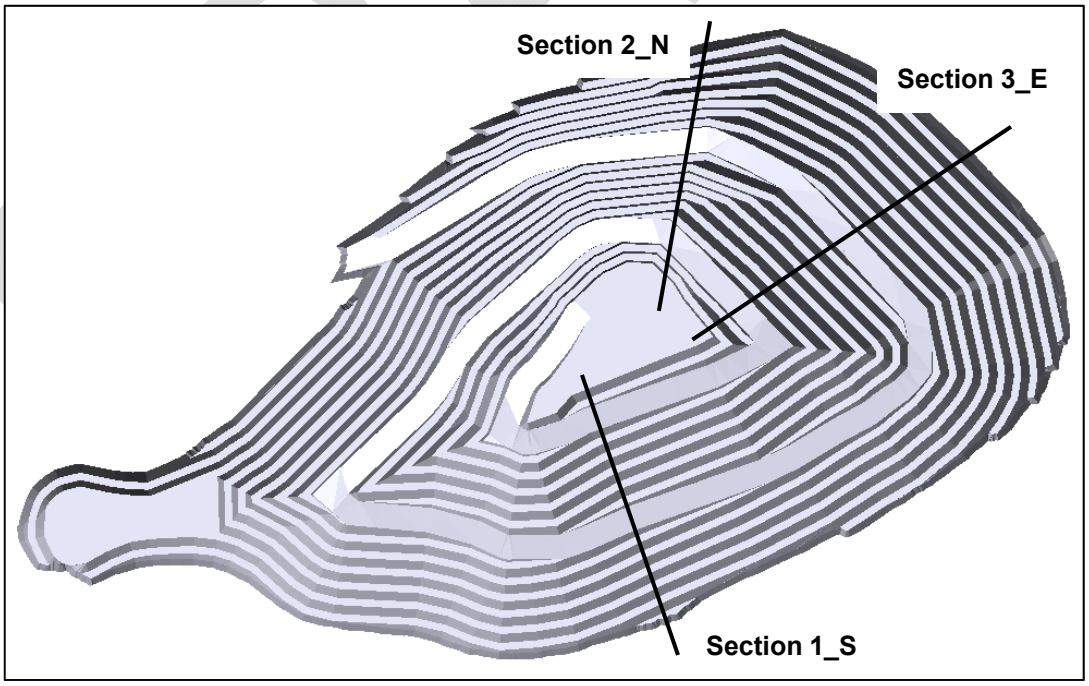

Figure 10-1: Location of geotechnical cross-sections

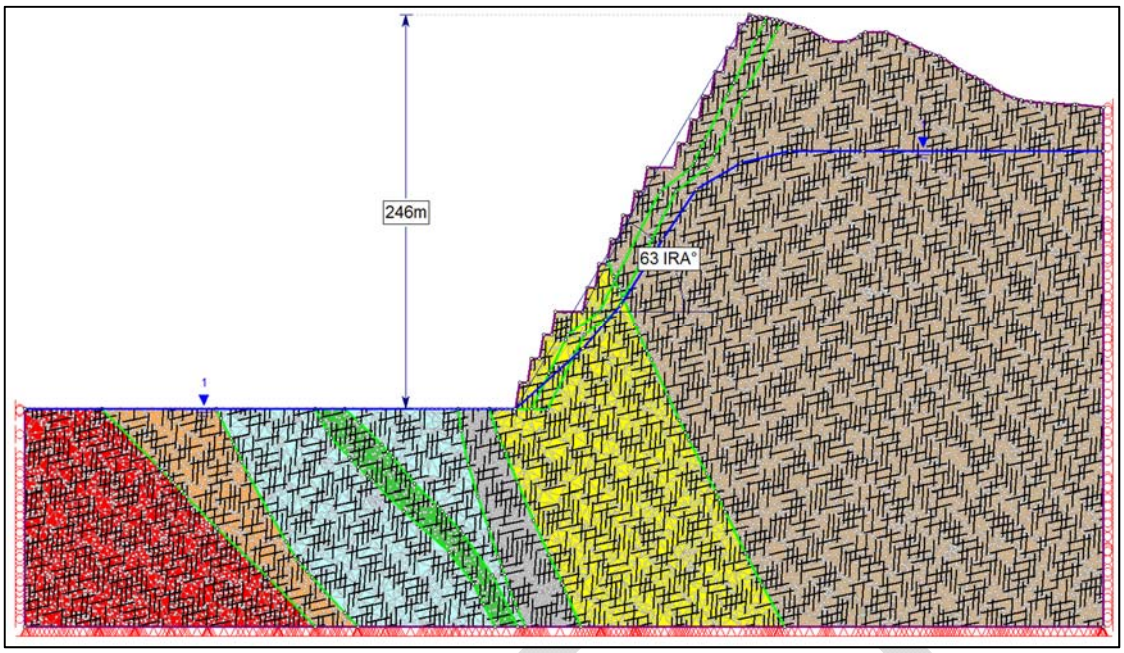

Figure 10-2: CS2_N cross-section showing joint network model

10.4 Input Design Parameters to Slope Stability Analysis

The modelling input parameters were collated from the data presented within the previous sections. The Hoek-Brown strength criterion was used for the fresh rock. The Hoek-Brown strength criterion is a non-linear criterion where the shear strength mobilised in any part of the rock mass is a function of the strength of the rock mass and the confining stress within the rock mass. These factors are summarised in Table 10-2 and Table 10-3. The calculation of this criterion requires a number of parameters. The main input parameters required are:

- Intact rock strength (IRS), Young's Modulus and Poisson's Ratio which have been defined within the laboratory testing programme.
- Geological Strength Index (GSI), for which average values for each geotechnical zone have been estimated based on the unadjusted RMR values. The two classifications are broadly similar and take into account similar properties, being the scale of the rock blocks and the condition of the discontinuities. The use of the RMR correlated to GSI is therefore considered acceptable, with GSI=RMR^{89}-5. For the modelling, it has been chosen to take the design RMR^{89} value as the value of the mean RMR^{89}.
- A material constant of the intact rock, *mi*. SRK have used data from triaxial testing.
- Hydrogeology: A phreatic surface defined on data collected during concurrent hydrogeological studies has been defined.
- Model Type: SRK assessed plane strain models. There may be an opportunity to use axisymmetric models to assess the influence of confinement as a result of the circular nature of the pit although SRK considers that this will be more applicable as the pit increases in depth.
- In addition to assessment assuming isotropic conditions, SRK has applied a fracture network model to incorporate the dominant joint sets in to the geotechnical model.
- The D value, which is the disturbance factor. This factor accounts for the disturbance and strength reduction of the in situ rock mass by blasting and stress relief. A 'D' factor of 0.7

indicating good blasting was applied to the outer skin of the model. An additional 'D' skin of 0.4 was also applied before the rock was modelled as undisturbed and 'D' 0 applied to the rock mass.

Table 10-2: Summary of rock mass strength used within modelling

Lithology	GSI	mi	UCS (MPa)
Gneiss	75	11	126
Leuco	72	12	207
Trans	70	20	289
Ferro	70	11	290
Amph	71	19	195
Alternating	70	15	150
Other	70	15	150

Table 10-3: Summary of fracture network parameters

Set ID	Dip	Dip Direction	Cohesion (kPa)	Friction Angle (°)	Spacing (m)	Persistence (m)
JS1	86	201	112	22	3	40
JS2	13	142	112	22	10	10

10.5 Finite Element Analysis Results

All models assessed that looked at both an isotropic rock mass and inclusion of fracture network returned Strength Reduction Factor ("SRF") results in excess of 3 indicating stable conditions in relation to significant instability through the rock mass. Failure through the intact rock bridges is unlikely given the extremely high intact rock strength, widely spaced joints, high rock mass strength and relatively low stress environment given the relatively small nature of the pit.

Given the initial models returning such high SRF values, it was not considered necessary to run a probabilistic analysis.

Table 10-4 presents a summary of the slope stability analysis results. Figure 10-3 to Figure 10-5 show outputs from the finite element analysis.

Table 10-4: Summary of finite element results

Model	Overall Slope Height (m)	Inter-Ramp Angle (°)	Groundwater	SRF (=FoS)	Failure Description
North - Isotropic	246	63	Yes	>5	Stable slope
North – Fracture Network	246	63	Yes	>4.5	Small build-up of strain at the toe of the slope
North – Fracture Network (topple)	246	63	Yes	3	Zones of localised potential toppling
South - Isotropic	175	63	Yes	>7	Stable slope
South – Fracture Network	175	63	Yes	>5	Stable Slope
East - Isotropic	253	63	Yes	>5	Small build-up of strain at the toe of the slope

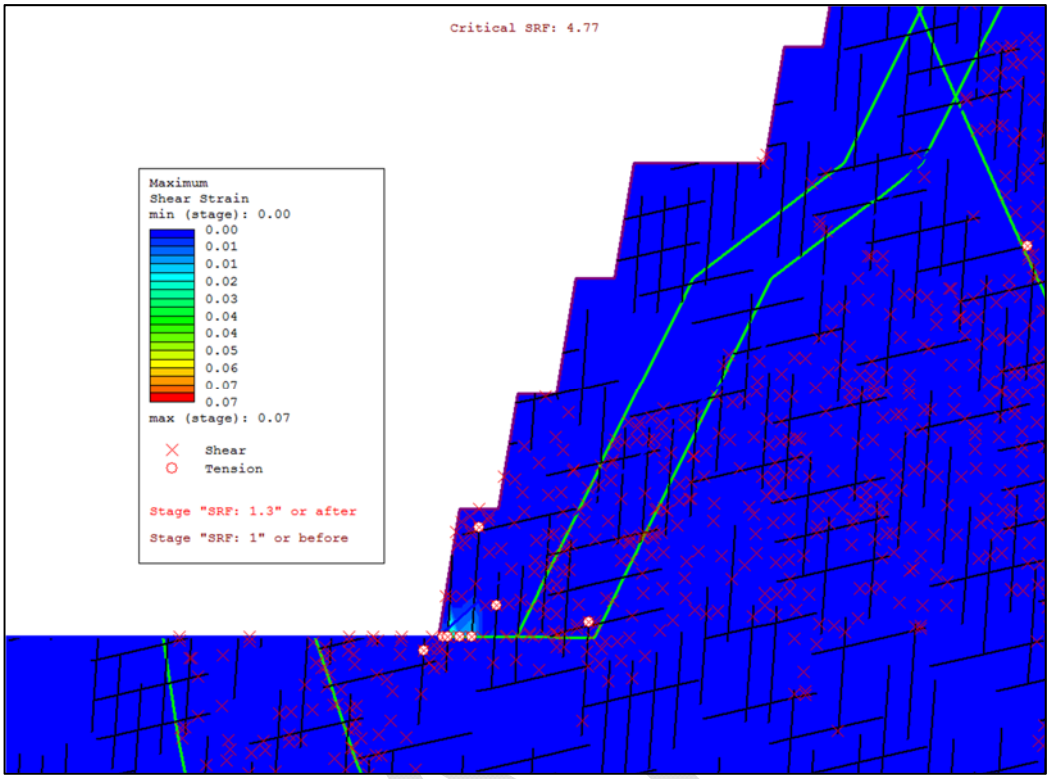

Figure 10-3: CS2_N joint network model showing minor strain build up at the toe of the slope

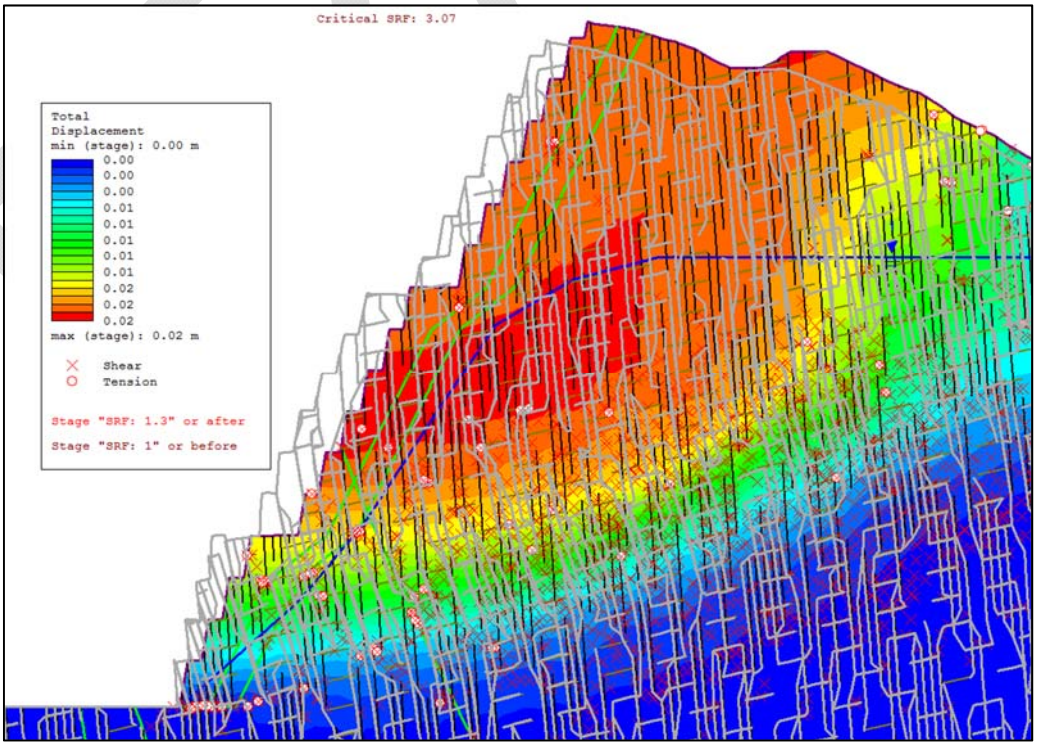

Figure 10-4: CS2_N joint network toppling model. Note grey mesh is an exaggerated simulation of direction of slope movement

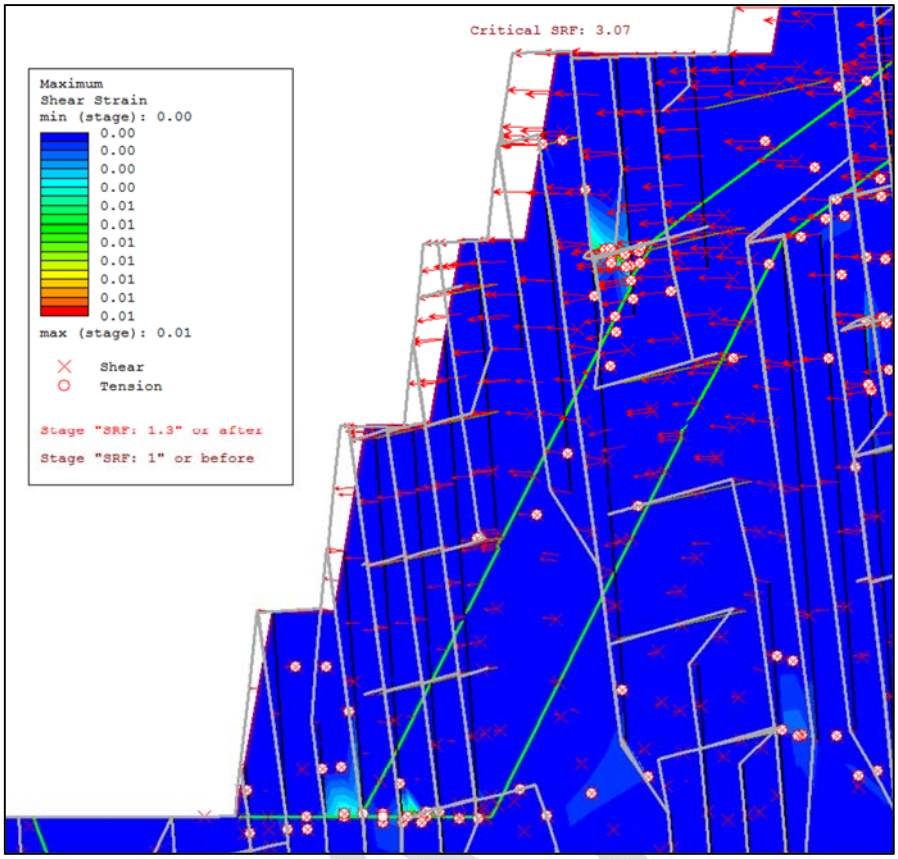

Figure 10-5: CS2_N joint network toppling model showing localised areas of potential toppling with strain build up in a rock bridge between the two modelled fracture sets

11 SLOPE DESIGN CRITERIA

Given the very limited presence of overburden and the fact that fresh rock conditions are observed at surface, SRK has only developed geotechnical design criteria for what can be considered fresh rock slopes.

Based on the structural conditions, kinematic analysis and slope stability modelling, SRK has identified two separate design domains (Domain 1 and Domain 2, respectively) which are differentiated as function of required berm width (Figure 11-1 and Figure 11-2). Analyses show that the maximum overall slope angles for the fresh rock is constrained by the bench and berm geometry, designed to minimise kinematic instability and trap potential rock fall. It should be noted that the maximum inter-ramp height should be 90 m, although a flexible approach to stack height may be required to ensure practical design. If no ramp is planned within the engineered pit slope design, a 17 m geotechnical berm should be constructed at the base of the stack. If a haul ramp is located at the toe of the 90 m stack, SRK recommends that a wider 10 m berm is designed within the stack to protect the ramp from rockfall. The other alternative would be to design wider ramps that can accommodate a rock fall containment trap and catch bund.

Analyses show that steep slope angles can technically be achieved, it may however be practically challenging to achieve the recommended inter-ramp angle and will require a strong design implementation strategy. Rock fall analysis results were based on clean berms. Scaling to remove loose rock from the bench faces, followed by clean-up of loose material along the bench toe should be implemented in order to significantly reducing the rock fall hazard. To achieve the recommended berm width, it will be essential to give special attention to blasting in order to minimise crest loss and formation of hard toe. Pre-splitting or good quality limit blasting on the slope face is therefore recommended. In order to maximise berm retention, all berms must be kept clean and free of loose blocks.

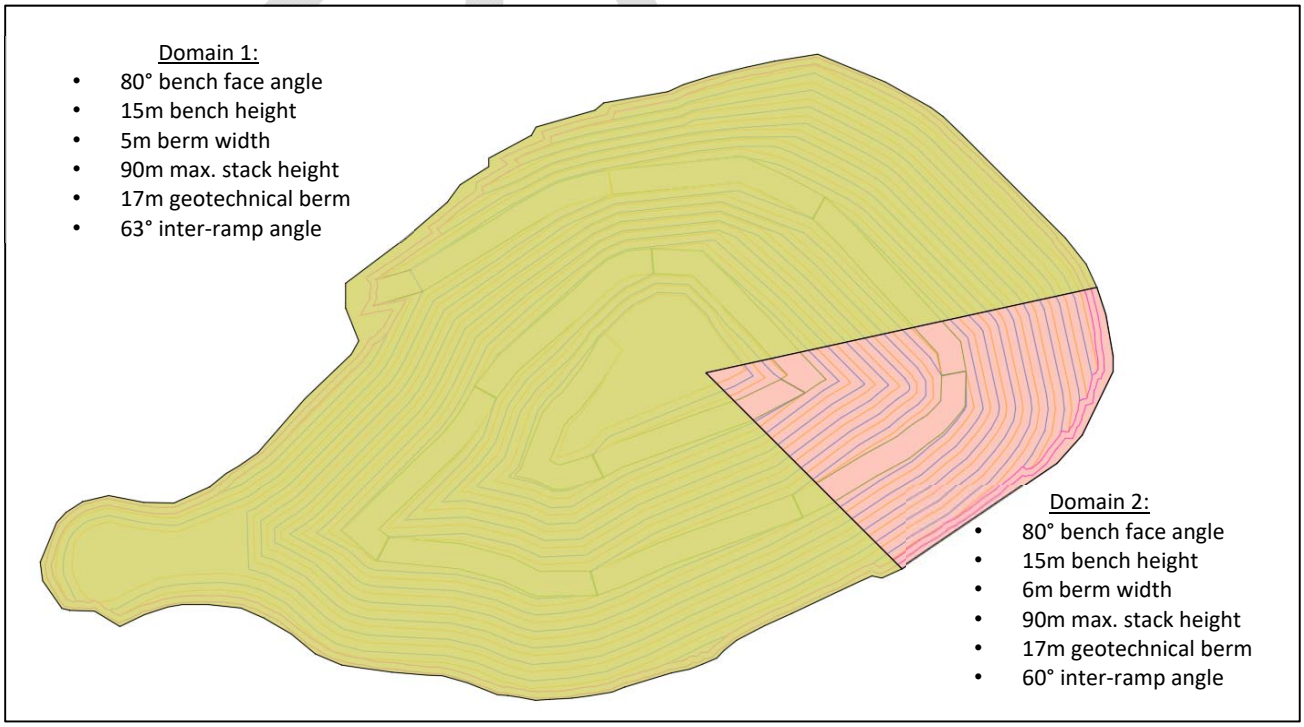

Figure 11-1: Geotechnical design domains

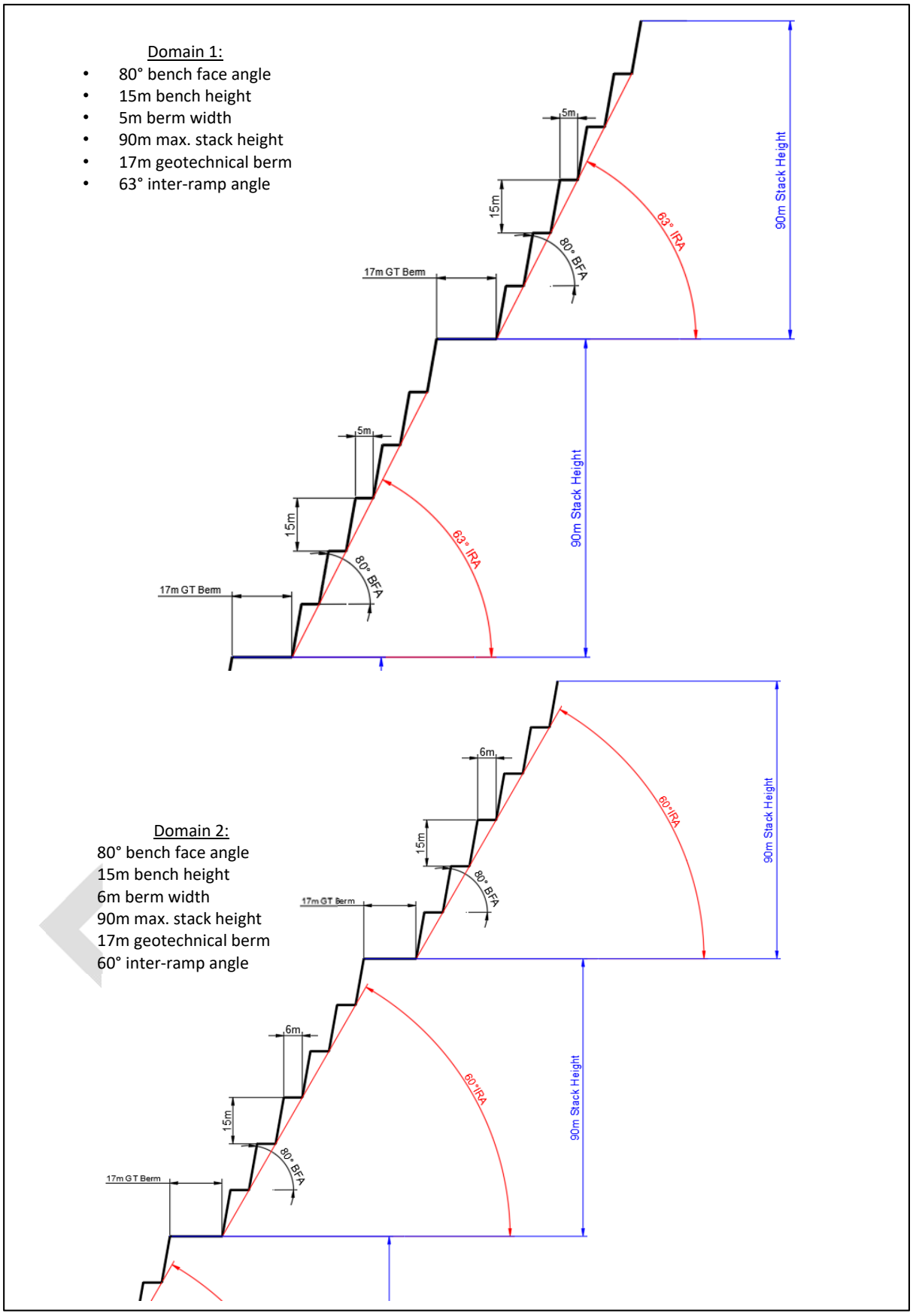

Figure 11-2: Slope design summary

12 ON-GOING DATA COLLECTION AND SLOPE MONITORING

Bench face mapping to update the geotechnical database should be carried out systematically. Mapping the extent and macro scale roughness of large structures, and their rock mechanical properties should be carried out. It will be critical to map and model high persistence joints as if these are orientated unfavourably to pit slope geometry then sliding of large blocks can occur. There will be sufficient opportunities to study the large-scale joints and faults and their impact on the slope stability during numerous push backs in the production phase of the pit. Slope stability analyses should be carried out as part of the on-going mine planning during production.

It will be critical that the slope monitoring strategy adopted for enabling the management of a design approach based upon 'controlled instability' is able to function well over a range of potential failure types. The selected combination of techniques, both observational and qualitative, must be able to handle all variations and combinations of potential failure size and rate.

Based on the experience and current levels of knowledge, the suitability of each of the monitoring techniques for varying failure sizes and rates are summarised in Table 12-1. It is noted that all the qualitative data acquisition systems do not have the capability of detecting rapid, small-scale surficial failures. For the detection of larger volumes in all areas of the open pit, a widespread survey prism network is currently considered to be the proven technique. By augmenting this system with other techniques such as radar, the management of potential instability in the operating areas of the pit is expected to be substantially enhanced.

Table 12-1: Summary of monitoring methods by potential failure size and implication

Block Size (m^3)	Speed of failure	Implications	Monitoring for detection	Typical remedial
1-10	Immediate	Rockall – safety	**Visual**	**Catchment**
10-1000	Very rapid to rapid	Safety	**Visual** Radar	**Catchment**
1000-100,000	Rapid to slow	Operational	Visual Surveying **Radar** Seismic (?)	**Manage** Modify slope (step-out)
100,000-1,000,000	Moderate to slow	Operational/financial	**Surveying** **Radar** TDR/inclinometer Seismic	**Manage** Modify slope (step-out) Re-cut
> 1,000,000	Slow to moderate	Force majeure	**Surveying** TDR/inclinometer Seismic Radar	**Modify slope (re-cut)** Mine closure (>10 Mn^3) Manage

Note: Bolding denotes most common approach for given block size.

SRK recommends using a Leica based survey system for the main component of the monitoring programme. This could start out as a manual system, but could be converted to an automated system with a number of prisms installed on the pit slopes faces; the requirement and extent of which would depend on the predicted risk. In addition, a slope stability radar ("SSR") based system for monitoring slope performance near active production areas at the Engebø pit would be invaluable as a real-time warning system for any potential instability.

In addition to the use of a survey system and SSR, the following is also required ensure appropriate pit slope management:

- Detailed structural and geological mapping using regular line mapping or a remote mapping system will be required as benches are continually excavated. Further material strength testing should also be undertaken as mining advances. This early information will be used to calibrate the proposed slope designs based on 3D exposure and the structures and the rock mass.
- Associated with the above programmes, it will be important undertake the following:
  - develop and maintain a dynamic mine hazard and evacuation plan;
  - regular face inspections;
  - record all failure histories; and
  - implement regular safety precautions around the pit slope areas.

13 UNDERGROUND INFRASTRUCTURE

A high-level assessment of the geotechnical conditions in the region of the planned underground infrastructure, namely the crusher station and silos has been undertaken. Borehole ENG18_10 intersected the infrastructure area in close proximity and rock mass and structural conditions assessed.

No clear signs of poor ground were noted within Borehole ENG18_10 in the region of the infrastructure, although the area is characterised by a number of strong joint sets which will have the potential to form unstable blocks given the likely dimensions of the infrastructure. In addition, the modelled fault that dips moderately to the north may intersect the proposed silo region (Figure 13-1). Indication from core photographs and geotechnical logging indicates that this fault is represented by an area of broken ground and may also act as a conduit for groundwater flow. Given their criticality to the mining process, the infrastructure will require an appropriate support design to ensure stability.

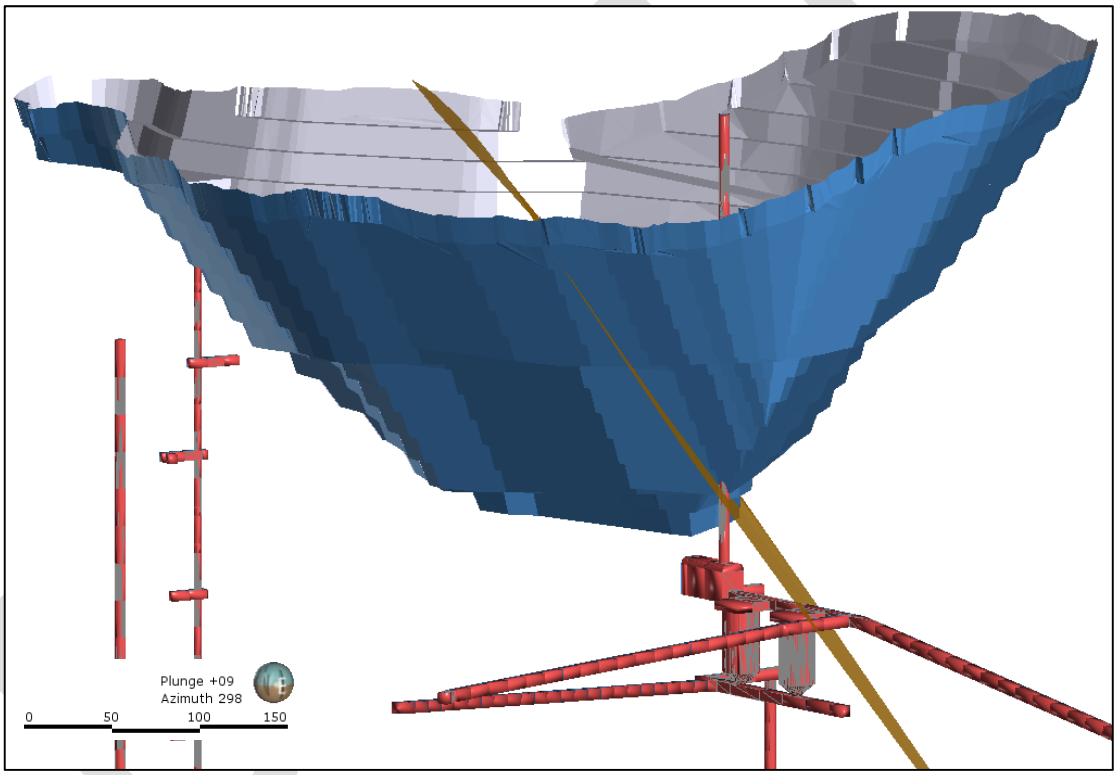

Figure 13-1: Fault intersection with proposed infrastructure

Average RMR[89] are approximately 70, which is similar to values generated for the rock mass within other areas of the pit.

Figure 13-2 shows the stereoplot of Borehole ENG18_10. A steeply dipping (to the west) joint set in addition to a shallow west dipping set can be seen. The development of unstable blocks should be assessed using appropriate software such as Dips and Unwedge and a support strategy implemented to ensure stable conditions are maintained.

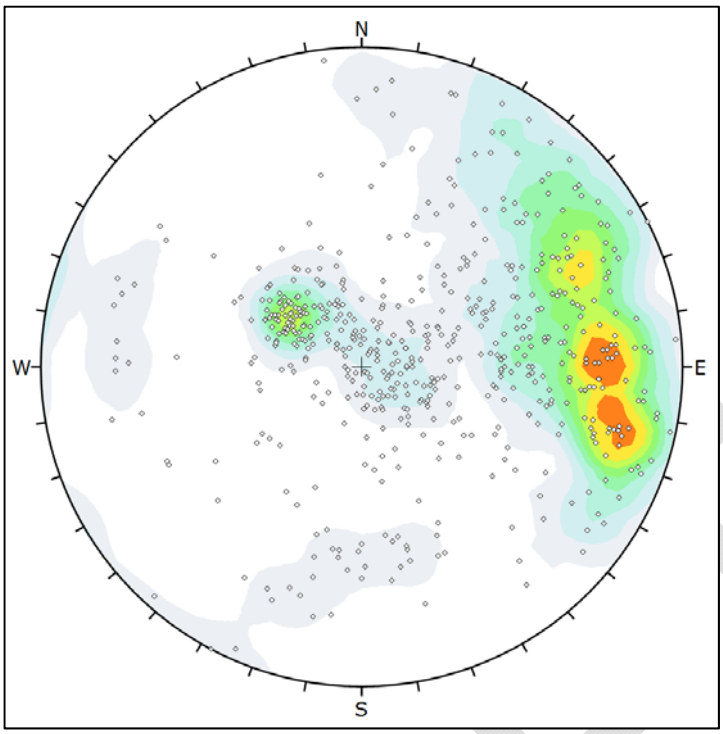

Figure 13-2: Borehole ENG18_10 stereoplot

A high-level assessment of the stability of the silo and crusher chamber has been undertaken using finite element modelling. Material parameters as defined in Section 10.4 have been maintained the location of the infrastructure in relation to the pit slope estimated according to the proposed current location and the 'Design 3' pit.

Figure 13-3 shows the location of the infrastructure and pit slope.

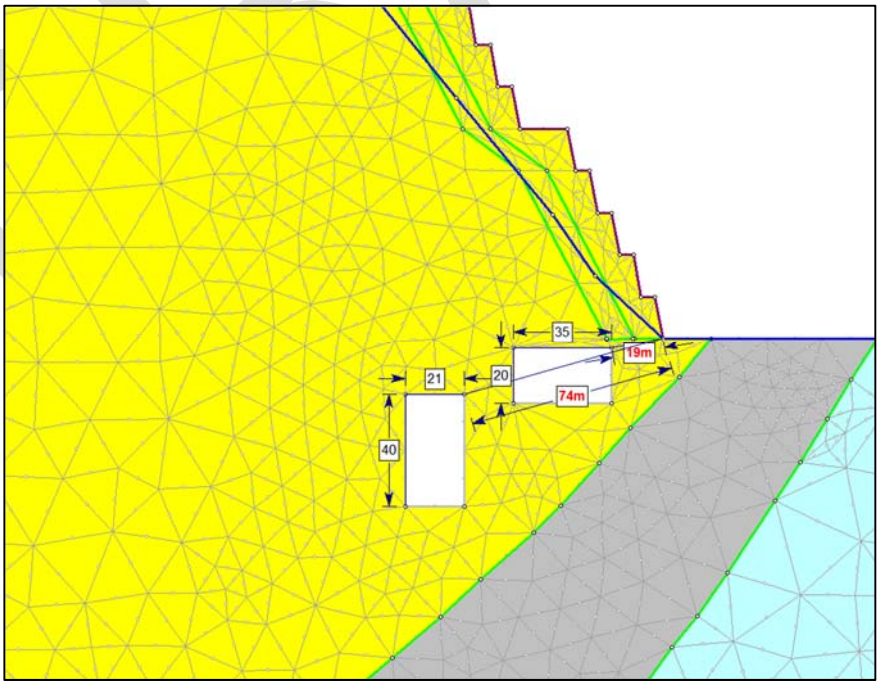

Figure 13-3: Infrastructure assessment cross section

Modelling of the interaction between the proposed infrastructure and the pit slope returns an SRF in excess of 3.5. Build-up of strain can be observed between the excavations although tangible displacement is evident (Figure 13-4). The development of an overall slope shear plane migrates through the excavations although the high SRF value indicates stable conditions (Figure 13-5). In addition, two-dimensional modelling assumed infinite out of plane geometry, which in this case assumes infinite excavation geometry. In reality, the underground infrastructure will be limited in span and should be modelled in three dimensions when the proposed location is defined.

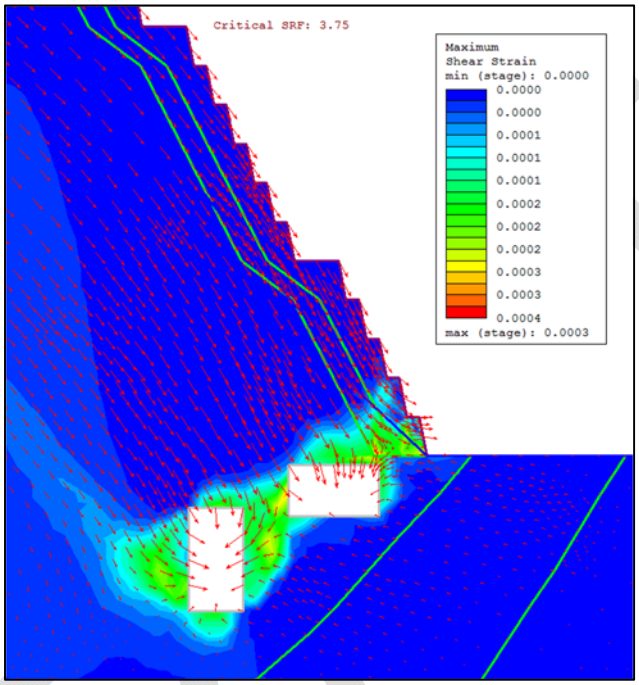

Figure 13-4: Shear strain development and displacement vectors within infrastructure area

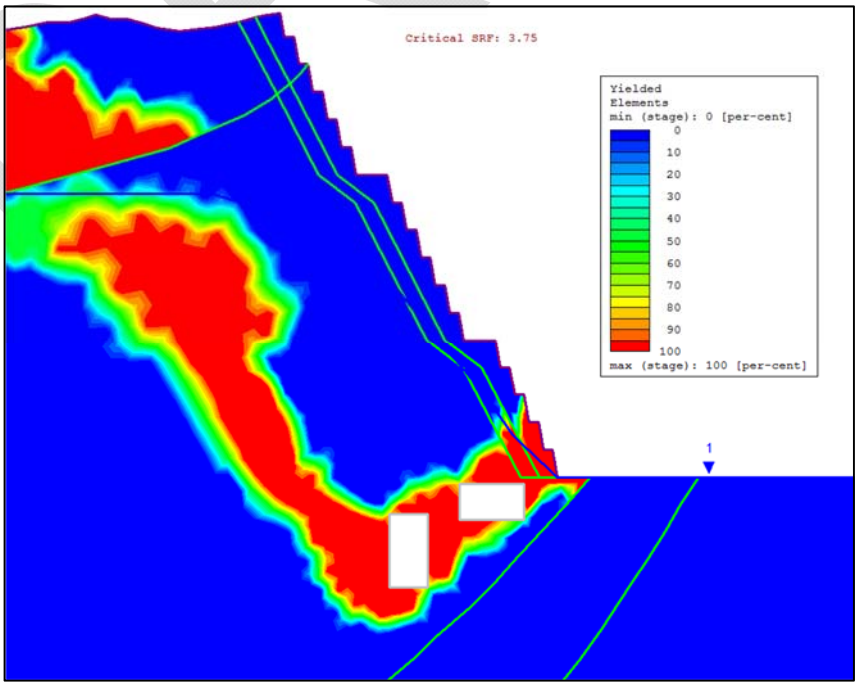

Figure 13-5: Yielded elements and interaction with open pit

14 CONCLUSIONS AND RECOMMENDATIONS

The following conclusions and recommendations are issued for the Engebø mine design study:

Data Sources

- Wardell Armstrong International completed a Pre-Feasibility study in 2016 which included drilling of a number of geotechnical boreholes, rock mass and structural logging and also strength testing of recovered core.
- Data sources were categorised based on format and quality of data collected. Recent data collected by SRK was deemed highest confidence.
    - ***Recommendation:*** Regular QA/QC protocol should be established to monitor geotechnical data collection through any on-going resource drilling at Engebø.

Geology and Structure

- In addition to data provided by the Client, SRK has developed a geological model based on assessment of 2016 and 2018 drill core in addition to historic geology maps based on detailed surface mapping.
- SRK completed a detailed 3D structural model which involved the generation of new major structures.
- Based on detailed analysis of the major faulting and small scale structure, it was not necessary to define individual structural domains within the pit. The singular domain defined for each pit containing discontinuity sets, major structures and rock fabric formed the basis of the kinematic assessment.
- Whilst assessment of core photos and televiewer logs indicates the presence of constrained faults, the complex geological setting has resulted in difficulty extrapolating data between boreholes. SRK has modelled a single fault plane located within the pit shell that dips moderately to the north.
    - ***Recommendation:*** Further definition of large scale structure during the early stages of mining.
- Alteration does not play a significant role in rock mass strength variability.

Rock Mass Model

- Supported through an assessment of rock mass parameters gained through diamond drilling, the following primary rock mass domains are defined:
    - trans Eclogite;
    - ferro Eclogite;
    - leuco Eclogite;
    - gneiss; and
    - amphibolite.
- Particular attention was paid to the assessment of intact rock strength within the Fresh Rock domain. Laboratory strength testing supported by point load testing and empirical estimates suggests the various lithological groups are reasonably homogenous.
- Mean values and ranges were defined for all rock mass parameters (fracture frequency, rock mass rating, etc.) within the defined rock mass domains. In addition to these standard rock mass parameters, Hoek-Brown parameters were generated for application to deterministic numerical models.

- ***Recommendation:*** Rock mass parameters should be validated through face mapping of exposures within the proposed pit areas.

Kinematics Assessment

- Based on available information, discontinuities through all rock mass domains were allocated a representative friction angle of 22°. No cohesion is applied to bench scale analyses.
- Figures and tables are provided that illustrate the kinematic design constraints within the proposed open pit. Full descriptions of toppling, planar and wedge risk are provided.
- The discontinuity sets and major structures identified are favourable in relation to slope design and performance.
  - ***Recommendation:*** Additional structural data collected during mining should be kinematically analysed to determine influence on pit slope performance. Persistence and spacing data should also be recorded for direct application to rock bridge assessment and discrete application of discontinuities in finite element and possibly discrete element modelling.

Hydrogeology

- Hydrogeological investigations have determined that groundwater flow is fracture driven
- At this time, residual pore pressure in Fresh Rock does not adversely affect slope stability, but sufficient monitoring and contingency must be assumed for mine plans.
  - ***Recommendation:*** As mining progresses, additional, coupled, sensitivity modelling should be completed to better understand the role and influence of the assumed damage zone on slope performance.

Stability Modelling

- Deterministic finite element (RS^2) was undertaken on three cross-sections within the pit.
- As a result of the tight nature of the fabric within the rock mass, anisotropy was not deemed suitable; however, a jointed rock mass model was developed to analyse the influence of persistent joint and rock bridge strength within the rock mass.
- A Disturbance Factor (D) of one was applied to all rock within approximately 30 m of the slope face.
- Acceptance criteria for Factor of Safety (FoS) was generated for each geotechnical cross-section.
- All cross-sections generated retuned favourable FoS values when modelled and slope angles established through kinematic analyses can be considered stable.
- ***Recommendation:*** As a better understanding of geotechnical conditions is developed as excavation commences, updated finite element modelling incorporating any critical overserved structures should be undertaken.

Slope Design

- Slope design criteria are issued based upon established kinematic and rock mass geometry constraints. Fresh Rock inter-ramp angles are set at 63° in Domain 1 and 60° in Domain 2.
  - ***Recommendation:***The majority of uncertainty and risk associated with the current slope design is related to interpretation of large scale structures intersection the pit slopes. As mining progresses, the structural model should be updated and its influence

on slope performance assessed. Trial slopes should be developed within the push-backs to assess slope performance prior to developing final pit walls.

14.1 Confidence in Pit Slope Design Recommendations

SRK uses a classification system of slope design based on three slope confidence classes (Steffen et al., 2006). The system was developed by SRK as a tool to report the confidence in the geotechnical information used in slope design. The three classes for slope design, inferred, probable, and proven, each represents an increased level of geotechnical knowledge and confidence. These classes refer to low, moderate and high confidence, respectively. For a feasibility study, a reasonable level of confidence is required, which relates to probable category. The three classes and their required levels of data confidence are explained as follows:

Category 3: Inferred Slope Angle

- Corresponds to application of typical slope angles based on experience in similar rocks. Quantification will be on the basis of rock mass classifications and a reasonable inference of the geological conditions within the affected rock mass.

Category 2: Probable Slope Angle

- Corresponds to a design based on information which allows a reasonable assumption to be made on the continuity of stratigraphic and lithological units. Some structural mapping will have been carried out utilising estimates of joint frequencies, lengths and conditions. All major features and joint sets should have been identified. Some testing (small sample) for the physical properties of the in situ rock and joint surfaces will have been carried out. Similarly, groundwater data will be based on water intersection in exploration holes with very few piezometer installations. Data will be such as to allow simplified design models to be developed in order to make sensitivity analyses possible.

Category 1: Proven Slope Angle

- Requires that the continuity of the stratigraphic and lithological units within the rock mass is confirmed in space from adequate intersections and/or mapping. Detailed structural mapping of the rock fabric is implied, orientations and types of penetrative fabrics and joint surfaces have been mapped and described from sufficient locations, that the foliation and joint trajectories are known to a high degree of confidence and can be extrapolated with a high confidence for the affected rock mass. Strength characteristics of the structural features and the in-situ rock have been determined by the appropriate testing procedures to allow reliable statistical interpretations to be made. Groundwater pressure distributions within the affected rock mass should have been measured using piezometer installations yielding a high confidence groundwater model. Data reliability should be such that an analytical model can be used to carry out the design to a confidence of 85%.

Based on the slope confidence classification described above, SRK has evaluated the available technical data critical to slope design as shown in Table 14-1.

Prior to the current geotechnical studies, the confidence in the slope angles used in the mine design were considered to lie in the “Inferred” category. This geotechnical study is considered to have raised the confidence to “Probable” and hence suitable for a definitive feasibility study. As mining progresses further geotechnical studies and monitoring of the behaviour of the pit walls according to the design criteria is recommended to raise the confidence and maximise /optimise the pit wall design criteria.

Overall, it is SRK’s opinion that the quality and amount of data obtained is reasonable and

allows for determining an appropriate pit design to the required feasibility level of confidence.

Table 14-1: Summary of slope confidence evaluation

Data	Comments	Level of confidence at Engebø	Recommendations for improvement
Geological Model	Geological model based upon borehole logging data.	Moderate confidence	
Structural model (major features)	Structural model based upon analysis and interpretation of historic boreholes and structural information generated from televiewer logging as part of the 2018 feasibility geotechnical programme.	Moderate confidence	Bench face mapping of faulting, foliation undulation, large scale roughness and persistence. Continual update of structural model as mining commences.
Structural model (jointing)	Reasonable understanding jointing and fabric. Appears to minimal variation in terms of structure orientation throughout the proposed pit. Televiewer surveys have produced a robust structural data set.	Moderate to high confidence	Bench face mapping when excavation develops to confirm major joint and fabric orientations.
Resource block model	Based on resource boreholes	High confidence.	
Intact Rock Strength	Detailed and comprehensive laboratory testing and PLT programme of unconfined compressive strength. Amount of results allow statistical interpretation	High confidence	
Strength of structural defects	Well sized laboratory testing programme of joint shear strength allows distinguishing shear strength by major lithologies. Not possible to determine joint shear strength for individual joint sets. Additional investigation and analysis of joint shear strength, especially joints that contain chloritic film infill. Low confidence in shear strength of major structures such as faults and shear zones.	Moderate to high confidence	Bench face mapping of large scale roughness, persistence, intact shear testing of fault and joints. Additional testing of joint shear strength.
Hydrogeological model	Hydrogeological investigation undertaken.	Moderate to high confidence	
Geotechnical model (rock mass strength)	Based on four new geotechnical boreholes in addition to the PFS data and televiewer surveys of historic boreholes. Rock mass strength is high and the orientation of structures and structure shear strength is the controlling factor to slope design and performance.	Moderate to high confidence	Continual update of rock mass model as mining commences.
Overall Confidence Rating		**PROBABLE**	

For and on behalf of SRK Consulting (UK) Limited

Max Brown, Principal Geotechnical Engineer, **Project Manager** SRK Consulting (UK) Limited	Neil Marshall, Corporate Consultant, **Project Director** SRK Consulting (UK) Limited

APPENDIX

A ROCK MASS LOGS

APPENDIX

B STRUCTURAL LOGS

APPENDIX

C LABORATORY TESTING

APPENDIX

D GEOLOGICAL AND STRUCTURAL REPORT

APPENDIX

E HYDROGEOLOGICAL REPORT